CHAPTER 3

Mechanistic Investigations of Palladium(II)-Catalyzed Oxidative Cyclizations

3.1 INTRODUCTION AND BACKGROUND

3.1.1 Introduction

Palladium(II)-catalyzed nucleophilic attack of an olefin by a heteroatom nucleophile can proceed by a variety of mechanisms. One key distinction to be made among them is whether attack occurs internally or externally, that is, with the metal and nucleophile on the same or opposite face of the olefin. Another subtlety is whether π-allyl palladium species are involved. Evidence for different reactive pathways has been demonstrated for several palladium(II)-catalyzed reactions, and it was not known by which pathway the oxidative cyclizations described in Chapter 2 proceeded. This question of mechanism is important on a fundamental, academic level, as well as from the practical standpoint of the development of successful reactions and for explaining and predicting stereochemical outcomes. For our oxidative cyclization reactions, we hypothesized that the sluggishness

of the asymmetric reaction could be attributed to the difference in ligand denticity between pyridine and (–)-sparteine (**22**). Thus, we wished to gain an understanding of the mechanism of the cyclization, and to determine whether the change from a mono- to a bidentate neutral ligand leads to a change in mechanism. The possible influence of anionic ligands and the nature of the nucleophile were also of interest. Our explorations into these effects are presented in this chapter.

3.1.2 Background

One commonly proposed mechanism for palladium(II)-catalyzed nucleophilic attack of an olefin by a heteroatom involves activation of the olefin by the metal followed by anti nucleophilic attack, i.e., anti oxypalladation (Figure 3.1.1). The resulting palladium alkyl intermediate (**186**) then undergoes β-hydrogen elimination. Such a mechanism is reminiscent of that proposed by Bäckvall, Stille and Kurosawa for the Wacker oxidation of ethylene to acetaldehyde.[1]

Figure 3.1.1 Anti oxypalladation.

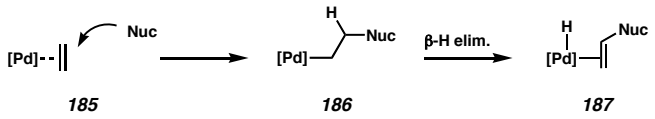

As evidence for anti oxypalladation in the Wacker oxidation of ethylene, Bäckvall has unraveled the stereochemical outcome of the oxidation, chlorination, and epoxidation sequence shown in Scheme 3.1.1.[1a,b] It is proposed that anti oxypalladation of ***trans*-15-d_2** is followed by S_N2 displacement by chloride, which is then displaced intramolecularly in an S_N2 fashion to provide *cis*-dideuteroepoxide **190**. For intramolecular reactions,

evidence for anti oxypalladation is scant, despite ongoing assertions that attack must occur in this fashion.[2]

Scheme 3.1.1

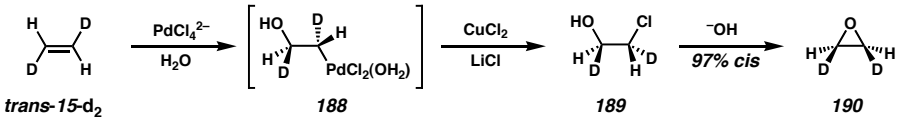

A second possible mechanism for palladium(II)-catalyzed nucleophilic attack, syn oxypalladation, is invoked in the alternative mechanism for the Wacker oxidation proposed by Henry and others.[3] The nucleophile is directly bound to palladium initially, as depicted by **185a** (Figure 3.1.2), and palladium-mediated bond formation between olefin and nucleophile occurs internally. The same palladium alkyl intermediate (**186**) results from both syn and anti oxypalladation, from which β-hydrogen elimination proceeds.

Figure 3.1.2 Syn oxypalladation.

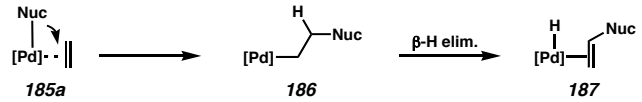

For intramolecular reactions, evidence of syn oxypalladation appears in recent reports from Hayashi and Wolfe. During the course of our work, Hayashi and coworkers described the reaction of a stereospecifically deuterium-labeled phenol substrate (**191**) under their conditions for enantioselective cyclization (see Section 2.1.2, Scheme 2.1.3).[4] After the oxypalladation step, the newly-formed C–O bond, palladium, and deuterium are all syn to each other (**192**). Syn β-deuterium elimination (see below) leads to initial product **193**, and then **194**. While significant olefin isomerization occurs to give **195** and **196**, all three products are consistent with syn oxypalladation. Interestingly, in the

presence of excess chloride ion, anti oxypalladation predominates, which indicates that subtle changes in reaction conditions can have dramatic effects on mechanism.

Scheme 3.1.2

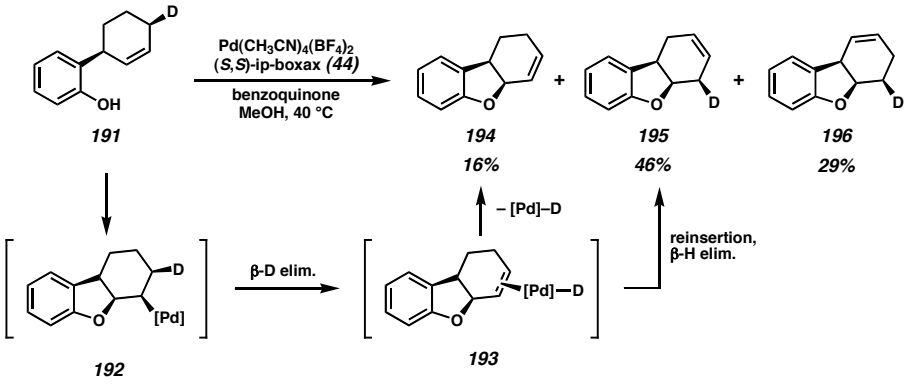

Wolfe and coworkers also provide evidence for syn oxypalladation in cyclizations with both oxygen and nitrogen nucleophiles.[5] In the example shown in Scheme 3.1.3, a pendant nitrogen nucleophile attacks a cyclopentene (**197**). *N*-Arylation, *C*-arylation, β-hydrogen elimination or a combination of the latter two leads to the various observed products (**199**, **201**, **203**, and **205**). The stereochemistry of the aryl group in **201** and **205** relative to the *cis*-5,5 ring system indicates syn oxypalladation.

Scheme 3.1.3

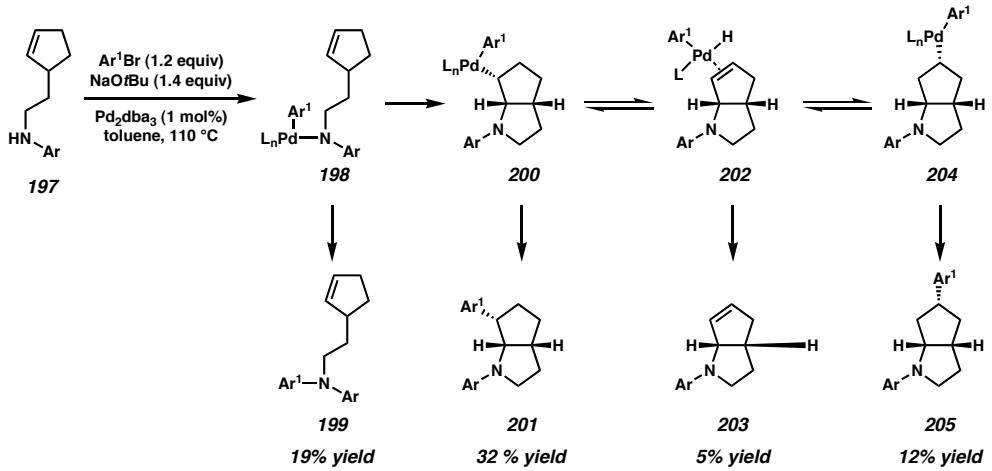

Wolfe further suggests that syn oxypalladation involves a formal olefin insertion into a palladium(II)–heteroatom bond.[6,7] However, Bäckvall and coworkers have studied computationally the reactivity of nucleophiles toward cis migration, i.e., olefin insertion, in (π-olefin)Pd(II) complexes and found that the HOMO-LUMO gap between the π* olefin orbital and a Pd–OH nucleophile is too large for migration to be frontier controlled.[8] Rather, the process is charge controlled, and thus likely does not occur through a concerted, 4-center transition state as in true olefin insertion reactions into palladium-alkyl and palladium-hydride bonds. The relevant frontier orbitals for a cis migration (olefin insertion) are depicted in Figure 3.1.3.

Figure 3.1.3 Frontier orbitals of the cis migration of an olefin in a palladium complex.

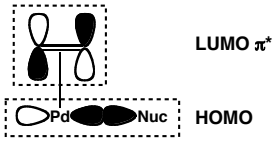

Another potential reaction pathway for palladium-olefin cyclization entails allylic C–H activation by palladium(II) to form an intermediate π-allyl species that would then undergo reductive elimination with the heteroatom nucleophile. Trost has shown that $Pd(TFA)_2$ will form π-allyl complexes by C–H activation of olefins in acetone.[9] In an intermolecular oxidative acetylation reaction of a deuterium-labeled cyclohexene **206**, Scheme 3.1.4), Bäckvall and coworkers reported a product outcome that supports a π-allyl intermediate (**207**).[10] The symmetrical π-allyl intermediate leads to a 1:1 mixture of products **208** and **209**, whereas anti oxypalladation would lead to only **208**.

Scheme 3.1.4

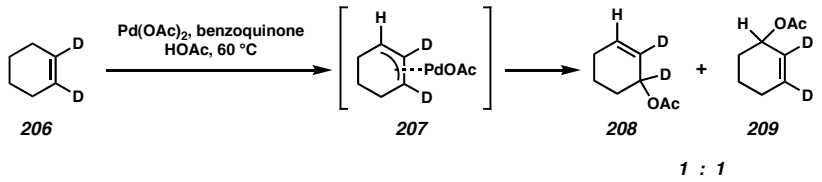

This chapter describes investigations into the mechanism of our oxidative cyclization reactions that establish the stereochemistry of oxypalladation for two types of substrates. On the basis of our results, we offer a rationale for the difficulty of developing the asymmetric reaction in toluene. As recent work by Hayashi, Wolfe, Sanford, White, Stahl, Sigman and others has also shown, our studies further demonstrate that oxidase-type catalysis by palladium(II) is both advantageously versatile in terms of reactivity and frustratingly promiscuous in terms of mechanism.

3.2 MECHANISTIC INVESTIGATIONS OF OXIDATIVE CYCLIZATIONS OF PRIMARY ALCOHOLS USING DEUTERIUM-LABELED SUBSTRATES

*3.2.1 Primary alcohol cyclizations of deuterium-labeled substrates with (pyridine)$_2$Pd(TFA)$_2$ (**144**).*

On the basis of the, until recently, commonly accepted mechanism for "Wacker" cyclizations, we initially operated under the supposition that the stereochemistry of oxypalladation in our reaction was anti.[11] But given the evidence for the existence of other reaction pathways under relatively similar conditions as described in part in Section 3.1.2, we wished to find support for this assumption. We set out to differentiate syn from anti oxypalladation through the synthesis of stereospecifically deuterium-labeled substrates, and by observing the products of the cyclization of these substrates in the presence of a mono- and a bidentate ligand. Deuterium-labeled alcohol substrates were

designed such that oxidative cyclization would result in either retention or elimination of the label, depending on the mode of nucleophilic attack. As mentioned above, during the course of this work, Hayashi and coworkers reported a similar study for the oxidative cyclization of olefin-appended phenols by palladium(II). We chose to focus on primary alcohols because of the interesting dichotomy between oxidative cyclization and alcohol oxidation and because a labeling study of this type had not yet been carried out for this substrate class.

Stereospecific deuterium incorporation into primary alcohol substrates could be effected with the Diels-Alder reaction shown Scheme 3.2.1 that completed the relatively straightforward synthesis of ***trans-*** and ***cis*-3-*d*-212**.[12]

Scheme 3.2.1

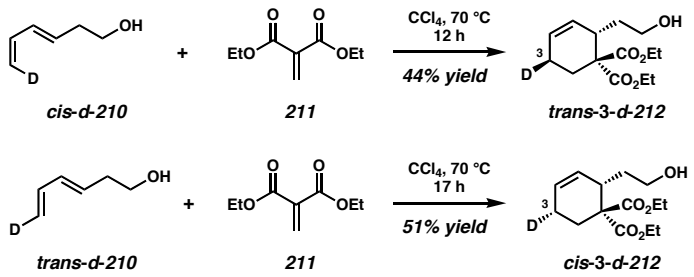

We assumed that the cyclization of **212** would preferentially form a cis 6-5 fused ring system, and that β-hydrogen elimination only occur when the palladium atom and eliminated H or D atom were syn to each other. Although examples of anti β-hydrogen elimination under various conditions have been reported, these involve aromatization or the formation of highly conjugated systems.[13] Given these two constraints, the presence or absence of a deuterium label in the product would then suggest the operative mechanistic pathway. While a π-allyl mechanism could be difficult to unambiguously

rule out with our test substrate, we hoped to at least distinguish syn from anti oxypalladation.[14]

Treatment of ***trans*-3-*d*-212** with 10 mol% $(pyridine)_2Pd(TFA)_2$ (**144**), 30 mol% pyridine, 2 equiv Na_2CO_3, 1 atm O_2 and 500 mg MS3Å/mmol substrate in toluene at 80 °C for 4.5 h provided **3-*d*-213** along with olefin isomer **3-*d*-214** in a 4:1 ratio and 91% overall yield (Scheme 3.2.2).[15] Likewise, reaction of the cis isomer (***cis*-3-*d*-212**) under the same conditions led to the formation of a 1:0.7 mixture of undeuterated **213** and ***cis*-2-*d*-214** in nearly quantitative yield.[16] Comparison of the ^1H and ^2H NMR spectra of the products of the above reactions with those formed from undeuterated **212** confirmed the presence or absence of a deuterium label.[17] Reaction of ***cis*-3-*d*-212** in the absence of Na_2CO_3 leads to an almost identical result: after 5.5 h, 99% yield of a 1:0.75 mixture of **213** and ***cis*-2-*d*-214** was obtained. To probe the origin of the isomerized product, reexposure of the product mixture (**213** and ***cis*-2-*d*-214**) to the same reaction conditions and an additional 10 mol% starting material (***cis*-3-*d*-212**) for 4 h resulted in 1:0.7 ratio of products in 90% isolated yield.

Scheme 3.2.2

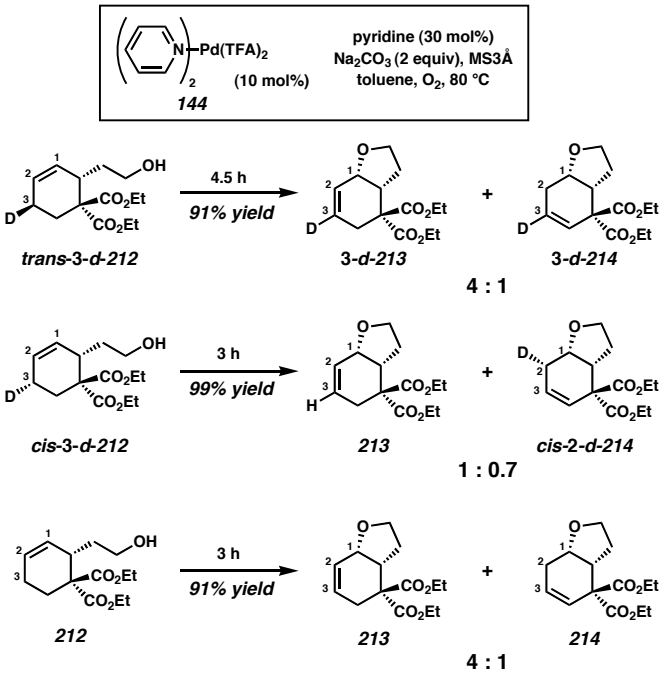

The stereochemistry of ***cis*-2-*d*-214** was confirmed via ^{1}H NMR spectroscopy. A homodecoupling experiment with **214** determined a coupling constant between H_A and H_B of 6.7 Hz (Figure 3.2.1). This value is consistent with a dihedral angle between the two C–H bonds of approximately 44°, which supports a cis relationship between H_A and H_B.[18] For nondeuterated product **214**, NOE interactions were observed between H_C and the protons indicated in Figure 3.2.1, and none was observed between H_C and H_D. This supports the spectral assignment of H_C, which does not appear in the ^{1}H NMR spectrum for ***cis*-2-*d*-214**.[17]

*Figure 3.2.1 Coupling constant and NOE interactions for **214**.*

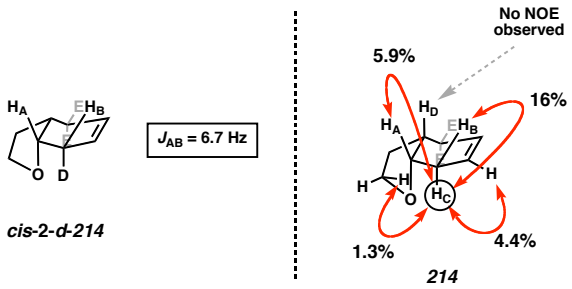

*3.2.2 Rationale for the product distribution from primary alcohol cyclizations of deuterium-labeled substrates with (pyridine)$_2$Pd(TFA)$_2$ (**144**).*

The mechanistic origin of the products, illustrated for the cis diastereomer (***cis*-3-*d*-212**), is shown in Figure 3.2.2. For comparison, all three possible pathways are shown. Path A involves anti nucleophilic attack of the palladium-coordinated olefin (**215**) by the pendant alcohol or alkoxide to provide palladium alkyl **216**. Subsequent β-hydrogen elimination and release of product from **217** would lead to the deuterium-labeled product **3-*d*-213**, but this product is not observed (see Scheme 3.2.2). In Path B, oxypalladation entails allylic C–H(D) activation to a π-allyl species (**218**) and subsequent formal reductive elimination to palladium(0) upon formation of the C–O bond in **219**. The stereochemistry of the reductive elimination would likely be anti, which is not supported by the observed product.[19] Further, unless selective C–D activation occurs, a mixture of labeled and unlabeled products would be expected; instead, a single product is observed. In Path C, a palladium alkoxide (**220**) undergoes syn oxypalladation followed by syn β-deuterium elimination to provide the observed major product, **213**, after dissociation of palladium from **222**. Reinsertion of the product olefin in the Pd–D intermediate **222** to give **223** followed by β-hydrogen elimination to **224** accounts for formation of the

observed minor product, ***cis*-2-*d*-214**.[16] The fact that an identical product mixture is obtained upon reexposure of the products to the reaction conditions supports the occurrence of reinsertion before dissociation of the product olefin from the Pd–D fragment. Because both Pd–D and Pd–H are formed, reinsertion *after* palladium dissociates from product **213** would lead to scrambling of the isotopic label. Finally, because the palladium(0) intermediate in Path B cannot easily account for the formation of olefin isomer ***cis*-2-*d*-214**, we favor the syn oxypalladation depicted in Path C.

Figure 3.2.2 Mechanistic rationale for the observed product distribution.

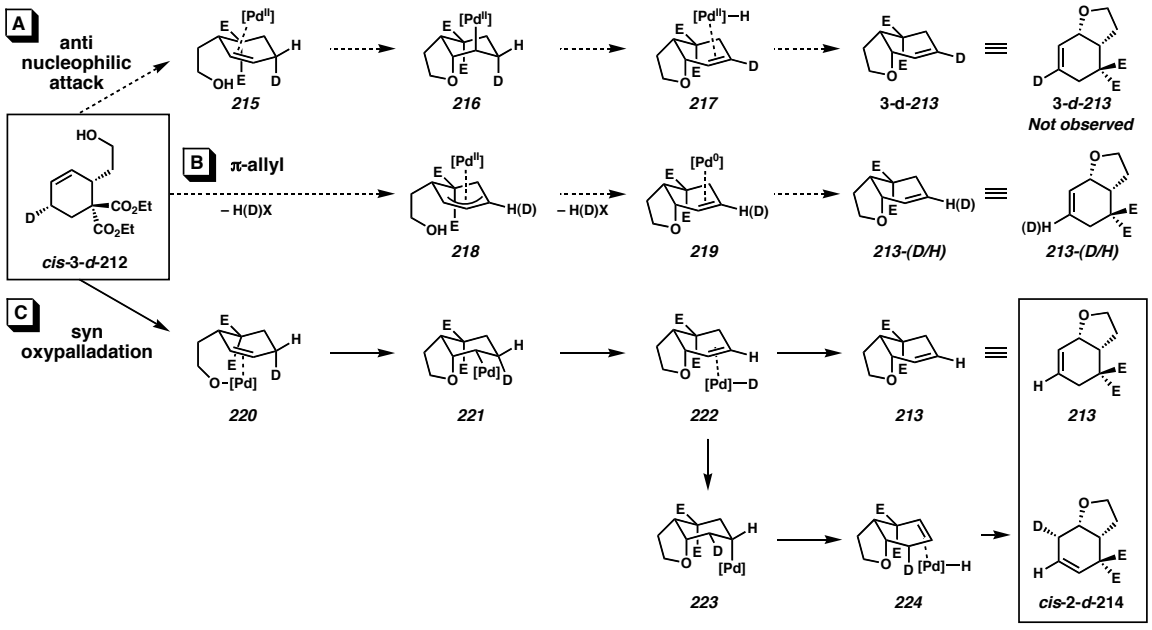

3.2.3 Possibilities for reactive pathways involving palladium(IV).

The remaining steps of the catalytic cycle involve reprocessing of palladium(II) by molecular oxygen. On the basis of earlier work by Murahashi and Takehira,[20,21] Uemura has proposed that this occurs by insertion of O_2 directly into the Pd(II)–H to form a palladium-hydroperoxide intermediate.[22] Stahl has elaborated the details of a mechanism

for aerobic oxidation catalysis by palladium(II) that entails reductive elimination of HX from Pd(II)–H to form palladium(0) which is then oxidized by O_2 in the formation of a palladium-peroxo intermediate.[23,24] In any case, these steps and those outlined in Figure 3.2.2 proceed through palladium(II) and palladium(0) intermediates; however, we cannot definitively discount a process involving palladium(IV).[25] In one scenario, oxidative activation of an allylic C–H bond would lead to a palladium(IV)-alkyl intermediate (**225**, Figure 3.2.3). Reductive elimination upon formation of the C–O bond would lead to a palladium(II) intermediate (**226**) that could undergo reprocessing by O_2 or a second reductive elimination of HX to form palladium(0), which would then be reoxidized. Alternatively, palladium(II) could undergo oxidative activation of an O–H bond to form a palladium(IV)-alkoxide (**227**). Syn oxypalladation would lead to palladium(IV)-alkyl **228**; β-hydrogen elimination to **229** followed by reductive elimination of HX would produce again a palladium(II) species (**61**). Although such pathways cannot be ruled out, the recently reported palladium oxidation reactions proposed to involve palladium(IV) also involve strong oxidizing agents such as $PhI(OAc)_2$.

Figure 3.2.3 Possibilities for reactive pathways involving palladium(IV).

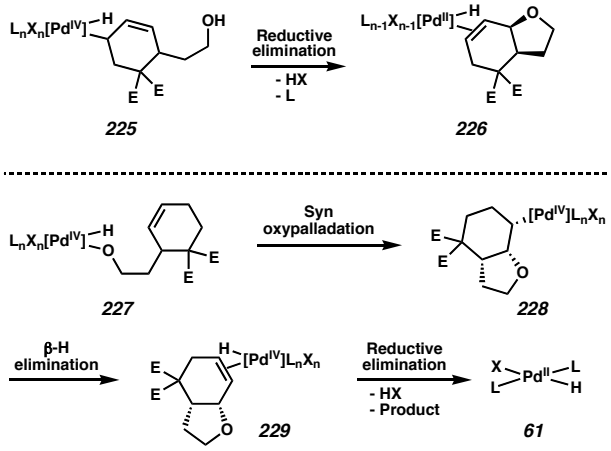

3.2.4 Considerations regarding a π-allyl mechanism.

We strove to further discount the π-allyl mechanism (Path B, Figure 3.2.2) by comparing the reactivity of two phenol substrates. As shown in Scheme 3.2.3, a phenol with a disubstituted pendant olefin (**28**) cyclizes in good yield to provide **29**. The most likely π-allyl species to form from **28** would involve activation of a benzylic proton, but intramolecular nucleophilic attack of this intermediate (**232**) would not lead to **29**. The π-allyl intermediate that would lead to **29**, i.e., **231**, could be expected to arise from terminal olefin **230** as well; both starting materials would lead to the same cyclized product (**29**). Instead, treatment of **230** with our standard nonenantioselective conditions leads to formation of a complex mixture and less than 5% yield of **29**. It may be that allylic or benzylic C–H activation does occur, but is not productive for cyclization.

Scheme 3.2.3

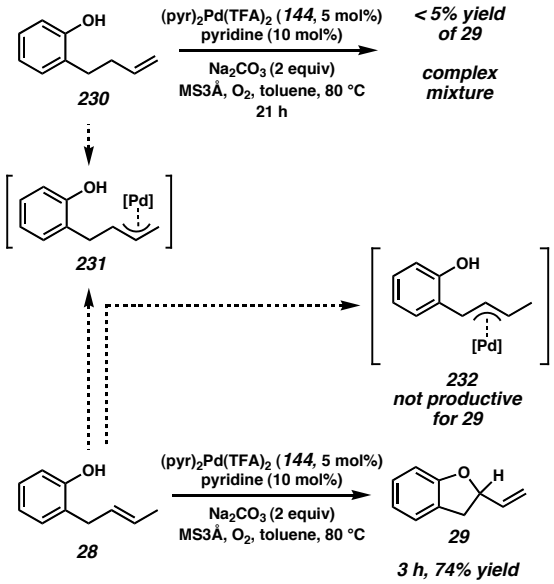

3.2.5 The effect of chloride ion on the stereochemistry of oxypalladation.

To explore whether the large effect of palladium(II) source on reactivity described in Chapter 2 originated from a change in mechanism, the cyclization of ***cis*-3-*d*-212** was carried out under the same reaction conditions but in the presence of $(pyridine)_2PdCl_2$ (Scheme 3.2.4).[26] The initial cyclization product (**213**) was identical to that obtained under the conditions employing $(pyridine)_2Pd(TFA)_2$ (**144**); however, the olefin isomer ***cis*-2-*d*-214** was now the major product. The cyclic ethers were obtained along with aldehyde ***cis*-3-*d*-233** in 74% overall yield after 20 h. The identity of the aldehyde was confirmed by oxidation of the alcohol by another method.[17] The formation of ethers **213** and ***cis*-2-*d*-214** implies that syn oxypalladation still occurs, contrary to what Hayashi observed for a similar phenol substrate, for which anti oxypalladation dominates upon the addition of chloride ion.[4] One explanation for the effect of chloride ion on product distribution is that it inhibits dissociation of palladium from the product olefin, leading to an increased amount of **214**. The formation of aldehyde ***cis*-3-*d*-233** likely occurs from a common alkoxide intermediate, and highlights the effect that subtle changes in reaction conditions can have on the mode of oxidation.

Scheme 3.2.4

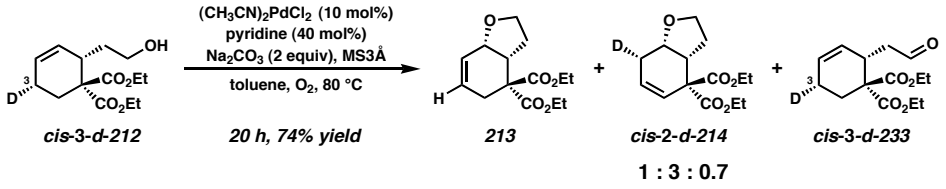

3.2.6 Deuterium-labeling studies of primary alcohol substrates in the presence of a bidentate ligand.

Next, we chose to examine the effect of a bidentate ligand on the product distribution of the cyclization. Treatment of both ***trans*-3-*d*-212** and ***cis*-3-*d*-212** with 10 mol% (dipyridyl)Pd(TFA)$_2$ (**149**), Na_2CO_3 (2 equiv), 1 atm O_2, 500 mg MS3Å/mmol substrate in toluene at 80 °C led to the formation of the same major products (**3-*d*-213** and **213**, respectively) observed with the conditions that use pyridine (Scheme 3.2.5). None of the olefin isomer **214** was observed; instead a small amount of aldehyde (***trans*-3-*d*-233** and ***cis*-3-*d*-233**) was formed for both starting material diastereomers. Both diastereomers were slower to cyclize in the presence of **149** than in the presence of (pyridine)$_2$Pd(TFA)$_2$ (**144**). However, the major product distribution from cyclization in the presence of both pyridine and dipyridyl (**74**) is the same. Presumably **233** arises from β-hydrogen elimination from a common alkoxide intermediate before oxypalladation can occur. The attempted cyclization of ***trans*-3-*d*-212** with (–)-sparteine (**22**) as a ligand led only to oxidation to the aldehyde.

Scheme 3.2.5

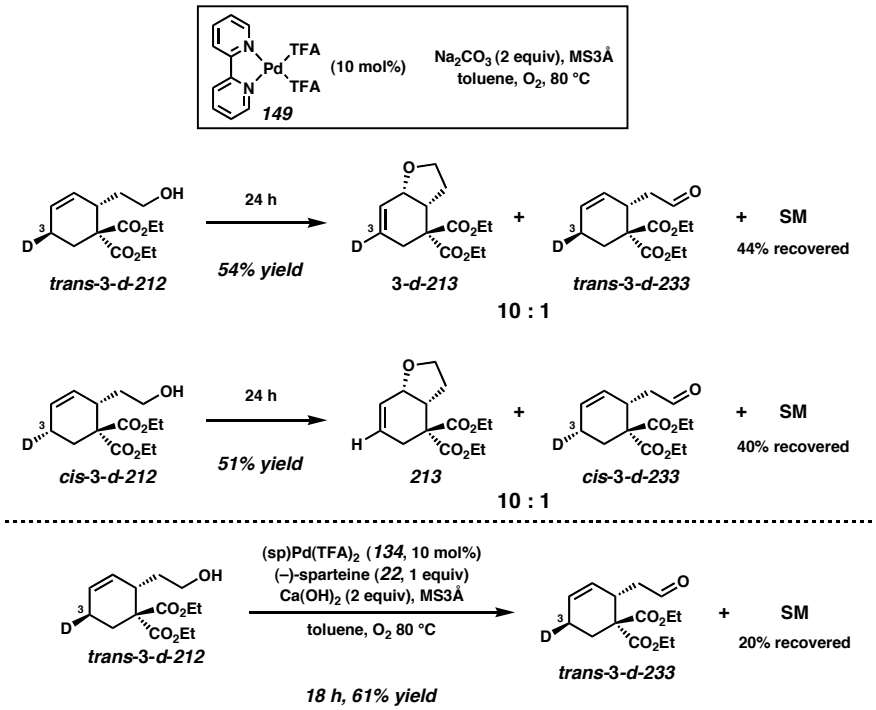

3.2.7 Considerations regarding mono- and bidentate ligands in the oxidative cyclization of primary alcohols.

On the basis of the results outlined above, we propose that, at least in the case of the alcohol substrates, reaction with a mono- or bidentate ligated catayst occurs by a similar pathway. The difference in reaction rate could arise from the degree to which each ligand can stabilize intermediates under otherwise identical reaction conditions. A neutral monodentate ligand such as pyridine can dissociate when necessary to free a coordination site for the substrate while maintaining charge-neutral intermediates (**235**-**237**, Figure 3.2.4A). When a bidentate ligand such as dipyridyl (**74**) is used, neutral ligand dissociation may be more difficult due to chelation, and instead an anionic ligand must dissociate, resulting in charged intermediates (**239** and **240**, Figure 3.2.4B). Such intermediates may be higher in energy under the reaction conditions, which in turn results

in decreased reactivity. The total failure of the substrates to cyclize when (–)-sparteine (**22**) is used as a ligand (cf. Scheme 3.2.5) is perhaps also due to steric congestion at the palladium center that prevents formation of the Pd–O–olefin chelate (**239**). We cannot rule out the possibility that the reaction with dipyridyl (**74**) as ligand proceeds through intermediates similar to those in Figure 3.2.4A with slow dissociation of one of the dipyridyl nitrogen atoms. If this is the case, (–)-sparteine (**22**), which is less likely to undergo partial dissociation due to its structural rigidity (see Chapter 4), would prevent cyclization.

Figure 3.2.4 Comparison of reaction pathways with a monodentate and bidentate ligand.

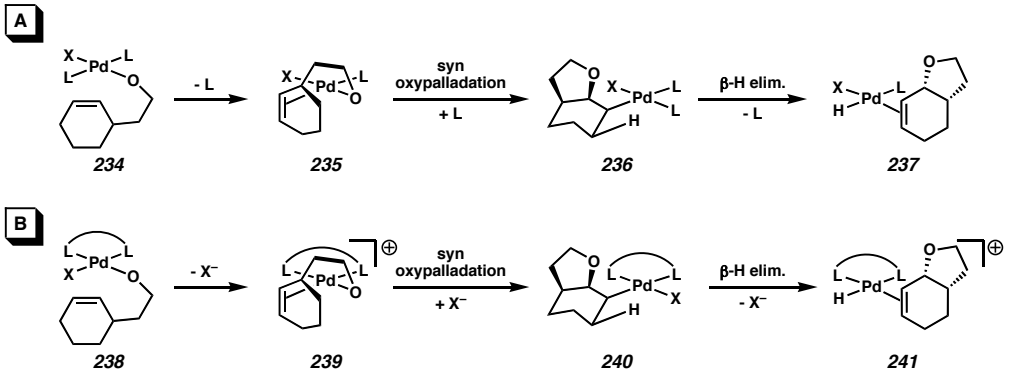

Although an extension of these mechanistic conclusions to the racemic and asymmetric phenol cyclizations may be tenuous, the same scenario would account for the slowness of the reactions catalyzed by ((–)-sparteine)Pd(TFA)$_2$ (**134**) relative to (pyridine)$_2$Pd(TFA)$_2$ (**144**) (see Chapter 2). Hayashi and coworkers' results also support this conclusion. Their system undergoes syn oxypalladation in the presence of a bidentate ligand with a dicationic palladium(II) catalyst in methanol using benzoquinone as the terminal oxidant.[4] The more polar solvent and dicationic catalyst may facilitate the formation of the charged intermediates shown in Figure 3.2.4B, whereas our toluene-

based conditions do not favor their formation. Because most chiral ligands that are effective in inducing asymmetry are bidentate, the mechanistic implication of the results described above is that selectivity *and* good reactivity will be difficult to attain in the palladium(II)/toluene/O_2 system.

3.3 MECHANISTIC INVESTIGATIONS OF THE OXIDATIVE CYCLIZATION OF CARBOXYLIC ACIDS USING DEUTERIUM-LABELED SUBSTRATES.

Alcohols ***trans*-3-*d*-212** and ***cis*-3-*d*-212** were oxidized[12] to the corresponding carboxylic acid derivatives (***trans*-3-*d*-242** and ***cis*-3-*d*-242**) and subjected to the cyclization with pyridine as a ligand (Scheme 3.3.1). Both substrates were slow to cyclize and formation of palladium black was observed; nevertheless, some product was obtained and analyzed by ^{1}H and ^{2}H NMR. In contrast to the alcohol substrates, the formation of unlabeled lactone **243** from ***trans*-3-*d*-242** and labeled lactone **3-*d*-243** from ***cis*-3-*d*-242** indicates that cyclization of the acid likely proceeds through anti oxypalladation. The olefin isomer arising from reinsertion was not observed. Cyclization of ***trans*-3-*d*-242** in the absence of Na_2CO_3 resulted in greatly diminished yield (4% yield after 24 h) of **243** but slower formation of palladium black, which indicates that the inorganic base does not affect the stereochemistry of oxypalladation, but may play a role in catalyst decomposition for this class of substrates.

Scheme 3.3.1

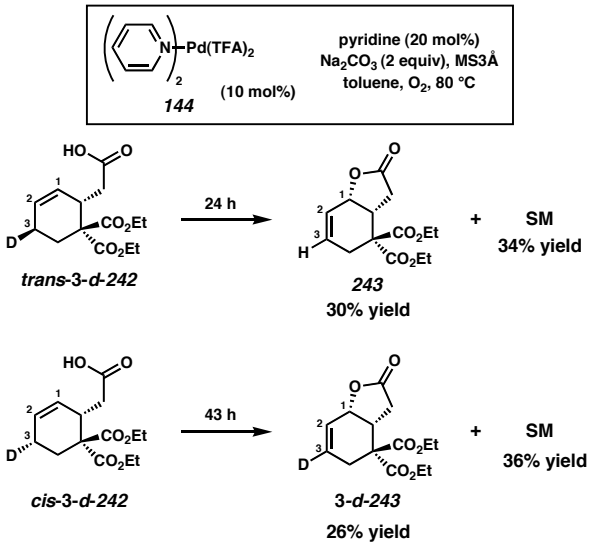

Although the reasons for the change in product distribution at this point remain unclear, geometrical constraints, pK_a differences, or differences in nucleophilicity between an acid and an alcohol are all possibilities. The additional unsaturation in the forming lactone could make geometrically unfavorable the Pd–O–olefin chelate that would precede syn oxypalladation. Whatever the case, these results confirm the versatility and undiscriminating reactivity of palladium(II) catalysts in oxidation reactions. As demonstrated by these results and the accumulating evidence from several groups, generalizations about reactivity and mechanism that span different substrates and different reaction conditions are difficult to make for palladium(II)-catalyzed oxidation reactions.[1,3,5,9,25,27]

3.4 SUMMARY AND CONCLUSION

Stereospecifically deuterated primary alcohol substrates were used to probe the stereochemistry of oxypalladation and to gain insight into the mechanism of cyclization.

Contrary to the common mechanistic proposal for reactions of this type (i.e., anti oxypalladation), cyclization of the primary alcohol substrates appears to occur via syn oxypalladation. This is in agreement with more recent reports from Hayashi and Wolfe on related systems. Neither the presence of chloride anion, nor the use of a bidentate instead of a monodentate ligand changes the stereochemistry of oxypalladation. The implications for the asymmetric reaction are that bidentate ligands may destabilize the intermediates necessary for a syn oxypalladation pathway. Thus, reactivity is decreased relative to the conditions employing a monodentate ligand. On the other hand, similarly deuterated carboxylic acid substrates react in the opposite sense, i.e., via anti oxypalladation.

As contemporary work in this rapidly developing, recently reborn field continues to demonstrate, oxidase-type catalysis by palladium(II) is highly versatile and adaptable to a variety of applications.[28] Our studies reported herein emphasize the subtleties of reactivity and mechanism in this field. Further development of dehydrogenation reactions using palladium(II) and molecular oxygen, racemic and asymmetric, is ongoing in this laboratory.

3.5 EXPERIMENTAL SECTION

3.5.1 Materials and Methods.

Unless stated otherwise, reactions were conducted in flame-dried glassware under a nitrogen atmosphere with freshly distilled solvents. All commercially obtained reagents were used as received. Reaction temperatures were controlled by an IKAmag temperature modulator. Thin-layer chromatography (TLC) was conducted with E. Merck silica gel 60 F254 precoated plates (0.25 mm) and visualized via UV and anisaldehyde or potassium permanganate staining. ICN silica gel (particle size 0.032-0.063 mm) was used for flash column chromatography. ^{1}H and ^{13}C NMR spectra were recorded on a Varian Mercury 300 spectrometer (at 300 MHz and 75 MHz respectively) and are reported relative to Me_4Si (δ 0.0). Some ^{1}H, ^{13}C, and all ^{2}H NMR spectra were recorded on a Varian Inova 500 spectrometer (at 500 MHz, 125 MHz, and 76 MHz, respectively) and are reported relative to Me_4Si (δ 0.0). Data for ^{1}H NMR spectra are reported as follows: chemical shift (δ ppm), multiplicity, coupling constant (Hz) and integration. Data for ^{13}C NMR spectra are reported in terms of chemical shift. Data for ^{2}H NMR spectra are reported in terms of chemical shift. NOE and homodecoupling experiments were recorded on a Varian Inova 500 spectrometer (at 500 MHz). IR spectra were recorded on a Perkin Elmer BXII spectrometer and are reported in frequency of absorption (cm^{-1}). High resolution mass spectra were obtained from the California Institute of Technology Mass Spectral Facility.

3.5.2 The preparation of deuterium-labeled primary alcohol substrates.

Scheme 3.5.1

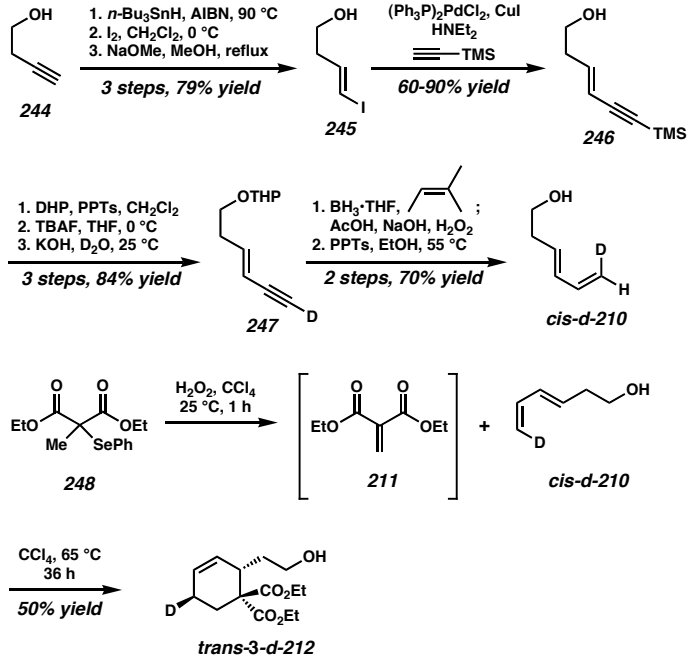

Deuterium-labeled cyclohexene *trans*-3-*d*-212. According to the procedure of Pilli:[29] a mixture of 3-butyn-1-ol (**244**, 3.0 g, 42.8 mmol), tri-*n*-butyltinhydride (16.1 mL, 59.9 mmol) and AIBN (210 mg, 1.28 mmol) was heated to 90 °C under argon. After 24 h, the reaction was cooled to 25 °C, diluted with CH_2Cl_2 (30 mL), and cooled to 0 °C in an ice bath. Iodine (16.3 g, 64.2 mmol) was added slowly in small portions, the flask was lightly capped, and the mixture was allowed to stir at 0 °C. After 1 h, the reaction was quenched with saturated aqueous $Na_2S_2O_3$ (20 mL). The mixture was extracted with Et_2O (3 x 40 mL). The organic layers were combined, washed with brine (15 mL), dried over Na_2SO_4, filtered, and concentrated in vacuo to give 30 g of crude material that was taken on to the next step without further purification. The resulting mixture of cis and trans vinyl iodides was dissolved in methanol (20 mL). Sodium metal (1.48 g, 64.2 mmol) was

added to additional methanol (40 mL), and the sodium methoxide solution added to the iodide. The mixture was heated to reflux under N_2 for 24 h, after which time elimination of the cis isomer was complete.[30] The reaction mixture was allowed to cool to 25 °C and the volatiles were removed in vacuo. The resulting brown residue was dissolved in saturated aqueous NH_4Cl (50 mL) and extracted with CH_2Cl_2 (3 x 50 mL). The organic extracts were combined, dried over $MgSO_4$, filtered, and concentrated in vacuo. The residue was further purfied by flash column chromatography on silica gel (hexanes → 6:1 → 1:1 hexanes/EtOAc eluent) to afford trans vinyl iodide **245** as a yellow-tinted oil (6.7 g, 33.7 mmol, 79% from **244**).

Iodide **245** (2.5 g, 12.6 mmol), trimethylsilylacetylene (2.68 mL, 18.9 mmol), and diethyl amine (20 mL) were combined in a Teflon-sealable Schlenk tube under argon. The mixture was degassed by one freeze-pump-thaw cycle (20 min). The flask was opened and CuI (24 mg, 0.13 mmol) and $(Ph_3P)_2PdCl_2$ (177 mg, 0.25 mmol) were quickly added as solids under a stream of argon. The flask was sealed again and the bright yellow-green mixture was allowed to stir in the dark at 25 °C. After 1.3 h, starting material was consumed and the volatiles removed in vacuo. The orange residue was taken up in benzene (25 mL) and H_2O (25 mL) and the layers were separated. The aqueous layer was extracted with benzene (3 x 25 mL). The organic layers were combined, dried over $MgSO_4$, filtered and concentrated in vacuo to provide a brown residue, which was purified by flash column chromatography on silica gel (4:1 hexanes/EtOAc eluent) to afford enyne **246** (1.75 g, 10.4 mmol, 83% yield).

Enyne **246** (1.75 g, 10.4 mmol), dihydropyran (1.42 mL, 15.6 mmol) and pyridinium-*p*-toluenesulfonate (261 mg, 1.04 mmol) were dissolved in CH_2Cl_2 (50 mL). Argon was

blown into the flask, and the flask sealed with a plastic cap. The mixture was allowed to stir at 25 °C for 3.25 h after which time reaction was complete. The solution was diluted with Et_2O (80 mL) and washed with a 1:1 solution of brine/H_2O (80 mL). Solvents were removed under reduced pressure to provide a yellow residue that was purified by flash column chromatography on silica gel (4:1 hexanes/EtOAc eluent) to provide the THP protected enyne as a light yellow oil (2.1 g, 8.4 mmol, 81% yield). The protected enyne (1.77 g, 7.0 mmol) was dissolved in THF (40 mL) under argon and cooled to 0 °C. A 1.0 M solution of tetrabutylammoniumfluoride in THF (7.0 mL, 7.0 mmol) was added dropwise to the cold stirring solution. After 10 min, starting material was consumed and the reaction was quenched by the addition of a 1:1 solution of sat. aq. NH_4Cl and H_2O (60 mL). The mixture was extracted with EtOAc (3 x 40 mL). The organics were combined, dried over $MgSO_4$, filtered, and concentrated in vacuo to provide a light brown oil. The oil was further purified by flash column chromatography on silica gel (9:1 hexanes/EtOAc eluent) to afford the free alkyne (990 mg, 5.5 mmol, 78% yield). Potassium hydroxide (127 mg, 2.26 mmol) was dissolved in D_2O (18.6 mL), and the solution was added to the deprotected enyne (990 mg, 5.5 mmol) under air.[31] The flask was sealed with a plastic cap and allowed to stir at 27 °C for 24 h. The opaque yellow mixture was extracted with CH_2Cl_2 (3 x 30 mL). The organic layers were combined, dried over $MgSO_4$, filtered, and concentrated in vacuo to provide deuterated alkyne **247** (893 mg, 4.93 mmol, 90%).

Hydroboration of the enyne (**247**) was carried out according to the procedure of Zweifel and Polston.[32] Borane•THF complex (1.0 M in THF, 5.4 mL, 5.40 mmol) was added to a solution of 2-methyl-2-butene (1.25 mL, 11.8 mmol) in THF (3 mL) at –5 °C

under argon. The mixture was allowed to stir for 2 h with the temperature maintained between –5 °C and 0 °C. Meanwhile, **247** (890 mg, 4.9 mmol) was dissolved in THF (6 mL) under argon and cooled to 0 °C. The prepared disiamylborane was transferred to the solution of alkyne via syringe, and the mixture was allowed to stir while the temperature was maintained between 0 °C and 5 °C. After 5 h, acetic acid (1.23 mL) was added, and the flask was heated to 57-60 °C. After another 6 h, the mixture was basified with 6 N NaOH (4.4 mL) and cooled to 25 °C. A solution of 30% aqueous hydrogen peroxide (0.62 mL) was added slowly, and the mixture was allowed to stir for another 15 min. The organic layer was separated, and the aqueous extracted with EtOAc (3 x 20 mL). The organic layers were combined, dried over $MgSO_4$, filtered, and concentrated in vacuo. The crude residue was purified on silica gel (99:1 → 19:1 hexanes/EtOAc eluent) to give the *cis*-deuterated diene as a clear, colorless oil (350 mg, 1.91 mmol, 39% yield). The THP ether was cleaved by combining the diene (350 mg, 1.91 mmol) with pyridinium-*para*-toluenesulfonate (48 mg, 0.191 mmol) in EtOH (19 mL) and heating to 55 °C in a flask sealed with a plastic cap. After 2.5 h the mixture was removed from heat and concentrated carefully under reduced pressure. The resulting crude material was purified by flash column chromatography on silica gel (9:1 → 1:1 pentane/Et_2O) to provide ***cis-d-*210** as a clear, colorless oil (175 mg, 1.76 mmol 92% yield): R_F 0.25 (4:1 hexanes/EtOAc eluent); ^{1}H NMR (500 MHz, $CDCl_3$) δ 6.32 (dd, J = 17.0, 10.5 Hz, 1H), 6.19-6.13 (m, 1H), 5.68 (ddd, J = 15.1, 7.2, 7.2 Hz, 1H), 5.13 (d, J = 17.0 Hz, 1H), 3.69 (t, J = 5.2 Hz, 2H), 2.39-2.34 (m, 1H), 1.42 (br s, 1H); ^{13}C NMR (125 MHz, $CDCl_3$) δ 136.9, 134.1 (t, $^2J_{CD}$ = 2 Hz), 130.7, 116.0 (t, $^1J_{CD}$ = 24 Hz), 62.1, 36.1; ^{2}H NMR (76 MHz, $CHCl_3$) δ 5.05 (s); HRMS (EI$^+$) m/z calc'd for $[C_6H_9OD]^+$: 99.07908, found: 99.07945.

The generation of diethyl methylenemalonate (**211**) in situ and subsequent Diels-Alder reaction was carried out according to the procedure of Raucher and Lawrence.[33] A solution of diethyl 2-methyl-2-(phenylseleno)malonate[34] (**248**, 1.16 g, 3.53 mmol) in CCl_4 (5 mL) was treated with 30% aqueous H_2O_2 (3.64 mL, 35.3 mmol) at 25 °C for 2 h, during which time a white milky precipitate formed in the aqueous layer. The organic layer was separated and filtered through a small plug of silica gel using CCl_4 (6 mL) into a flask containing the diene (***cis-d*-210**, 175 mg, 1.76 mmol). The mixture was heated to 70 °C under argon for 12 h, at which point the starting material was consumed. The slightly yellow solution was cooled to 25 °C and concentrated under reduced pressure. The residue was purified by flash column chromatography on silica gel (2:1 hexanes/EtOAc eluent) to afford cyclohexene ***trans*-3-*d*-212** as a clear colorless oil (208 mg, 0.77 mmol), 44% yield, 94% deuterium incorporation: R_F 0.06 (4:1 hexanes/EtOAc eluent); ^{1}H NMR (500 MHz, $CDCl_3$) δ 5.79 (ddd, J = 10.1, 4.8, 1.8 Hz, 1H), 5.65 (dd, J = 10.1, 4.5 Hz, 1H), 4.26-4.12 (comp. m, 4H), 3.79-3.68 (comp. m, 2H), 3.04-3.00 (m, 1H), 2.21 (dd, J = 13.6, 2.7 Hz, 1H), 2.17 (br s, 1H), 2.03 (dd, J = 13.6, 6.0 Hz, 1H), 1.64-1.52 (comp. m, 3H), 1.25 (t, J = 7.2 Hz, 3H), 1.23 (t, J = 7.1 Hz, 3H); ^{13}C NMR (125 MHz, $CDCl_3$) δ 171.1, 171.1, 128.8, 126.0, 61.6, 61.4, 61.0, 57.3, 35.8, 35.2, 24.4, 22.5 (t, J_{CD} = 19.2 Hz), 14.30, 14.28; ^{2}H NMR (76 MHz, $CHCl_3$) δ 1.88 (s); HRMS (EI$^+$) *m/z* calc'd for $[C_{14}H_{21}O_5D]^+$: 271.1530, found: 271.1526.

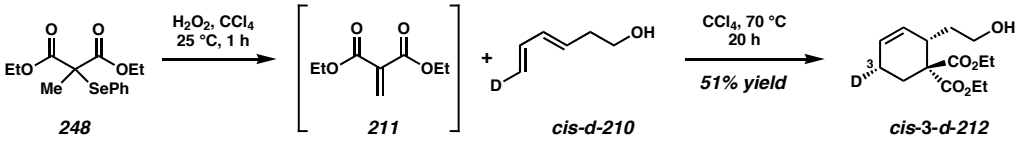

Deuterium-labeled cyclohexene *cis*-3-*d*-212. ***cis*-3-*d*-212** was synthesized according to the above procedure in comparable yields with the following differences: the alkyne was not deuterated (***H*-247**), and the hydroboration reaction was carried out with acetic acid-d_1, >97% deuterium incorporation: 51% yield from **210**, R_F 0.06 (4:1 hexanes/EtOAc); ^{1}H NMR (500 MHz, $CDCl_3$) δ 5.79 (ddd, J = 10.0, 4.8, 2.4 Hz, 1H), 5.65 (d, J = 10.1 Hz, 1H), 4.27-4.12 (comp. m, 4H), 3.79-3.68 (comp. m, 2H), 3.02 (t, J = 4.6 Hz, 1H), 2.21 (dd, J = 13.7, 6.2 Hz, 1H), 2.03 (dd, J = 10.7, 13.6 Hz, 1H), 1.94-1.88 (m, 1H), 1.63-1.52 (comp. m, 3H), 1.26 (t, J = 7.1 Hz, 3H), 1.24 (t, J = 7.2 Hz, 3H); ^{13}C NMR (125 MHz, $CDCl_3$) δ 171.4, 171.1, 128.8, 126.0, 61.6, 61.4, 61.1, 35.8, 35.2, 24.4, 22.5 (t, J_{CD} = 19.7 Hz), 14.3, 14.3; ^{2}H NMR (76 MHz, $CHCl_3$) δ 2.15 (s); HRMS (FAB$^+$) m/z calc'd for $[C_{14}H_{21}O_5D + H]^+$: 272.1608, found 272.1616.

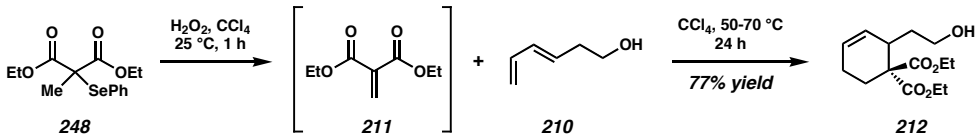

Cyclohexene 212. 3,5-Hexadien-1-ol (**210**) was synthesized from ethyl sorbate using the method of Batey and Miller.[35] The Diels-Alder reaction was carried out as above for ***trans*-3-*d*-212**: 77% yield, R_F 0.06 (4:1 hexanes/EtOAc); ^{1}H NMR (500 MHz, $CDCl_3$) δ 5.80-5.76 (ddd, J = 10.0, 4.8, 2.4 Hz, 1H), 5.65 (dd, J = 10.1, 4.5 Hz, 1H), 4.25-4.13 (comp. m, 4H), 3.87-3.67 (comp. m, 2H), 3.02 (t, J = 5.0 Hz, 1H), 2.24-2.20 (m, 1H),

2.17-2.11 (m, 1H), 2.07-2.01 (m, 1H), 1.97-1.89 (m, 1H), 1.64-1.51 (comp. m, 2H), 1.38-1.34 (m, 1H), 1.25 (t, J = 7.1 Hz, 3H), 1.23 (t, J = 7.1 Hz, 3H); ^{13}C NMR (125 MHz, $CDCl_3$) δ 171.1, 171.1, 128.7, 126.0, 61.6, 61.4, 61.0, 57.3, 35.8, 35.2, 24.4, 22.8, 14.3, 14.3; IR (film) 3464, 2942, 2980, 1734, 1236 cm^{-1}; HRMS (EI$^+$) m/z calc'd for $[C_{14}H_{22}O_5]^+$: 271.1545, found, 271.1557.

Figure 3.5.1 Comparison ^{1}H NMR spectrum of alcohol substrates.

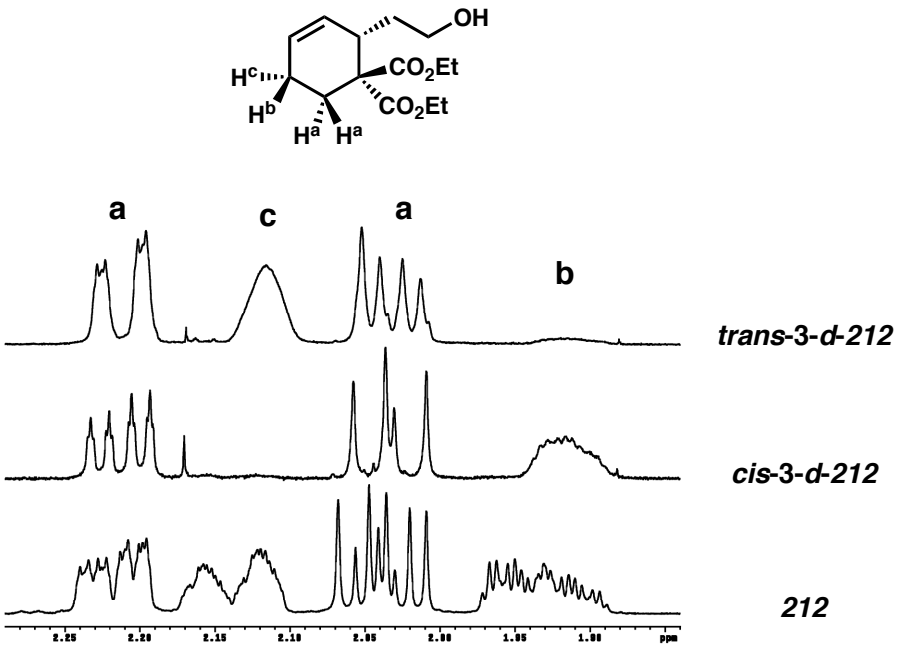

3.5.3 Representative procedure for the cyclization of deuterium-labeled alcohol substrates **trans-*3*-d-*212*** *and* **cis-*3*-d-*212***, *and cyclohexene* ***212*** *shown in Scheme 3.2.2.*

A thick-walled oven-dried 25 mL, 15 cm long tube (1.5 cm OD) equipped with magnetic stir bar was charged with powdered molecular sieves (MS3Å, 66 mg, 500 mg/mmol), which were flame dried immediately prior to use. $(Pyridine)_2Pd(TFA)_2$ (**144**, 9.1 mg, 0.019 mmol, 0.10 equiv) and Na_2CO_3 (39 mg, 0.37 mmol, 2.0 equiv) were added, followed by toluene (1.0 mL), pyridine (4.5 mL, 0.056 mmol, 0.30 equiv), and primary

alcohol substrate (50 mg, 0.185 mmol, 1.0 equiv). The tube was evacuated and back-filled with O_2 (3 x, balloon), heated to 80 °C in an oil bath, and allowed to stir under O_2 (1 atm, balloon). After reaction was complete, the crude mixture was loaded directly onto a column of silica gel and the product eluted with 4:1 hexanes/EtOAc.

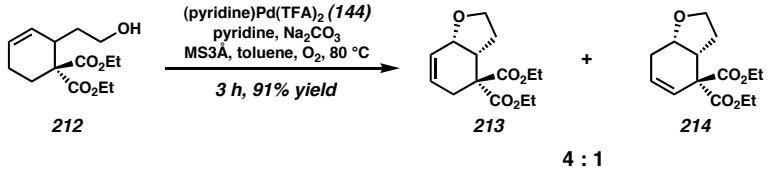

212 *213* *214*

4 : 1

Cyclohexene 213. 3 h. Clear, colorless oil (45.4 mg, 0.169 mmol, 91% yield): R_F 0.46 (2:1 hexanes/EtOAc); ^{1}H NMR (500 MHz, $CDCl_3$) δ 5.70 (dddd, *J* = 10.2, 5.4, 2.3, 0.97 Hz, 1H), 5.60-5.57 (m, 1H), 4.79-4.77 (m, 1H), 4.24-4.14 (comp. m, 4H), 3.86-3.76 (comp. m, 2H), 3.13 (ddd, *J* = 8.9, 8.7, 8.6 Hz, 1H), 2.72-2.59 (m, 1H), 1.89-1.82 (m, 1H), 1.77-1.70 (m, 1H), 1.26 (t, *J* = 7.2 Hz, 3H), 1.24 (t, *J* = 7.2 Hz, 3H); ^{13}C NMR (125 MHz, $CDCl_3$) δ 171.1, 170.6, 128.0, 125.3, 74.7, 66.0, 61.9, 61.8, 56.5, 40.6, 27.0, 26.1, 14.3, 14.2; IR (film) 2979, 1732, 1244, 1101, 1059 cm^{-1}; HRMS (EI$^+$) *m/z* calc'd for $[C_{14}H_{20}O_5]^+$: 268.1311, found, 268.1319.

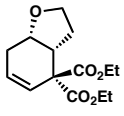

214

Cyclohexene 214. R_F 0.46 (2:1 hexanes/EtOAc); ^{1}H NMR (500 MHz, $CDCl_3$) δ 6.07 (dddd, *J* = 9.8, 2.7, 1.3, 1.2 Hz, 1H), 5.95 (dddd, *J* = 9.8, 5.3, 3.4, 0.46 Hz, 1H), 4.58 (ddd, *J* = 7.4, 7.0, 3.7 Hz, 1H), 4.28-4.08 (comp. m, 4H), 3.89 (ddd, *J* = 8.5, 8.4, 2.0 Hz, 1H), 3.63 (ddd, *J* = 14.7, 8.6, 6.1 Hz, 1H), 3.17 (dddd, *J* = 12.6, 8.0, 7.8, 1.2 Hz, 1H),

2.30 (dddd, J = 18.0, 6.6, 3.4, 2.8 Hz, 1H), 2.14 (dddd, J = 17.9, 5.4, 3.9, 1.4 Hz, 1H), 1.80-1.75 (m, 1H), 1.63-1.55 (m, 1H), 1.28 (t, J = 7.1 Hz, 3H), 1.22 (t, J = 7.1 Hz, 1H); ^{13}C NMR (125 MHz, $CDCl_3$) δ 170.2, 169.4, 129.6, 123.5, 74.4, 66.25, 61.84, 61.74, 56.98, 41.64, 28.89, 28.53, 14.33, 14.17; IR (film) 2979, 1732, 1246, 1060 cm^{-1}; HRMS (EI$^+$) m/z calc'd for $[C_{14}H_{20}O_5]^+$: 268.1311, found, 268.1309.

Figure 3.5.2 NOE analysis of cyclohexene ***214****.*

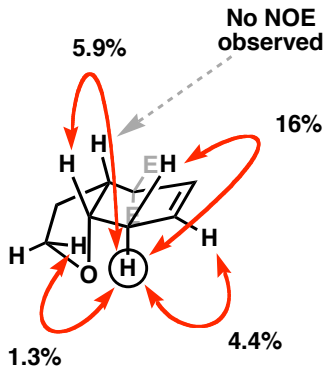

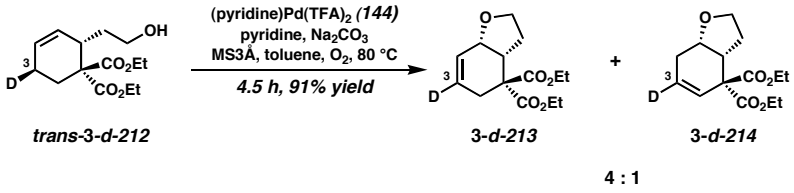

Cyclization of *trans*-3-*d*-212. This cyclization was carried out with 0.110 mmol ***trans*-3-*d*-212** (30.0 mg). After 4.5 h, the crude reaction mixture was loaded onto a short column of silica gel topped with Celite and chromatographed (4:1 hexanes/EtOAc eluent) to provide a 4:1 mixture of **3-*d*-213** and **3-*d*-214** (27 mg, 0.100 mmol, 91% yield): ^{2}H NMR (76 MHz, $CHCl_3$) δ 5.97 (s, minor), 5.72 (s, major), 2.12 (s, trace).

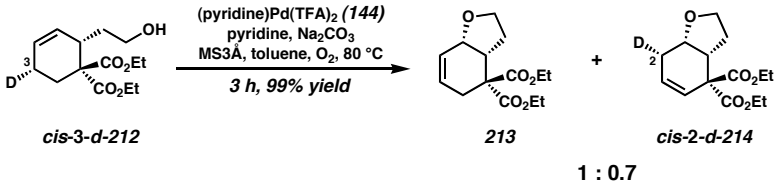

Cyclization of *cis*-3-*d*-212. This cyclization was carried out with 0.150 mmol ***cis*-3-*d*-212** (40.7 mg). After 3 h, the crude reaction mixture was loaded onto a short column of silica gel topped with Celite and chromatographed (4:1 hexanes/EtOAc eluent) to provide a 1:0.7 mixture of **213** and ***cis*-2-*d*-214** (40 mg, 0.148 mmol, 99% yield): ^{2}H NMR (76 MHz, $CHCl_3$) δ 5.70 (s, trace), 2.11 (s, major).

Figure 3.5.3 Homodecoupling analysis of **cis-*2*-d-*214*.**

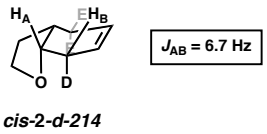

Figure 3.5.4 ^{1}H NMR comparison spectrum of cyclized products.

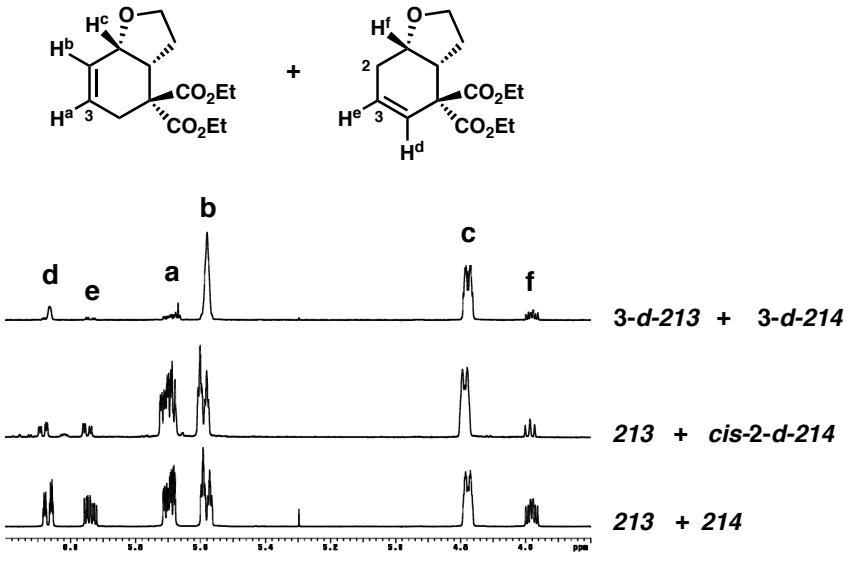

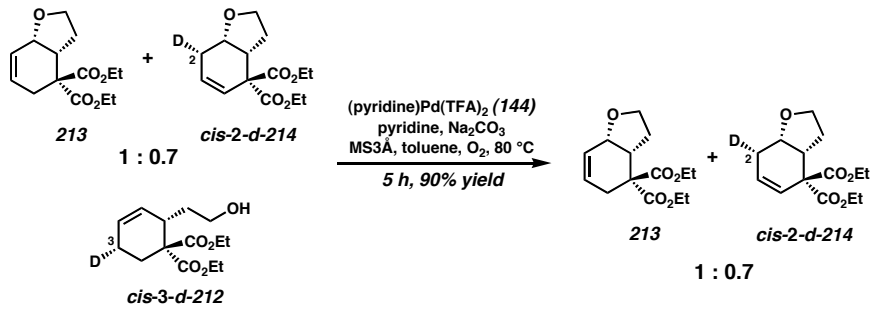

Reexposure of 213 and *cis*-3-*d*-214 to the cyclization conditions. An oven dried, 25 mL, 15 cm long tube equipped was magnetic stir bar was charged with MS3Å (60 mg, 500 mg MS3Å/mmol substrate) which were flame dried immediately prior to use. $(Pyridine)_2Pd(TFA)_2$ (**144**, 5.8 mg, 0.012 mmol, 0.10 equiv), and Na_2CO_3 (25 mg, 0.24 mmol, 2.0 equiv) were added, followed by pyridine (2.9 μL, 0.036 mmol, 0.30 equiv), ***cis*-3-*d*-212** (3.2 mg, 0.012 mmol, 0.10 equiv) and a 1:0.7 mixture of **213** and ***cis*-2-*d*-214** (32 mg, 0.12 mmol, 1.0 equiv). The tube was evacuated and backfilled with O_2 (3 x, balloon) and then heated to 80 °C in an oil bath under O_2 (1 atm, balloon). After 5 h, the crude reaction mixture was filtered through a pad of silica gel topped with Celite (4:1 hexanes/EtOAc eluent) to provide a 1:0.7 mixture of **213** and ***cis*-2-*d*-214** (29 mg, 0.11 mmol, 90% yield) as indicated by the ^1H NMR spectrum.

3.5.4 Attempted cyclization of a terminal olefin-appended phenol as shown in Scheme 3.2.3.

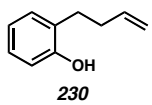

Homoallyl phenol 230. Synthesized from dihydrocoumarin using the procedure of Yates.[36] Spectroscopic data was in accordance with that reported by Macas.[37]

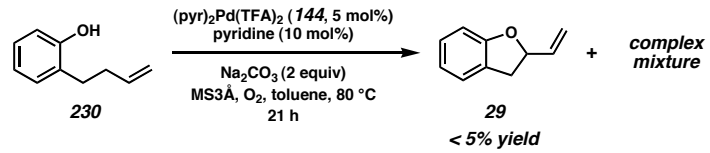

A thick-walled, oven dried 25 mL 15 cm long tube equipped with magnetic stir bar was charged with MS3Å (125 mg, 500 mg MS3Å/mmol substrate), which were flame dried immediately prior to use. (Pyridine)$_2$Pd(TFA)$_2$ (**144**, 6.1 mg, 0.0125 mmol, 0.05 equiv) and Na_2CO_3 (53 mg, 0.50 mmol, 2.0 equiv) were added, followed by pyridine (2.0 μL, 0.025 mmol, 0.10 equiv), toluene (1.0 mL), phenol **230** (37 mg, 0.25 mmol, 1.0 equiv) and additional toluene (1.5 mL). The tube was purged with O_2 (3 x, ballon) and heated to 80 °C in an oil bath under O_2 (1 atm, balloon). After 24 h, the crude reaction mixture was filtered through silica gel (hexanes → 9:1 hexanes/EtOAc eluent) to yield a complex mixture of unidentified products along with <5% of 24 as determined by analysis of the ^{1}H NMR spectrum of the fraction containing **29** (2.8 mg).

*3.5.5 Cyclization of **cis-3-d-212** with (pyridine)$_2$PdCl$_2$ as shown in Scheme 3.2.4.*

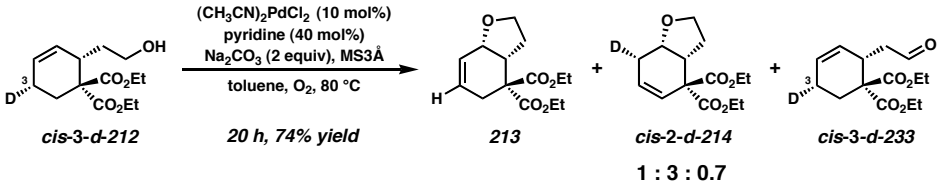

In a thick-walled, oven-dried 10 mL 15 cm tube, MS3Å (50 mg, 500 mg MS3Å/mmol substrate) were flame-dried immediately prior to use. $(CH_3CN)_2PdCl_2$ (3.5 mg, 0.010 mmol, 0.10 equiv) and Na_2CO_3 (21 mg, 0.20 mmol, 2.0 equiv) were added, followed by pyridine (3.2 μL, 0.040 mmol, 0.40 equiv) and toluene (1.0 mL). The mixture was heated to 80 °C under argon for 15 min. Alcohol ***cis*-3-*d*-212** (27 mg, 0.10

mmol, 1.0 equiv) was added, the tube purged with O_2 (3 x, balloon), and heated to 80 °C in an oil bath under O_2 (1 atm, balloon). After 20 h, the crude reaction mixture was filtered over silica gel topped with Celite (4:1 hexanes/EtOAc eluent) to provide a mixture of **213**, ***cis*-3-*d*-214**, and ***cis*-3-*d*-233** (20 mg, 0.074 mmol, 74% yield) as indicated by analysis of the ^{1}H NMR spectrum of the product mixture.

*3.5.6 Representative procedure for the cyclization of deuterium-labeled alcohol substrates **trans-3-d-212** and **cis-3-d-212** with (dipyridyl)Pd(TFA)$_2$ (**149**) and (sp)Pd(TFA)$_2$ (**134**) shown in Scheme 3.2.5.*

A thick-walled oven dried 25 mL, 15 cm-long tube equipped with magnetic stir bar was charged with powdered molecular sieves (MS3Å, 55 mg, 500 mg/mmol), which were flame dried immediately prior to use. (Dipyridyl)$_2$Pd(TFA)$_2$ (**149**, 5.4 mg, 0.011 mmol, 0.10 equiv) and Na_2CO_3 (23 mg, 0.22 mmol, 2.0 equiv) were added, followed by toluene (1.0 mL) and primary alcohol substrate (30 mg, 0.11 mmol, 1.0 equiv). The tube was evacuated and back-filled with O_2 (3 x, balloon), heated to 80 °C in an oil bath, and allowed to stir under O_2 (1 atm, balloon). After reaction was complete, the crude mixture was loaded directly onto a column of silica gel and chromatographed (19:1 → 1:1 hexanes/EtOAc). The product mixtures were analyzed by ^{1}H NMR.

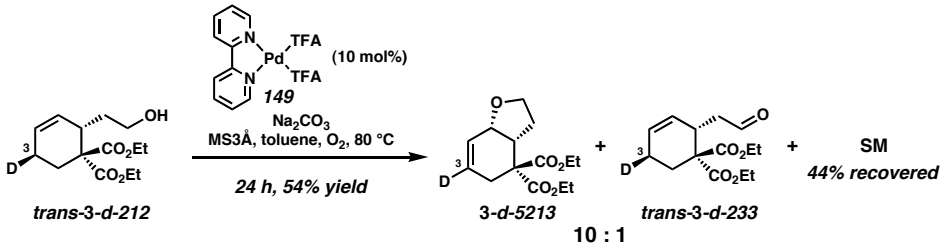

Cyclization of *trans*-3-*d*-212 with (dipyridyl)Pd(TFA)$_2$ (149). 24 h, 10:1 mixture of **3-*d*-213** and aldehyde ***trans*-3-*d*-233** (16 mg, 0.059 mmol, 54% yield) isolated, along with recovered starting material (***trans*-3-*d*-212**, 13 mg, 0.050 mmol, 44% yield).

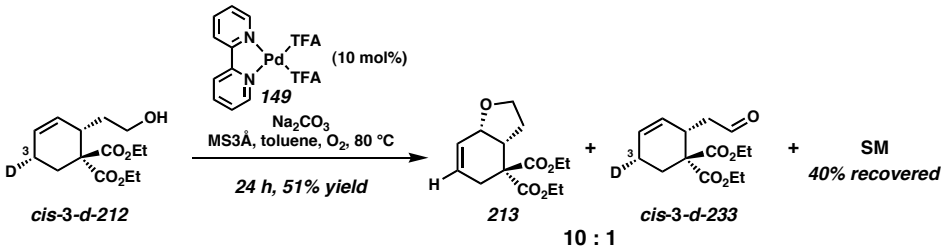

Cyclization of *cis*-3-*d*-212 with (dipyridyl)Pd(TFA)$_2$ (149). 24 h, 10:1 mixture of **213** and aldehyde ***cis*-3-*d*-233** (15 mg, 0.055 mmol, 51% yield) isolated, along with recovered starting material (***trans*-3-*d*-212**, 12 mg, 0.044 mmol, 40% yield).

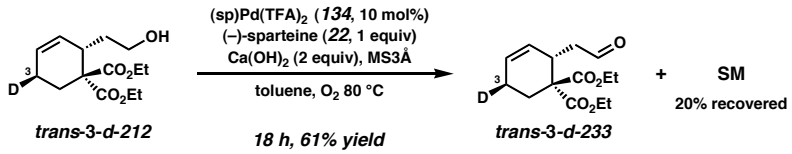

Cyclization of *trans*-3-*d*-212 with (sp)Pd(TFA)$_2$ 134). A thick-walled oven-dried 10 mL, 15 cm-long tube equipped with magnetic stir bar was charged with powdered molecular sieves (MS3Å, 46 mg, 500 mg/mmol), which were flame dried immediately prior to use. (sp)$_2$Pd(TFA)$_2$ (**134**, 5.2 mg, 0.009 mmol, 0.10 equiv) and Ca(OH)$_2$ (14 mg,

0.18 mmol, 2.0 equiv) were added, followed by toluene (0.92 mL) and ***trans*-3-*d*-212** (25 mg, 0.092 mmol, 1.0 equiv). The tube was evacuated and back-filled with O_2 (3 x, balloon), heated to 80 °C in an oil bath, and allowed to stir under O_2 (1 atm, balloon). After 18 h, the crude reaction mixture was filtered through silica gel (9:1 → 1:1 hexanes/EtOAc) to provide aldehyde ***trans*-3-*d*-233** (15 mg, 0.056 mmol, 61% yield) along with recovered starting material (5 mg, 0.018 mmol, 20% yield).

*3.5.7 The preparation of deuterium-labeled carboxylic acid substrates **cis-3-d-242** and **trans-3-d-242**.*

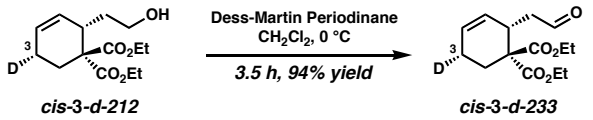

***cis*-3-*d*-212** ***cis*-3-*d*-233**

Oxidation of *cis*-3-*d*-212 to aldehyde *cis*-3-*d*-233. A solution of cyclohexene ***cis*-3-*d*-212** (46 mg, 0.17 mmol) in CH_2Cl_2 (2 mL) under argon was treated with a 10% *w*/*v* CH_2Cl_2 solution of Dess-Martin periodinane (0.42 mL, 0.13 mmol) at 25 °C. The mixture was allowed to stir for 3.5 h, after which time reaction was complete. The reaction was quenched by the addition of a 1:1 solution of sat. aq. $NaHCO_3$/sat. aq. $Na_2S_2O_3$ (5 mL) and extracted with EtOAc (3 x 6 mL). The organic extracts were combined, dried over $MgSO_4$, filtered, and concentrated in vacuo. The residue was purified by flash column chromatography on silica gel (4:1 hexanes/EtOAc) to provide aldehyde ***cis*-3-*d*-233** as a clear, colorless oil (42 mg, 0.156 mmol, 92% yield), >95% deuterated: R_F 0.31 (4:1 hexanes/EtOAc); ^{1}H NMR (500 MHz, $CDCl_3$) δ 9.74 (t, *J* = 1.6 Hz, 1H), 5.69-5.65 (m, 2H), 4.23-4.07 (comp. m, 4H), 3.53-3.50 (m, 1H), 2.58-2.48 (comp. m, 2H), 2.29 (dd, *J* = 13.4, 5.6 Hz, 1H), 2.10 (br s, 1H), 2.05-2.00 (m, 1H), 1.24

(comp. m, 7.1, 6H); ^{13}C NMR (125 MHz, $CDCl_3$) δ 200.6, 170.7, 170.7, 128.5, 126.5, 61.8, 61.6, 56.6, 47.0, 33.3, 25.1, 22.3 (t, J_{CD} = 20.6 Hz), 14.3, 14.2; ^{2}H NMR (76 MHz, $CHCl_3$) δ 2.12 (s); IR (film) 2980, 1732, 1447, 1235, 1043 cm^{-1}; HRMS (EI$^+$) *m/z* calc'd for $[C_{14}H_{19}O_5D]^+$: 269.1373, found: 269.1362.

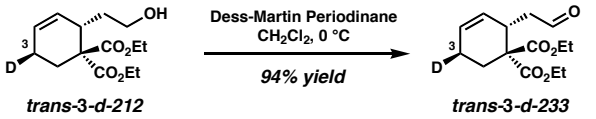

***trans*-3-*d*-212** ***trans*-3-*d*-233**

Aldehyde *trans*-3-*d*-222. Alcohol ***trans*-3-*d*-212** was oxidized by the same procedure outlined above for ***cis*-3-*d*-212** to give ***trans*-3-*d*-233** (94% yield), 95% deuterated: R_F 0.61 (2:1 hexanes/EtOAc); ^{1}H NMR (500 MHz, $CDCl_3$) δ 9.74 (t, *J* = 1.7 Hz, 1H), 5.70-5.64 (comp. m, 2H), 4.23-4.07 (comp. m, 4H), 3.53-3.49 (m, 1H), 2.58-2.49 (comp. m, 2H), 2.23 (dd, *J* = 13.6, 6.0 Hz, 1H), 2.10 (br s, 1H), 2.02 (dd, *J* = 13.6, 4.0 Hz, 1H), 1.24 (t, *J* = 7.1, 3H), 1.241 (t, *J* = 7.1 Hz, 3H); ^{13}C NMR (125 MHz, $CDCl_3$) δ 200.6, 170.8, 170.7, 128.5, 126.5, 61.75, 61.62, 56.59, 46.93, 33.43, 25.15, 22.25 (t, J_{CD} = 19.5 Hz), 14.26, 14.19; ^{2}H NMR (76 MHz, $CHCl_3$) δ 2.1 (s, minor), 2.0 (s, major); IR (film) 2981, 1732, 1236, 1191, 1050 cm^{-1}; HRMS (EI$^+$) *m/z* calc'd for $[C_{14}H_{19}O_5D]^+$: 269.1373, found: 269.1370.

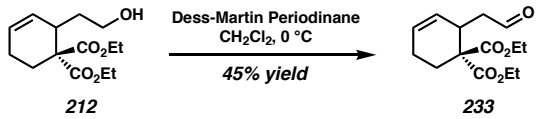

212 ***233***

Aldehyde 233. **212** was oxidized by the same procedure outlined above for ***cis*-3-*d*-212** to provide **233** (45% yield): R_F 0.61 (2:1 hexanes/EtOAc); ^{1}H NMR (500 MHz, $CDCl_3$) δ 9.76 (t, *J* = 1.7 Hz, 1H), 5.72-5.67 (comp. m, 2H), 4.25-4.19 (comp. m, 4H), 4.16-4.09

(comp. m, 2H), 3.55-3.52 (m, 1H), 2.60-2.50 (comp. m, 2H), 2.28-2.23 (m, 1H), 2.17-2.11 (m, 1H), 2.08-2.03 (m, 1H), 2.02-1.97 (m, 1H), 1.262 (t, J = 7.1 Hz, 3H), 1.261 (t, J = 7.1 Hz, 3H); ^{13}C NMR (125 MHz, $CDCl_3$) δ 200.6, 170.8, 170.7, 128.4, 126.6, 61.7, 61.6, 56.6, 46.9, 33.3, 25.2, 22.6, 14.3, 14.4; IR (film) 2980, 1731, 1238, 1174 cm^{-1}; HRMS (EI$^+$) m/z calc'd for $[C_{14}H_{20}O_5]^+$: 268.1311, found: 268.1321.

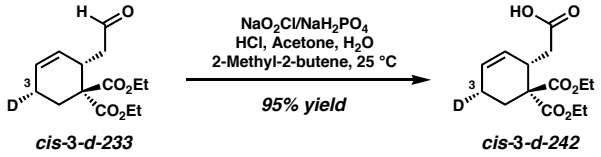

***cis*-3-*d*-233** ***cis*-3-*d*-242**

Deuterium-labeled acid *cis*-3-*d*-242. **Aldehyde *cis*-3-*d*-233** (42 mg, 0.16 mmol) was dissolved in acetone (30 mL) and treated with a saturated solution of NaH_2PO_4 that had been acidified to *p*H 2 with 1 N HCl (3.6 mL). The mixture was cooled to 0 °C and 2-methyl-2-butene (0.083 mL, 0.78 mmol) was added. Finally, a solution of $NaOCl_2$ (28 mg, 0.31 mmol) in H_2O (3 mL) was added dropwise to the cold stirring solution over 5 min, after which time starting material was consumed. The reaction mixture was poured into ice water (20 mL) and extracted with CH_2Cl_2 (3 x 30 mL). The organic layers were combined, dried over $MgSO_4$, filtered, and concentrated in vacuo. The residue was purified by flash column chromatography on silica gel (4:1 → 2:1 hexanes/EtOAc eluent) to provide ***cis*-3-*d*-242** as a waxy solid (42 mg, 0.15 mmol, 95% yield): R_F 0.17 (2:1 hexanes/EtOAc), >95% deuterated; ^{1}H NMR (500 MHz, $CDCl_3$) δ 5.75 (ddd, J = 9.9, 3.9, 1.9 Hz, 1H), 5.66 (m, 1H), 4.26-4.08 (comp. m, 4H), 3.39-3.34 (m, 1H), 2.53-2.35 (comp. m, 2H), 2.21 (dd, J = 12.7, 5.2 Hz, 1H), 2.24-1.90 (comp. m, 2H), 1.24 (t, J = 7.2 Hz, 3H), 1.24 (t J = 7.2 Hz, 3H); ^{13}C NMR (125 MHz, $CDCl_3$) δ 178.1, 170.7, 170.7, 128.2,

126.6, 61.7, 61.6, 56.6, 37.1, 35.1, 25.1, 22.3 (t, J_{CD} = 17.6 Hz), 14.2, 14.2; IR (film) 3313, 2981, 1734, 1713, 1236, 1073 cm^{-1}; HRMS (EI^+) *m/z* calc'd for $[C_{14}H_{19}O_6D]^+$: 285.1323, found: 285.1315.

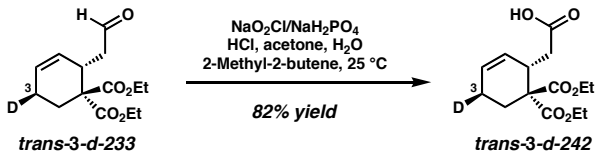

trans-3-*d*-233 *trans*-3-*d*-242

Deuterium-labeled acid *trans*-3-*d*-242. The trans isomer was synthesized from ***trans*-3-*d*-233** according to the procedure outlined above for ***cis*-3-*d*-242** to afford ***trans*-3-*d*-242** (82% yield): R_F 0.17 (2:1 hexanes/EtOAc), 95% deuterated; ^1H NMR (500 MHz, $CDCl_3$) δ 5.76 (ddd, *J* = 10.1, 4.3, 2.0 Hz, 1H), 5.67 (ddd, *J* = 10.1, 4.0, 1.6 Hz, 1H), 4.25-4.11 (comp. m, 4H), 3.37 (ddd, *J* = 8.8, 4.0, 4.0 Hz, 1H), 2.52-2.39 (comp. m, 2H), 2.21 (dd, *J* = 13.6, 4.2 Hz, 1H), 2.11 (br s, 1H), 2.04 (dd, *J* = 13.6, 6.0 Hz, 1H), 1.25 (t, *J* = 7.1 Hz, 3H), 1.25 (t, *J* = 7.1 Hz, 3H); ^{13}C NMR (125 MHz, $CDCl_3$) δ 176.5, 170.7, 170.7, 128.2, 126.7, 61.7, 61.6, 56.6, 36.9, 35.1, 25.2, 22.3 (t, J_{CD} = 17.7 Hz), 14.3, 14.2; ^2H NMR (76 MHz, $CHCl_3$) δ 1.97 (s); IR (film) 3313, 2982, 2915, 1734, 1713, 1261, 1235, 1192, 1057 cm^{-1}; HRMS (EI^+) *m/z* calc'd for $[C_{14}H_{19}O_6D]^+$: 285.1323, found: 285.1305.

*3.5.8 Representative procedure for the cyclization of deuterium-labeled acid substrates **cis-3-d-242** and **trans-3-d-242** as shown in Scheme 3.3.1.*

A thick-walled oven-dried 15 cm-long tube (1cm OD) equipped with magnetic stir bar was charged with powdered molecular sieves (MS3Å, 36 mg, 500 mg MS3Å/mmol substrate), which were flame dried immediately prior to use. $(Pyridine)_2Pd(TFA)_2$ (**144**, 3.6 mg, 0.007 mmol, 0.10 equiv) and Na_2CO_3 (16 mg, 0.15 mmol, 2 equiv) were added,

followed by pyridine (1.2 μL, 0.015 mmol, 0.20 equiv), and a toluene solution of acid substrate (0.1 M solution, 0.073 mmol). The tube was evacuated and back-filled with O_2 (3 x, balloon), heated to 80 °C in an oil bath, and allowed to stir under O_2 (1 atm, balloon). After reaction was complete, the crude mixture was loaded directly onto a column of silica gel and the product eluted with 4:1 hexanes/EtOAc.

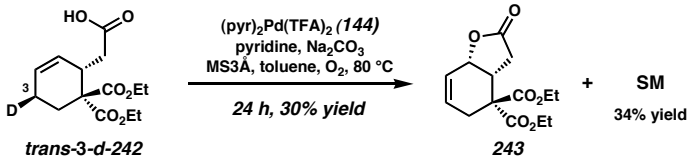

trans-3-*d*-242 243

Lactone 243. The cyclization was carried out with 0.073 mmol ***trans*-3-*d*-242** (21 mg). After 24 h the crude reaction mixture was loaded onto a short column of silica gel topped with Celite and chromatographed (4:1 → 1:1 hexanes/EtOAc eluent) to give **243** (21 mg, 0.073 mmol) as a clear colorless oil (6.2 mg, 0.022 mmol, 30% yield) along with recovered starting material (7.0 mg, 0.025 mmol, 34% yield): R_F 0.66 (1:1 hexanes/EtOAc); ^{1}H NMR (500 MHz, $CDCl_3$) δ 5.89 (dddd, *J* = 10.3, 4.6, 3.2, 1.2 Hz, 1H), 5.77-5.73 (m, 1H), 5.29-5.26 (m, 1H), 4.27-4.16 (comp. m, 4H), 3.51 (ddd, *J* = 10.4, 10.4, 7.6 Hz, 1H), 2.79-2.70 (comp. m, 2H), 2.44 (d, *J* = 10.4 Hz, 2H), 1.26 (t, *J* = 7.1 Hz, 3H), 1.25 (t, *J* = 7.1 Hz, 3H); ^{13}C NMR (125 MHz, $CDCl_3$) δ 175.3, 169.9, 169.4, 127.7, 124.8, 77.4, 76.2, 62.4, 55.3, 37.3, 30.0, 26.2, 14.2, 14.2; IR (film) 2982, 1783, 1730, 1245, 1186, 997 cm^{-1}; HRMS (EI$^+$) *m/z* calc'd for $[C_{14}H_{18}O_6]^+$: 282.1103, found: 282.1092.

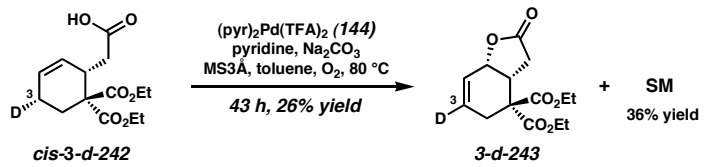

Lactone 3-*d*-243. The cyclization was carried out with 0.081 mmol ***cis*-3-*d*-242** (23 mg). After 43 h, the crude reaction mixture was loaded onto a short column of silica gel topped with Celite and chromatographed (4:1 hexanes/EtOAc eluent) to yield **3-*d*-243** as a clear colorless oil (6.0 mg, 0.021 mmol, 26% yield) along with recovered starting material (8.4 mg, 0.029 mmol, 36% yield): R_F 0.66 (1:1 hexanes/EtOAc); ^{1}H NMR (300 MHz, $CDCl_3$) δ 5.88 (m, 1H), 5.75 (m, 1H), 5.27 (dddd, *J* = 9.6, 2.9, 2.6, 2.2 Hz, 1H), 4.30-4.13 (comp. m, 4H), 3.51 (ddd, *J* = 10.5, 10.5, 8.3 Hz, 1H), 2.80-2.67 (comp. m, 2H), 2.44 (d, *J* = 10.5 Hz, 2H), 1.26 (t, *J* = 7.2 Hz, 3H), 1.25 (t, *J* = 7.2 Hz, 1H); ^{13}C NMR (125 MHz, $CDCl_3$) δ 175.3, 169.9, 169.4, 127.4 (t, J_{CD} = 23.0 Hz), 124.7, 77.4, 76.2, 62.4, 55.3, 37.3, 30.0, 26.1, 14.2, 14.2; IR (film) 2977, 2930, 1781, 1728, 1241, 1184, 996 cm^{-1}; HRMS (EI$^+$) *m*/*z* calc'd for $[C_{14}H_{17}O_6D]^+$: 283.1166, found: 283.1177.

3.6 NOTES AND REFERENCES

[1] (a) Bäckvall, J.-E.; Åkermark, B.; Ljunggren, S. O. *J. Chem. Soc., Chem. Commun.* **1977**, 264-265. (b) Bäckvall, J.-E.; Åkermark, B.; Ljunggren, S. O. *J. Am. Chem. Soc.* **1979**, *101*, 2411-2416. (c) James, D. E.; Hines, L. F.; Stille, J. K. *J. Am. Chem. Soc.* **1976**, *98*, 1806-1809. (d) Stille, J. K.; Divakaruni, R. *J. Am. Chem. Soc.* **1978**, *100*, 1303-1304. (e) Majima, T.; Kurosawa, H. *J. Chem. Soc., Chem. Commun.* **1977**, 610-611.

[2] (a) Coleman, J. P.; Hegedus, L. S. *Principles and Applications of Organometallic Chemistry*; University Science Books: Mill Valley, CA, 1980, pp 401-424. (b) Hegedus, L. S.; Allen, G. F.; Bozell, J. J.; Waterman, E. L. *J. Am. Chem. Soc.* **1978**, *100*, 5800-5807.

[3] (a) Francis, J. W.; Henry, P. M. *Organometallics* **1991**, *10*, 3498-3503. (b) Zaw, K.; Henry, P. M. *Organometallics* **1992**, *11*, 2832-2836. (c) Francis, J. W.; Henry, P. M. *Organometallics* **1992**, *11*, 2008-2015. (d) Hamed, O.; Henry, P. M. *Organometallics* **1997**, *16*, 4903-4909. (e) Hamed, O.; Thompson, C.; Hernry, P. M. *J. Org. Chem.* **1997**, *62*, 7082-7083. (f) Hamed, O.; Henry, P. M.; Thompson, C. *J. Org. Chem.* **1999**, *64*, 7745-7750. (g) ten Brink, G.-J.; Arends, I. W. C. W.; Papadogianakis, G.; Sheldon, R. A. *Appl. Catal., A* **2000**, *194-195*, 435-442. (h) Nelson, D. J.; Li, R.; Brammer, C. *J. Am. Chem. Soc.* **2001**, *123*, 1564-1568.

[4] Hayashi, T.; Yamasaki, K.; Mimura, M.; Uozumi, Y. *J. Am. Chem. Soc.* **2004**, *126*, 3036-3037.

[5] For systems containing oxygen nucleophiles, see: (a) Hay, M. B.; Hardin, A. R.; Wolfe, J. P. *J. Org. Chem.* **2005**, *70*, 3099-3107. For systems containing nitrogen nucleophiles, see: (b) Ney, J. E.; Wolfe, J. P. *Angew. Chem., Int. Ed.* **2004**, *43*, 3605-3608. (c) Ney, J. E.; Wolfe, J. P. *J. Am. Chem. Soc.* **2005**, *127*, 8644-8657.

[6] For experimental evidence of insertion of tetrafluoroethylene into a Pt–O bond, see: Bryndza, H. E. *Organometallics* **1985**, *4*, 406-408.

[7] For a recent example of olefin insertion into a rhodium amide, see: Zhao, P.; Krug, C.; Hartwig, J. F. *J. Am. Chem. Soc.* **2005**, *127*, 12066-12073.

[8] (a) Bäckvall, J.-E.; Björkman, E. E.; Pettersson, L.; Siegbahn, P. *J. Am. Chem. Soc.* **1984**, *106*, 4369-4373. (b) Bäckvall, J.-E.; Björkman, E. E.; Pettersson, L.; Siegbahn, P. *J. Am. Chem. Soc.* **1985**, *107*, 7265-7267.

[9] Trost, B. M.; Metzner, P. J. *J. Am. Chem. Soc.* **1980**, *102*, 3572-3577.

[10] (a) Grennberg, H.; Simon, V.; Bäckvall, J.-E. *J. Chem. Soc. Chem. Commun.* **1994**, 265-266. (b) Grennberg, H.; Bäckvall, J.-E. *Chem. Eur. J.* **1998**, *4*, 1083-1089.

[11] Trend, R. M.; Ramtohul, Y. K.; Ferreira, E. M.; Stoltz, B. M. *Angew. Chem. Int. Ed.* **2003**, *42*, 2892-2895.

[12] See Section 3.5.1 for details of the synthesis.

[13] (a) Toyota, M.; Ilangovan, A.; Okamoto, R.; Masaki, T.; Arakawa, M.; Ihara, M. *Org. Lett.* **2002**, *4*, 4293-4296. (b) Lautens, M.; Fang, Y.-Q. *Org. Lett.* **2003**, *5*, 3679-3682. (c) Hughes, C. C.; Trauner, D. *Angew. Chem. Int. Ed.* **2002**, *41*, 1569-1572. (d) Buchwald, S. L.; Hennessy, E. J. *J. Am. Chem. Soc.* **2003**, *125*, 12084-12084.

[14] For a study that attempts to differentiate between oxypalladation and a π-allyl route for a Pd(II)-catalyzed cyclization, see: Zanoni, G.; Porta, A.; Meriggi, A.; Franzini, M.; Vidari, G. *J. Org. Chem.* **2002**, *67*, 6064-6069.

[15] These are the standard conditions for nonenantioselective cyclization described in Chapter 2.

[16] The difference in the product ratios formed from the trans and cis isomers could be accounted for by an isotope effect in the reinsertion step. Possibilities include: slower reinsertion for the [Pd]–H bound olefin than for the [Pd]–D bound olefin, faster dissociation for the [Pd]–H bound olefin, faster reductive elimination of HX before dissociation or reinsertion, or faster coordination and insertion of O_2 into the [Pd]–H bond, if turnover of the catalyst occurs by that mechanism. At this time we cannot rule out any of or distinguish among these possibilities.

[17] See Section 3.5 for details.

[18] As determined by the program Mestre-J.

[19] For a Pd(II)-π-allyl electrophile, a primary alcohol (or alkoxide) would fall into the class of "soft" nucleophiles, the conjugate acids of which as defined by Trost have a $pK_a < 25$, see: Trost, B. M.; Van Vranken, D. L. *Chem. Rev.* **1996**, *96*, 395-422.

[20] Hosokawa, T.; Murahashi, S.-I. *Acc. Chem. Res.* **1990**, *23*, 49-54.

[21] Takehira, K.; Hayakawa, T.; Orita, H. *Chem. Lett.* **1985**, 1835-1838, and references therein.

[22] Nishimura, T.; Onoue, T.; Ohe, K.; Uemura, S. *J. Org. Chem.* **1999**, *64*, 6750-6755.

[23] (a) Stahl, S. S.; Thorman, J. L.; Nelson, R. C.; Kozee, M. A. *J. Am. Chem. Soc.* **2001** *123*, 7188-7189. (b) See also: Steinhoff, B. A.; Stahl, S. S. *Org. Lett.* **2002**, *4*, 4179-4181.

[24] Keith, J. M.; Nielsen, R. J.; Oxgaard, J.; Goddard, W. A., III; *J. Am. Chem. Soc.* **2005**, *127*, 13172-13179.

[25] For recent articles invoking Pd(IV) in Pd-catalyzed oxidative processes, see: (a) Dick, A. R.; Hull, K. L.; Sanford, M. S. *J. Am. Chem. Soc.* **2004**, *126*, 2300-2301. (b) Dick, A. R.; Kampf, J. W.; Sanford, M. S. *Organometallics* **2005**, *24*, 482-485. (c) Alexanian, E. J.; Lee, C.; Sorensen, E. J. *J. Am. Chem. Soc.* **2005**, *127*, 7690-7691. (d) Yoneyama, T.; Crabtree, R. H. *J. Mol. Catal. A* **1996**, *108*, 35-40. (e) For a related Pd-catalyzed iodination system, see: Giri, R.; Chen, X.; Yu, J.-Q. *Angew. Chem., Int. Ed.* **2005**, *44*, 2112-2115.

[26] The catalyst was generated in situ by heating $(CH_3CN)_2PdCl_2$ and all other reagents except the substrate for 15 min before addition of the substrate.

[27] (a) Thorarensen, A.; Palmgren, A.; Itami, K.; Bäckvall, J.-E. *Tetrahedron Lett.* **1997**, *38*, 8541-8544. (b) Itami, K.; Palmgren, A.; Thorarensen, A.; Bäckvall, J.-E. *J. Org. Chem.* **1998**, *38*, 6466-6471. (c) Cotton, H. K.; Verboom, R. C.; Johansson, K.; Plietker, B. J.; Bäckvall, J.-E. *Organometallics* **2002**, *21*, 3367-3375.

[28] (a) Sohn, J.-H.; Waizumi, N.; Zhong, H. M.; Rawal, V. H. *J. Am. Chem. Soc.* **2005**, *127*, 7290-7291. (b) Garg, N. K.; Caspi, D. D.; Stoltz, B. M. *J. Am. Chem. Soc.* **2005**, *127*, 5970-5978. (c) Tietze, L. F.; Sommer, K. M.; Zinngrebe, J.; Stecker, F. *Angew. Chem., Int. Ed.* **2004**, *44*, 257-259.

[29] Pilli, R. A.; de Andrade, C. K. Z.; Souto, C. R. O.; de Meijere, A. *J. Org. Chem.* **1998**, *63*, 7811-7819.

[30] Munakata, R.; Ueki, T.; Katakai, H.; Takau, K.; Tadano, K.-i. *Org. Lett.* **2002**, *3*, 3029-3033.

[31] Halter, R. J.; Fimmen, R. L.; McMahon, R. J.; Peebles, S. A.; Kuczkowski, R. L.; Stanton, J. F. *J. Am. Chem. Soc.* **2001**, *123*, 12353-12363.

[32] Zweifel, G.; Polston, N. L. *J. Am. Chem. Soc.* **1970**, *92*, 4068-4071.

[33] Raucher, S.; Lawrence, R. F. *Tetrahedron Lett.* **1983**, *24*, 2927-2930.

[34] Curran, D. P; Martin-Esker, A. A.; Ko, S. B.; Newcomb, M. *J. Org. Chem.* **1993**, *58*, 4691-4695.

[35] Miller, C. A.; Batey, R. A. *Org. Lett.* **2004**, *6*, 699-702.

[36] Bhamare, N. K.; Granger, T.; John, C. R.; Yates, P. *Tetrahedron Lett.* **1991**, *32*, 4439-4442.

[37] Yates, P.; Macas, T. S. *Can. J. Chem.* **1988**, *66*, 1-10.

APPENDIX 3.1

Spectra Relevant to Chapter 3

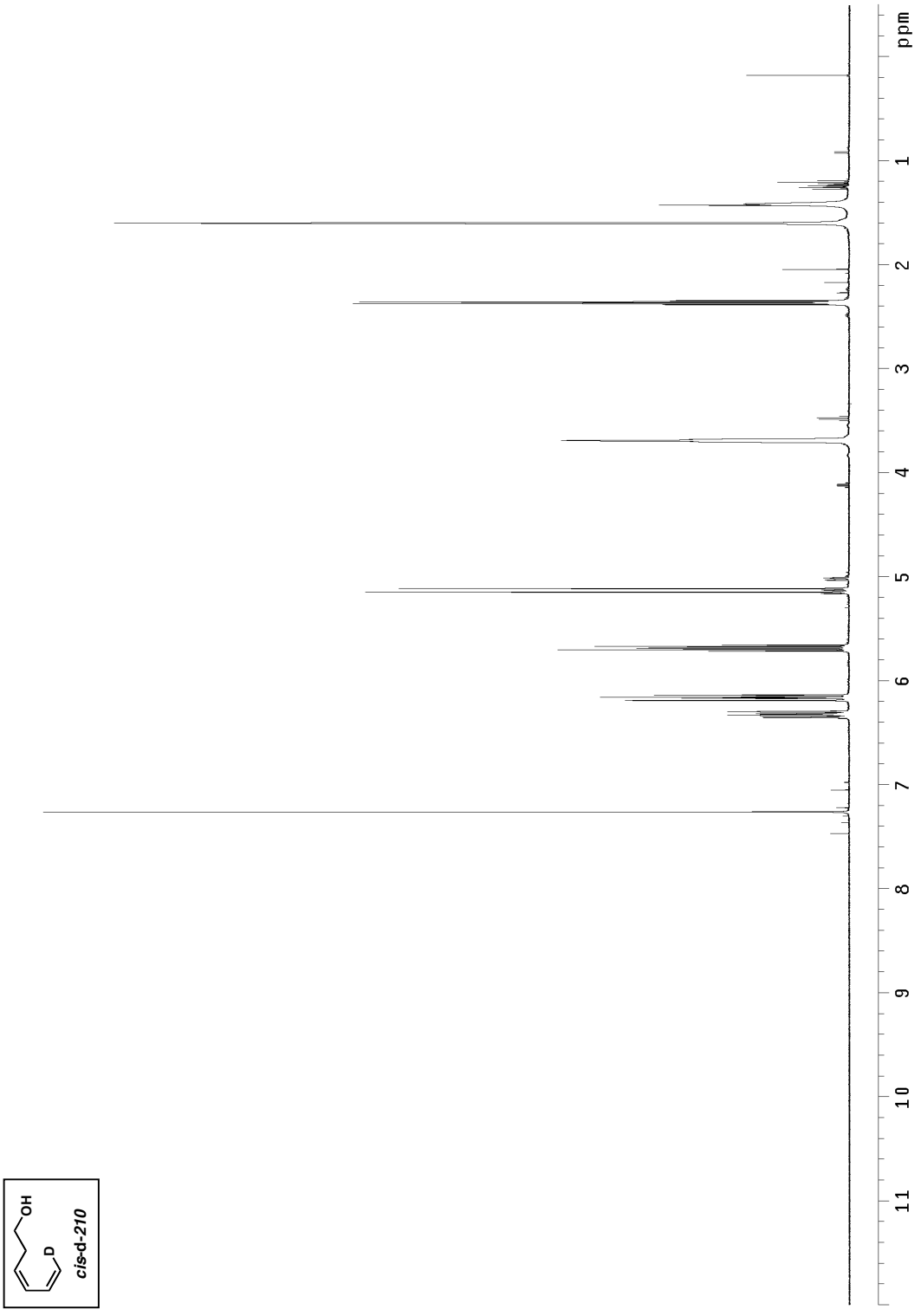

Figure A3.1.1 ^{1}H NMR spectrum (500 MHz, $CDCl_3$) of ***cis-d-210***.

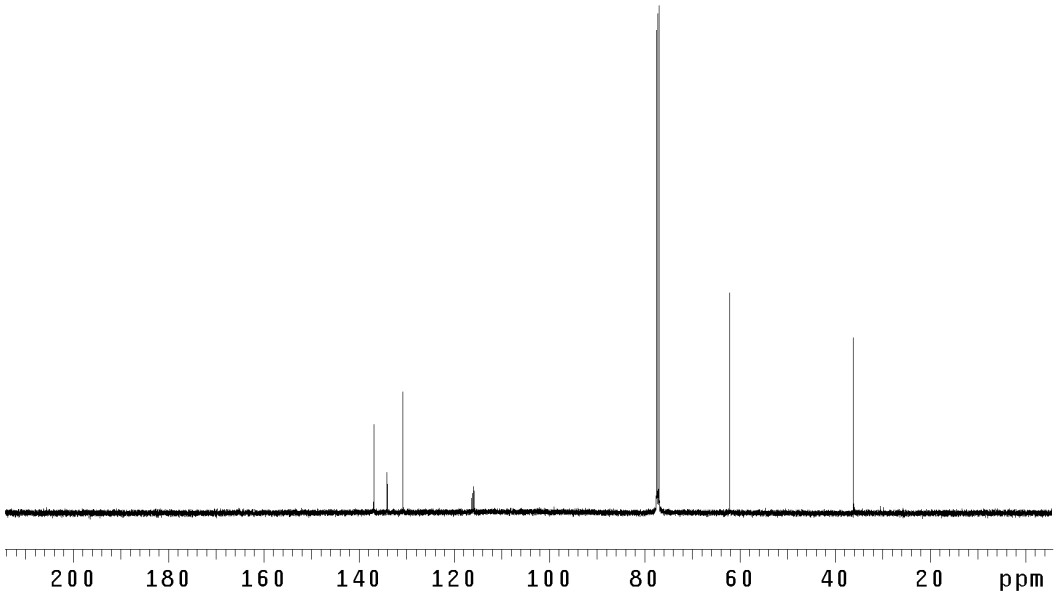

Figure A3.1.2 ^{13}C NMR spectrum (125 MHz, $CDCl_3$) of ***cis-d-210****.*

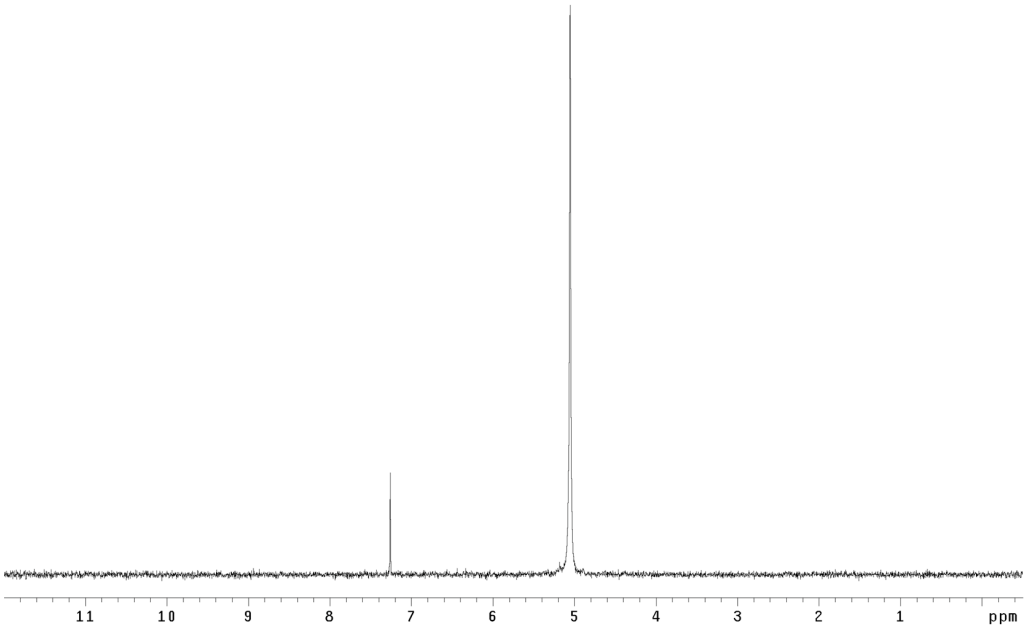

Figure A3.1.3 ^{2}H NMR spectrum (76 MHz, $CHCl_3$) of ***cis-d-210****.*

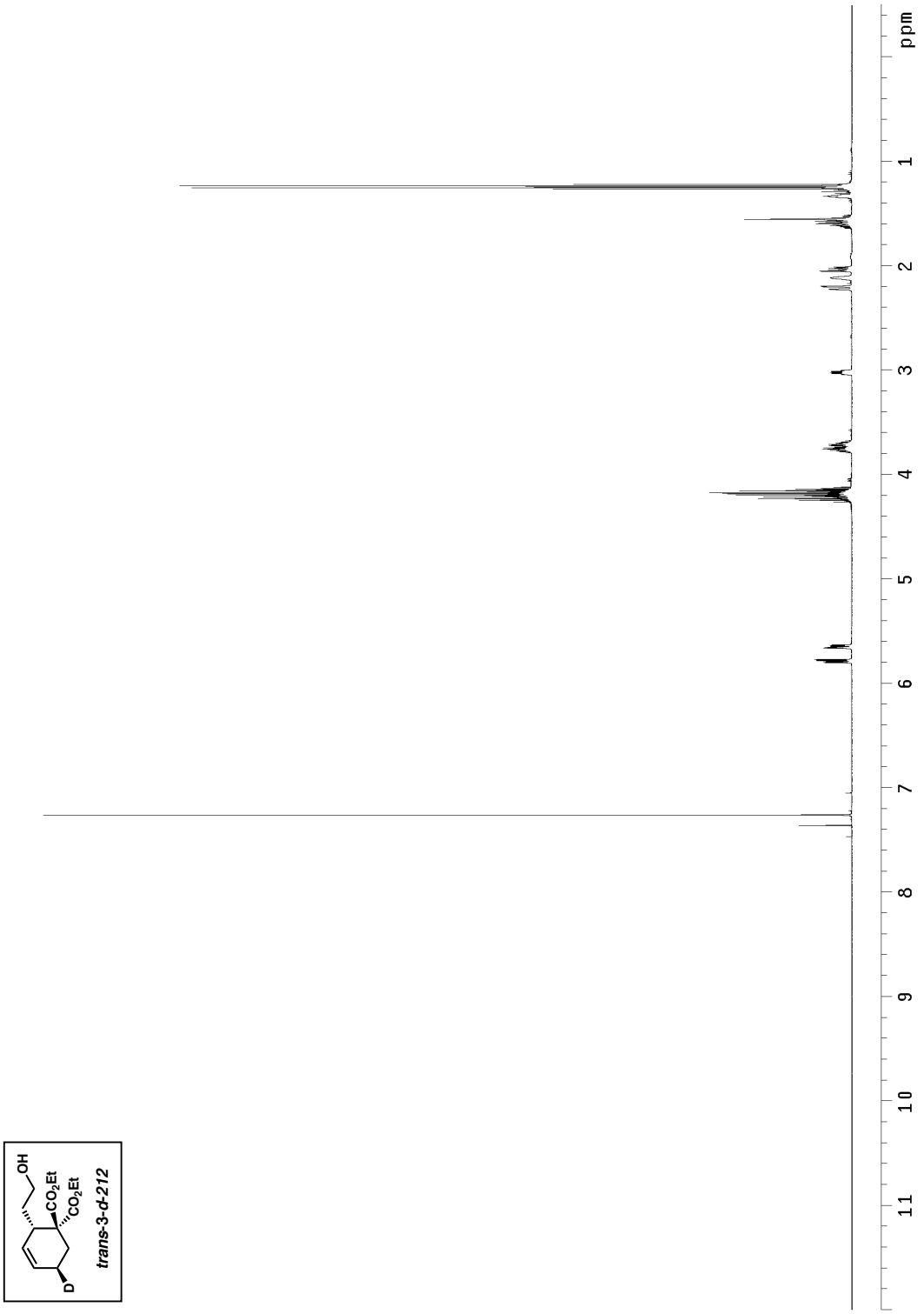

Figure A3.1.4 ^{1}H NMR spectrum (500 MHz, $CDCl_3$) of ***trans*-3-*d*-212**.

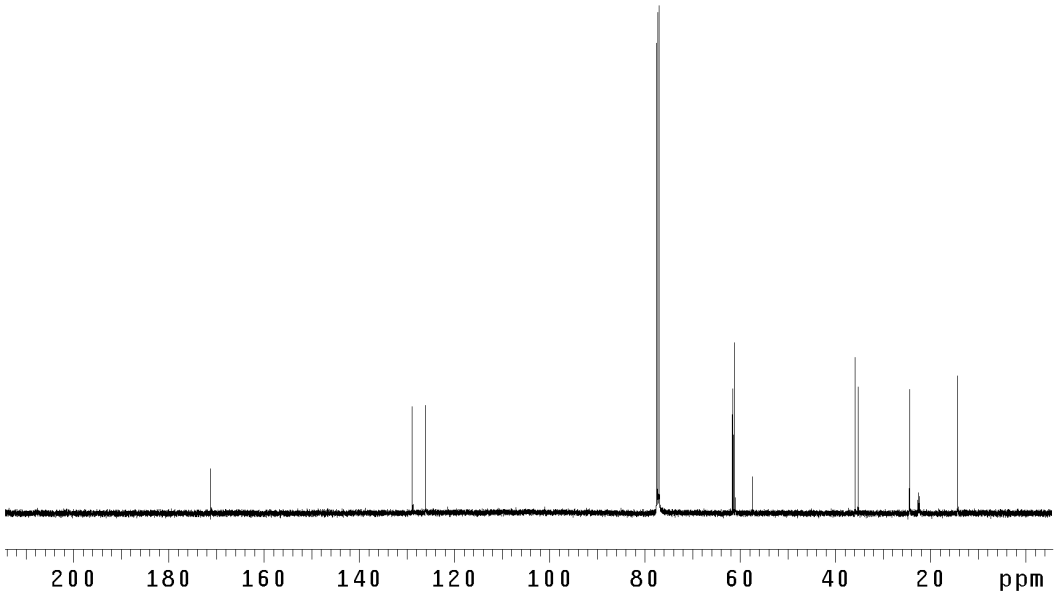

Figure A3.1.5 ^{13}C NMR spectrum (125 MHz, $CDCl_3$) of ***trans*-3-*d*-212**.

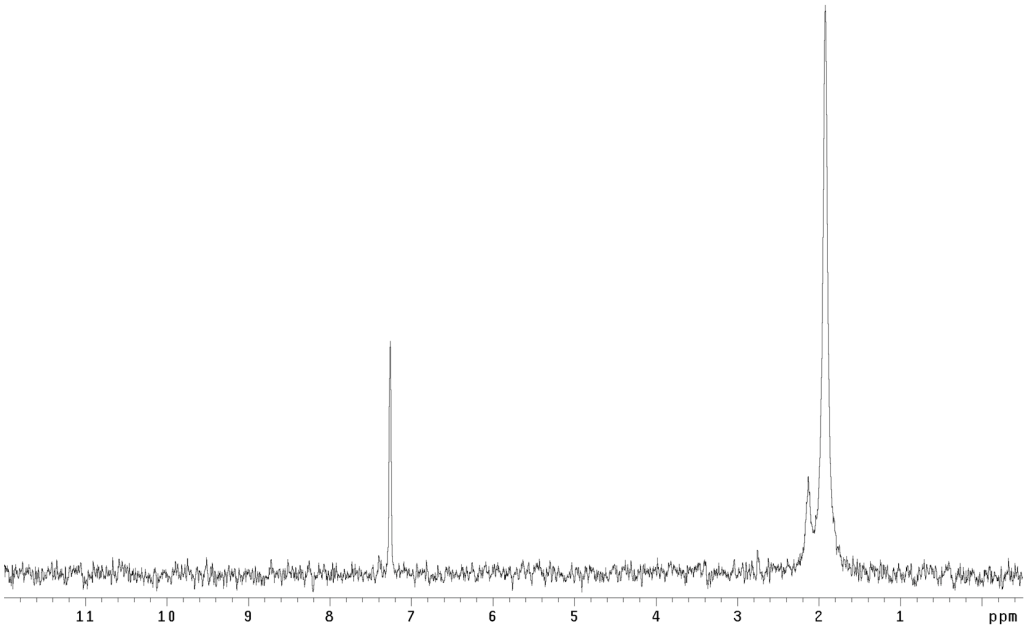

Figure A3.1.6 ^{2}H NMR spectrum (76 MHz, $CHCl_3$) of ***trans*-3-*d*-212**.

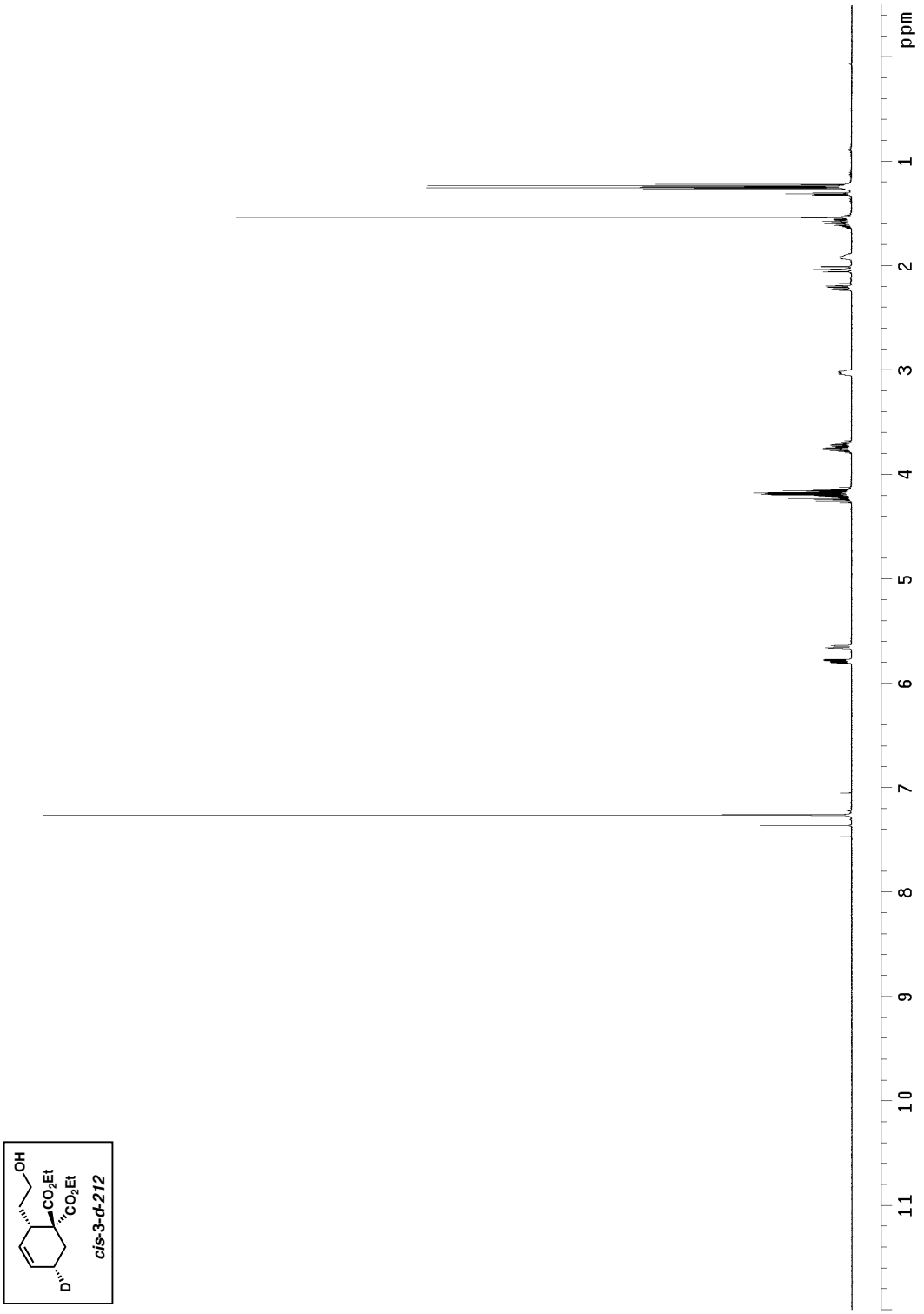

Figure A3.1.7 ^{1}H *NMR spectrum (500 MHz,* $CDCl_3$*) of* ***cis*-3-*d*-212**.

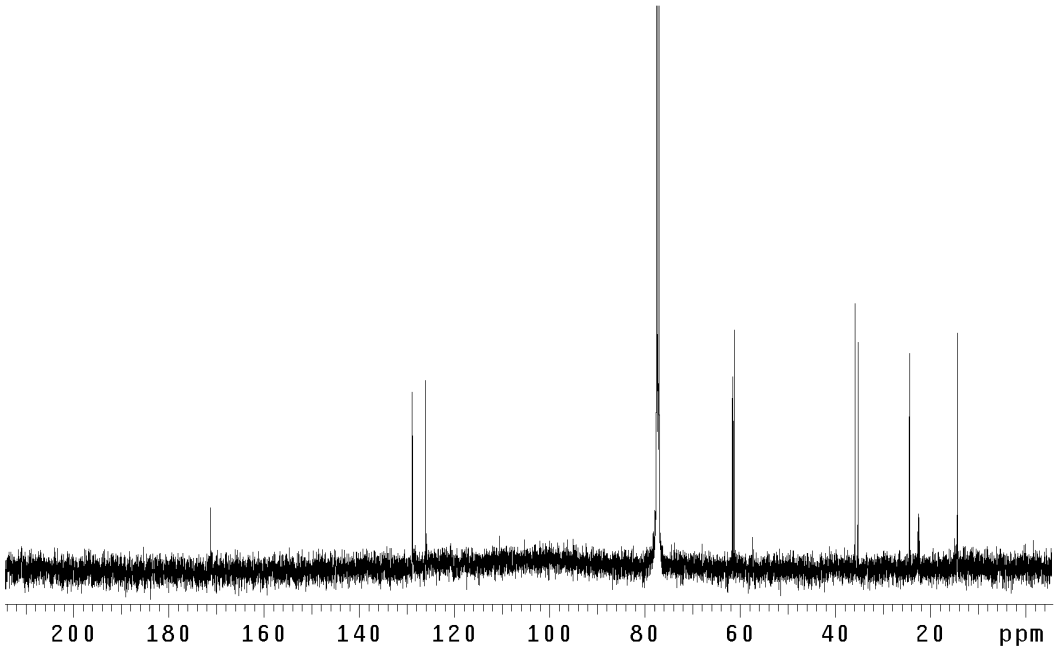

Figure A3.1.8 ^{13}C *NMR spectrum (125 MHz,* $CDCl_3$*) of* ***cis*-3-*d*-212**.

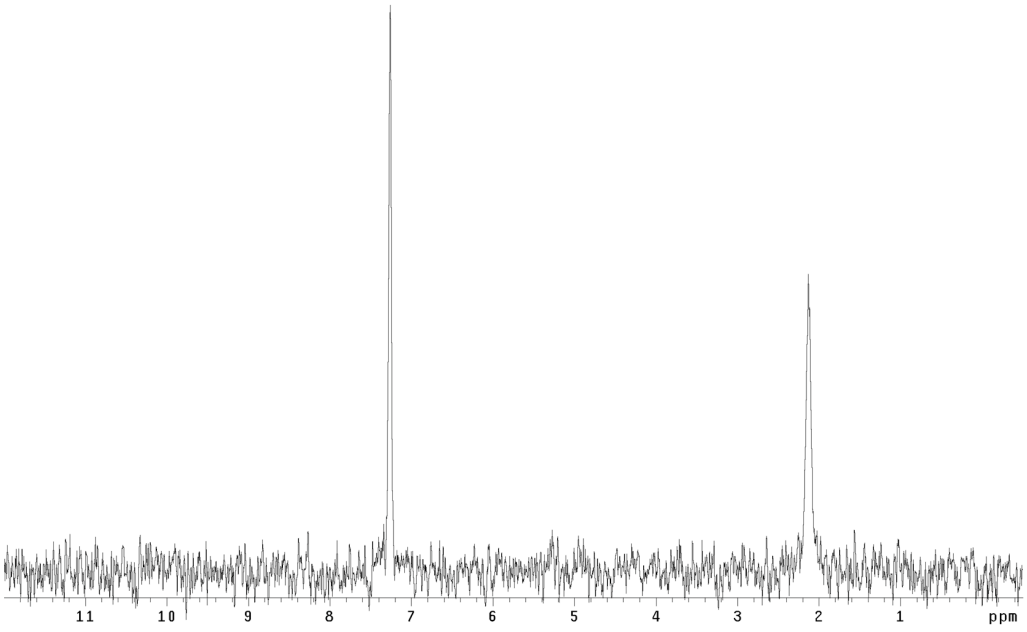

Figure A3.1.9 ^{2}H *NMR spectrum (76 MHz,* $CHCl_3$*of* ***cis*-3-*d*-212**.

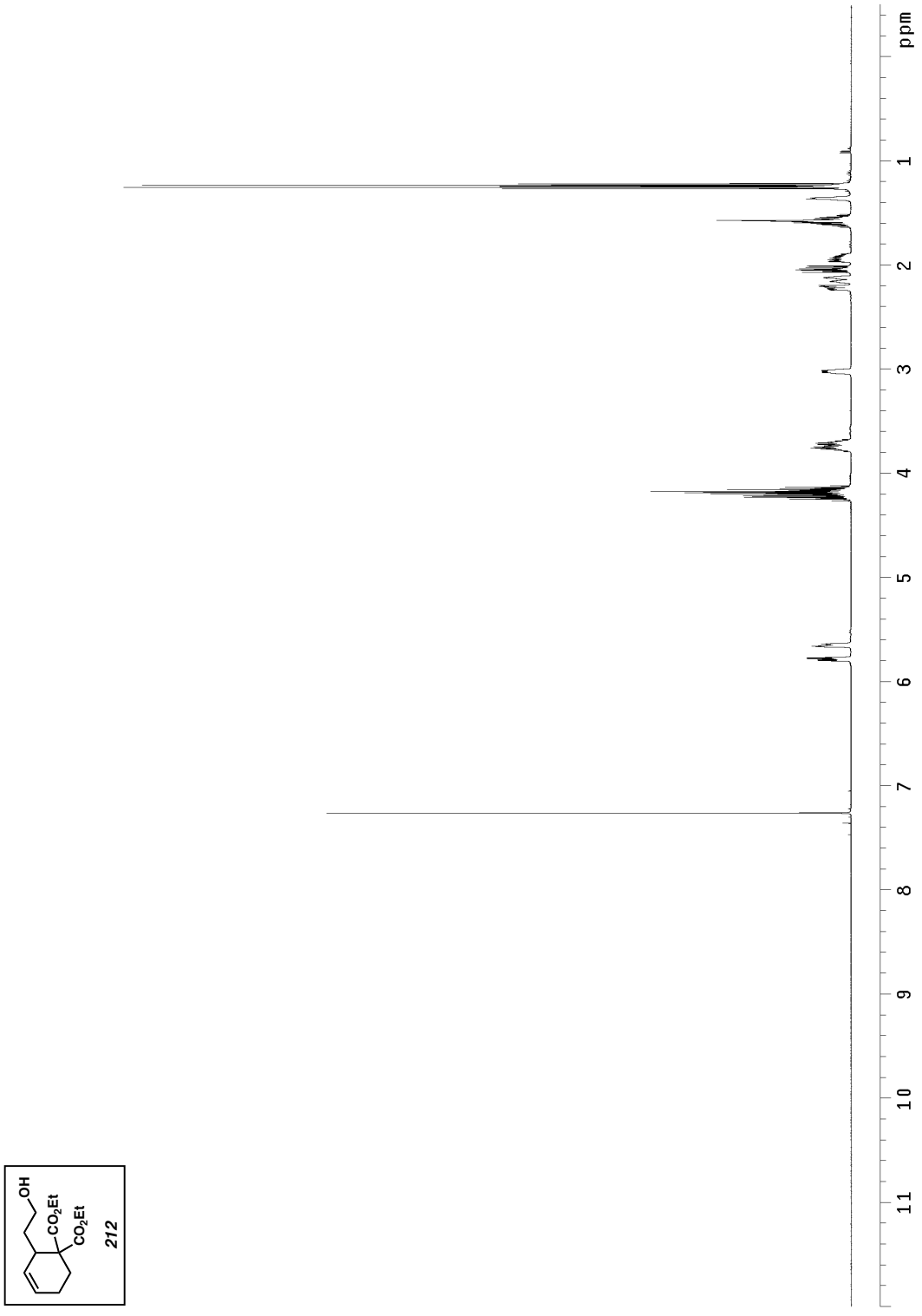

*Figure A3.1.10 ^{1}H NMR spectrum (500 MHz, $CDCl_3$) of **212**.*

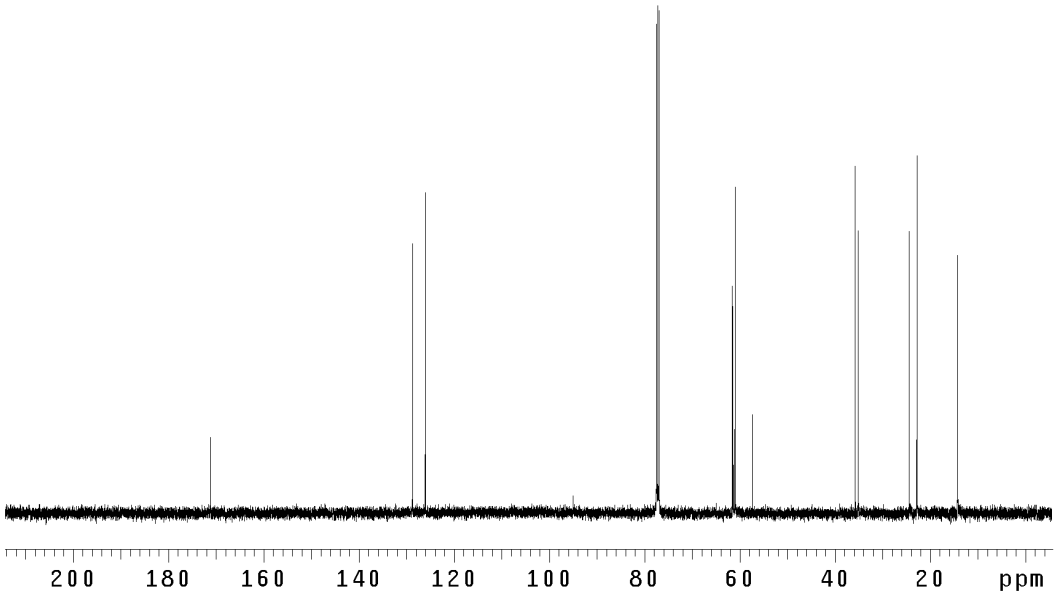

*Figure A3.1.11 ^{13}C NMR spectrum (125 MHz, $CDCl_3$) of **212**.*

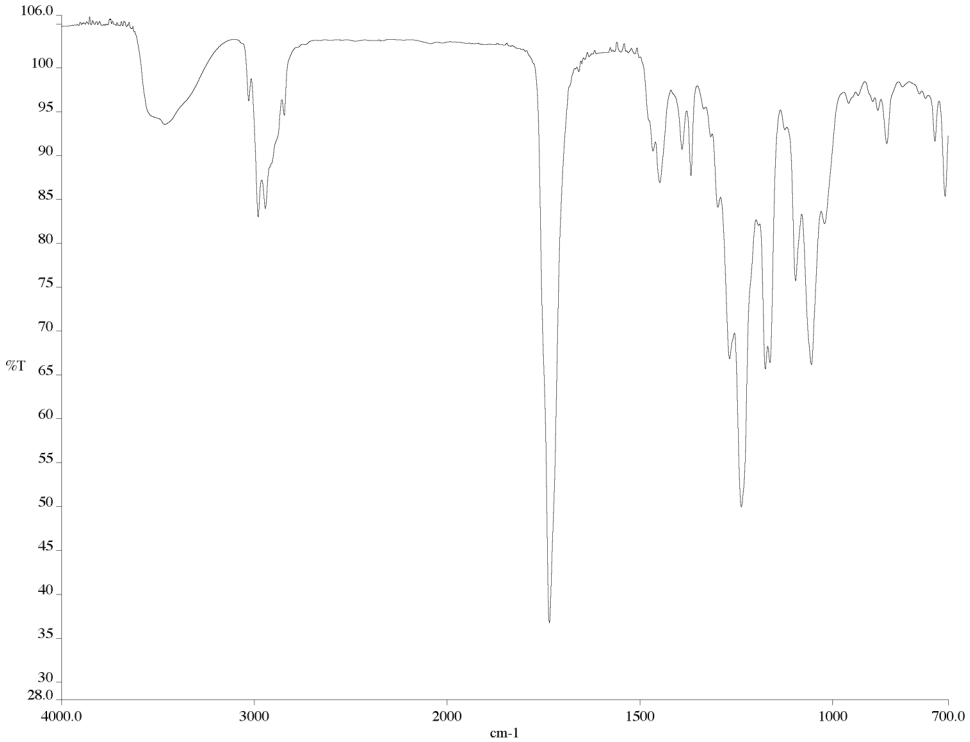

*Figure A3.1.12 IR spectrum (thin film/NaCl)) of **212**.*

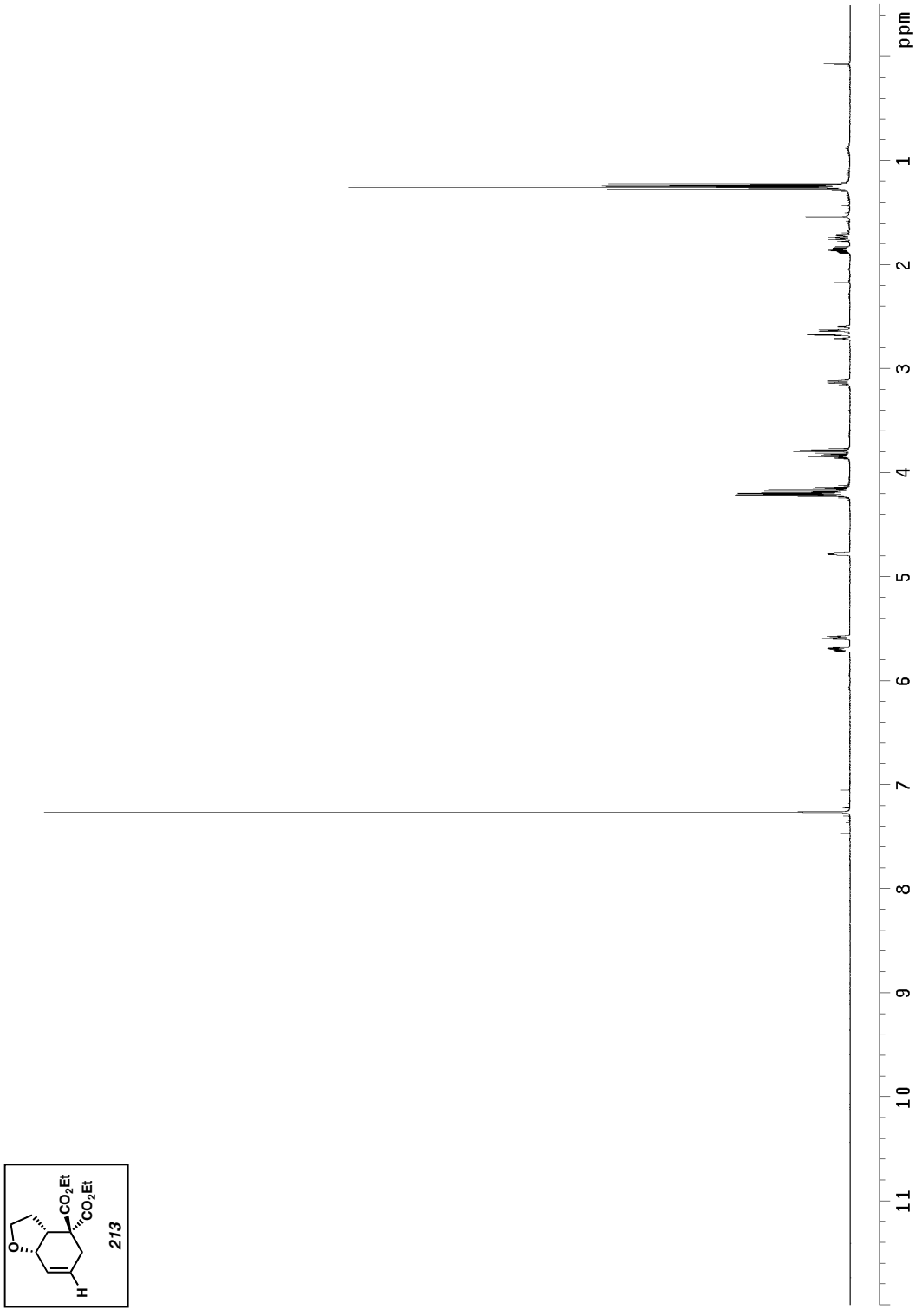

*Figure A3.1.13 ^{1}H NMR spectrum (500 MHz, $CDCl_3$) of **213**.*

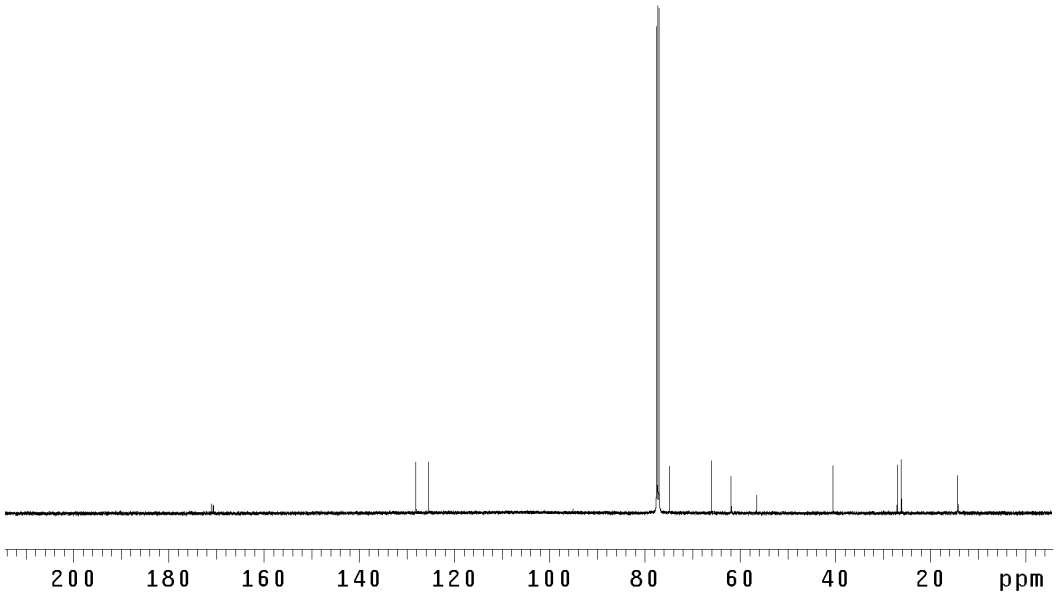

*Figure A3.1.14 ^{13}C NMR spectrum (125 MHz, $CDCl_3$) of **213**.*

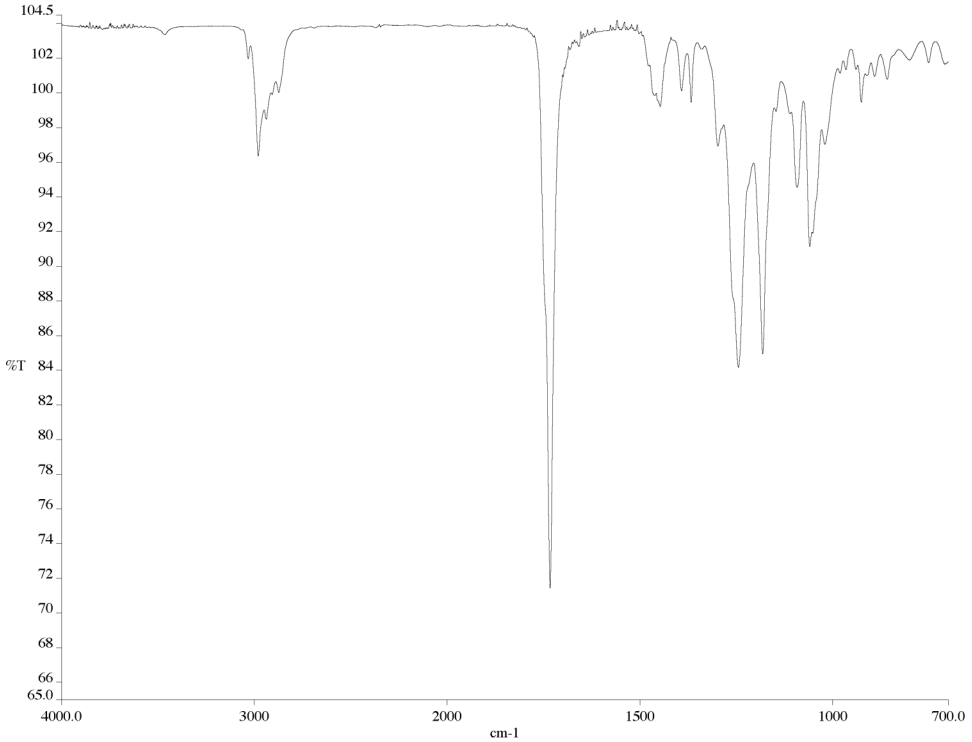

*Figure A3.1.15 IR spectrum (thin film/NaCl)) of **213**.*

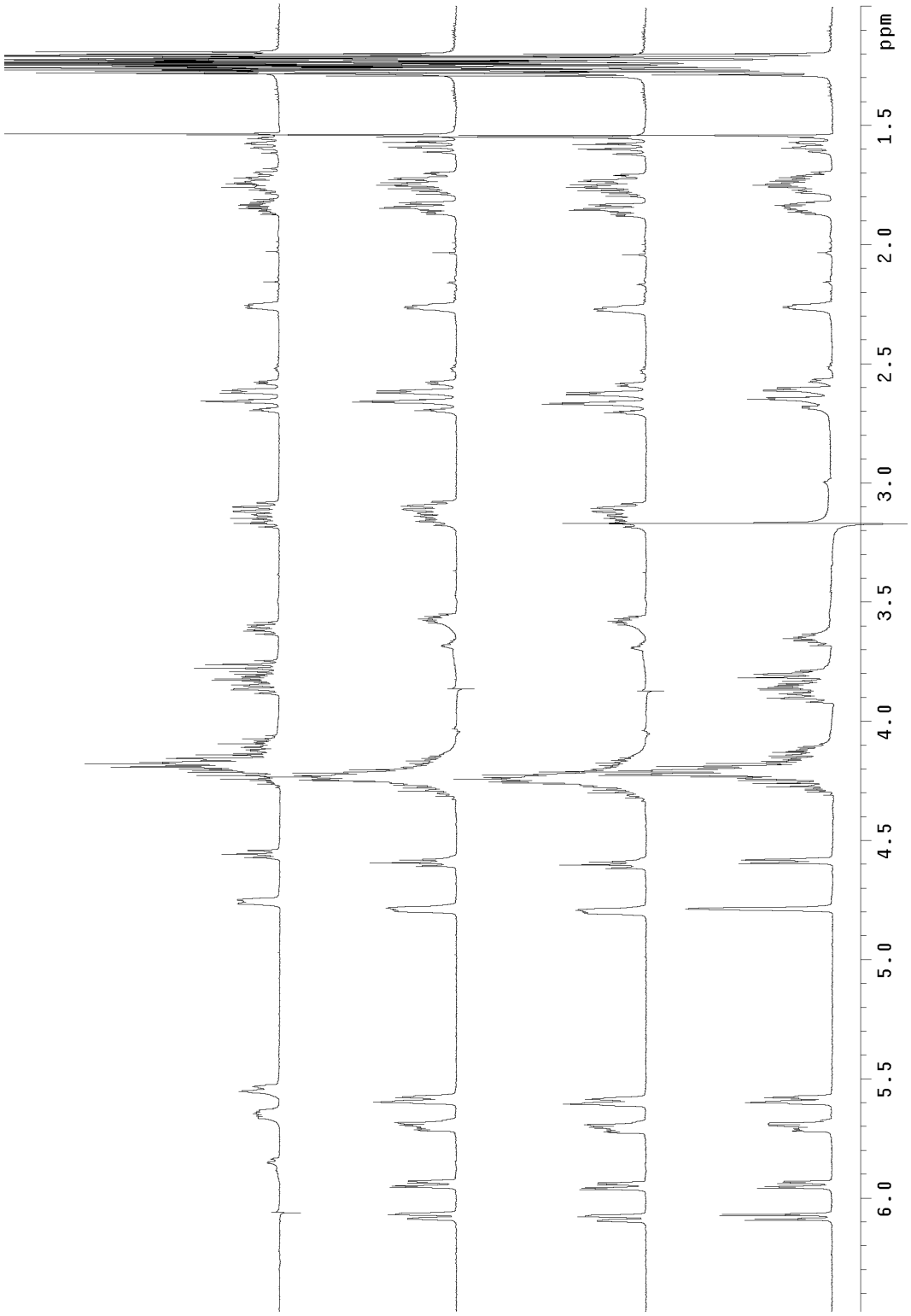

*Figure A3.1.16 ^{1}H NMR spectrum (500 MHz, $CDCl_3$) of **cis-2-d-214**, homodecoupling at 3.17, 3.87, 5.94, and 6.1 ppm (from bottom to top).*

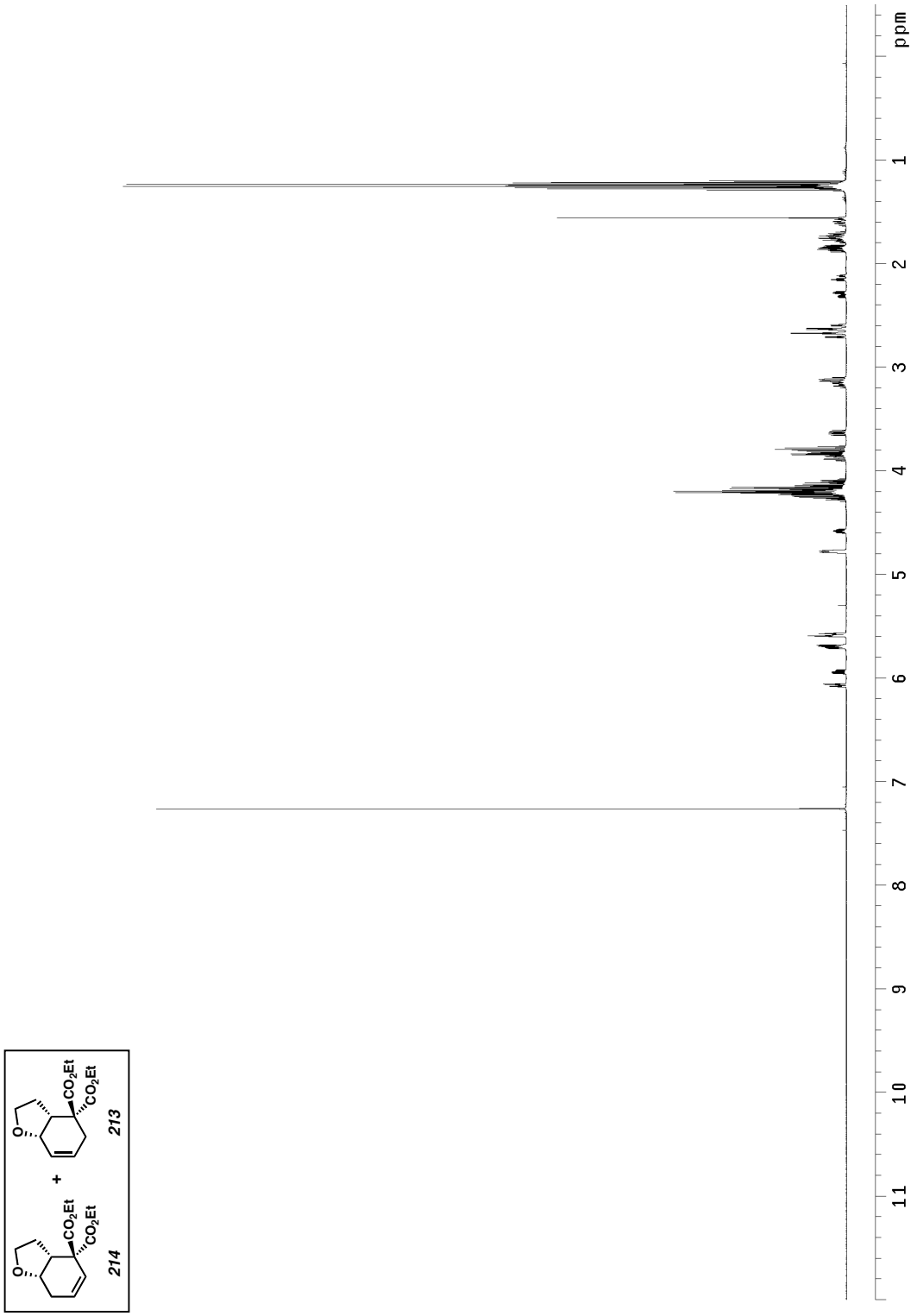

*Figure A3.1.17 ^{1}H NMR spectrum (500 MHz, $CDCl_3$) of **214**, the minor component is **213**.*

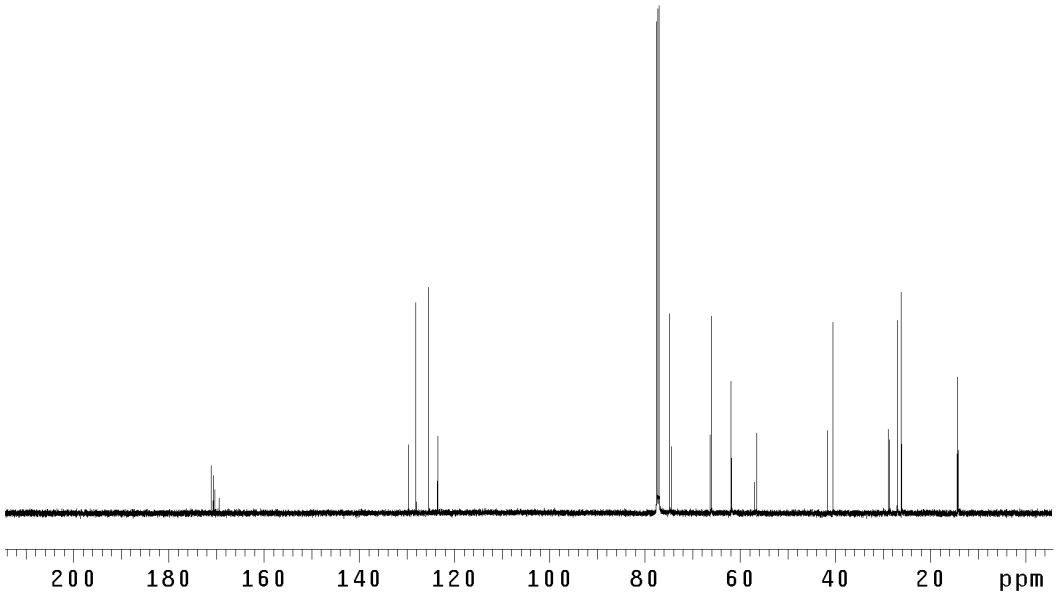

*Figure A3.1.18 ^{13}C NMR spectrum (125 MHz, $CDCl_3$) of **214**, the minor component is **213**.*

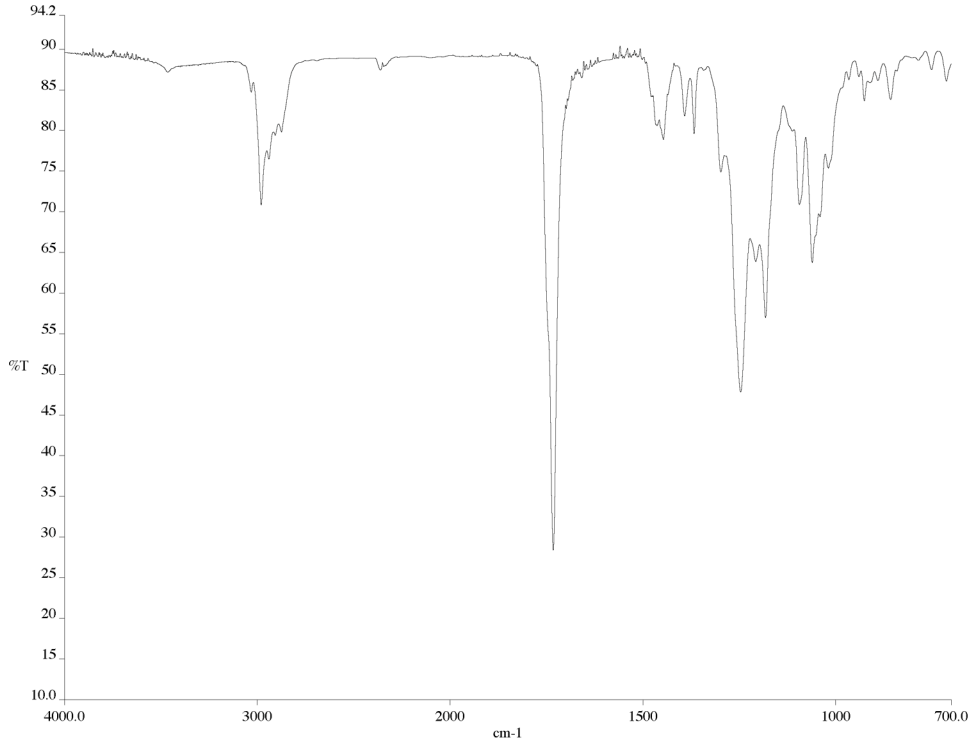

*Figure A3.1.19 IR spectrum (thin film/NaCl)) of **214** in a mixture with **213**.*

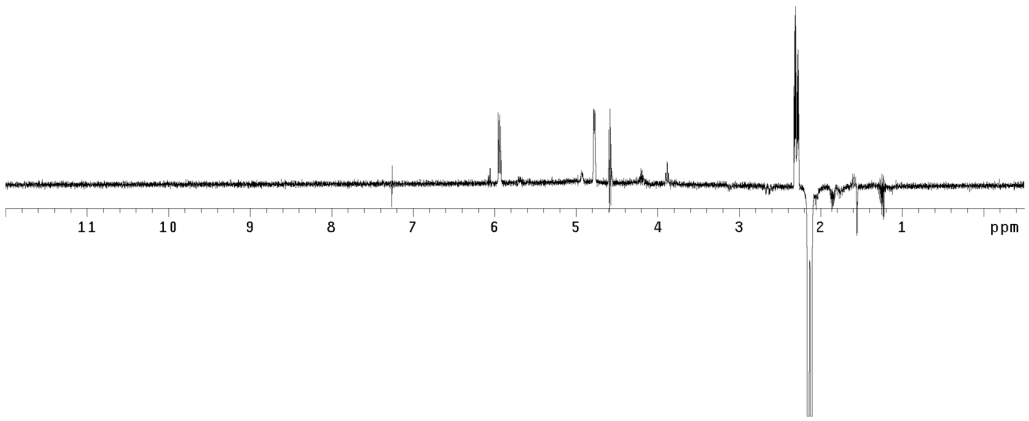

*Figure A3.1.20 ^{1}H NMR spectrum (500 MHz, $CDCl_3$) of **214** in a mixture with **213**. CycleNOE experiment with irradiation at 2.14 ppm.*

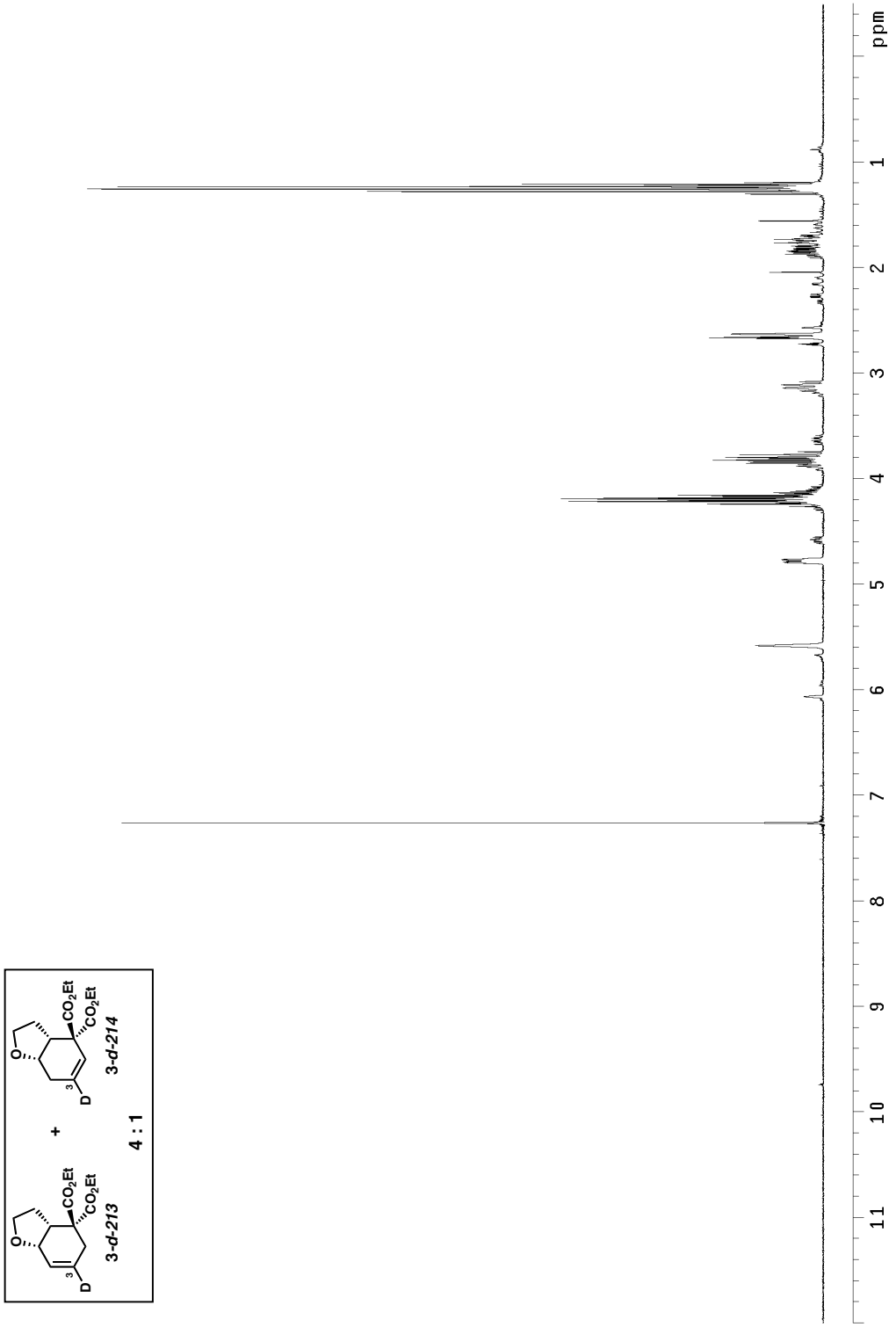

*Figure A3.1.21 ^{1}H NMR spectrum (300 MHz, $CDCl_3$) of **3-d-213** and **3-d-214**.*

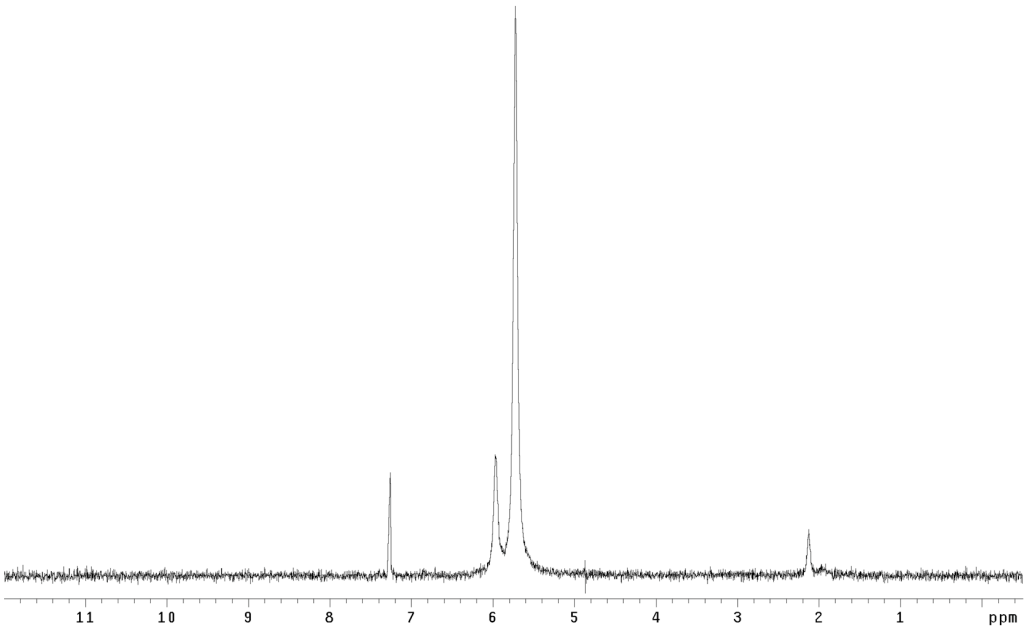

*Figure A3.1.22 ^{2}H NMR spectrum (76 MHz, $CHCl_3$) of **3-d-213** and **3-d-214**.*

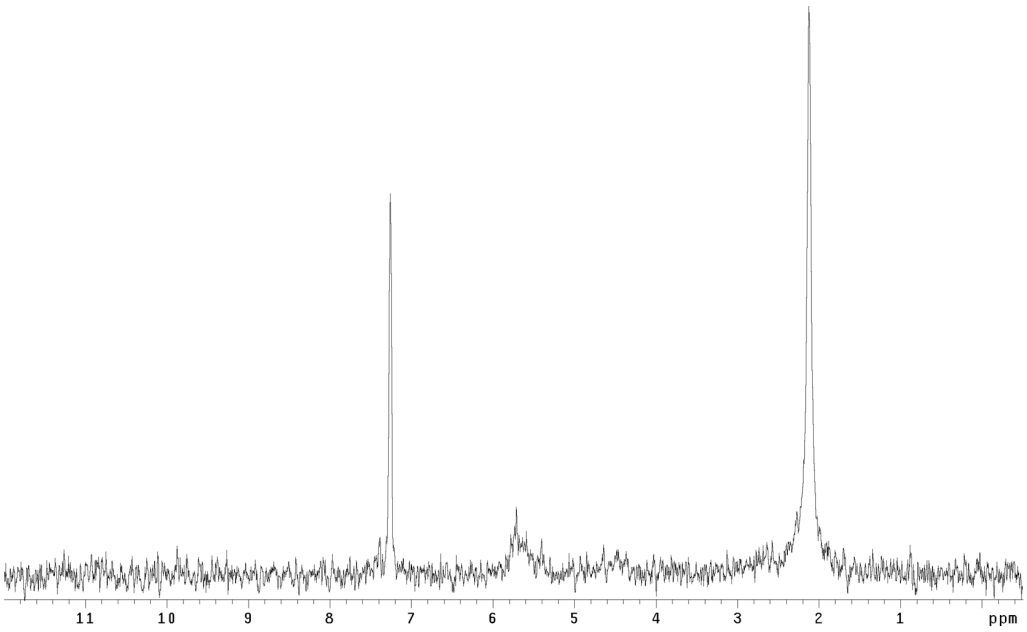

*Figure A3.1.23 ^{2}H NMR spectrum (76 MHz, $CHCl_3$) of **213** and **cis-2-d-214**.*

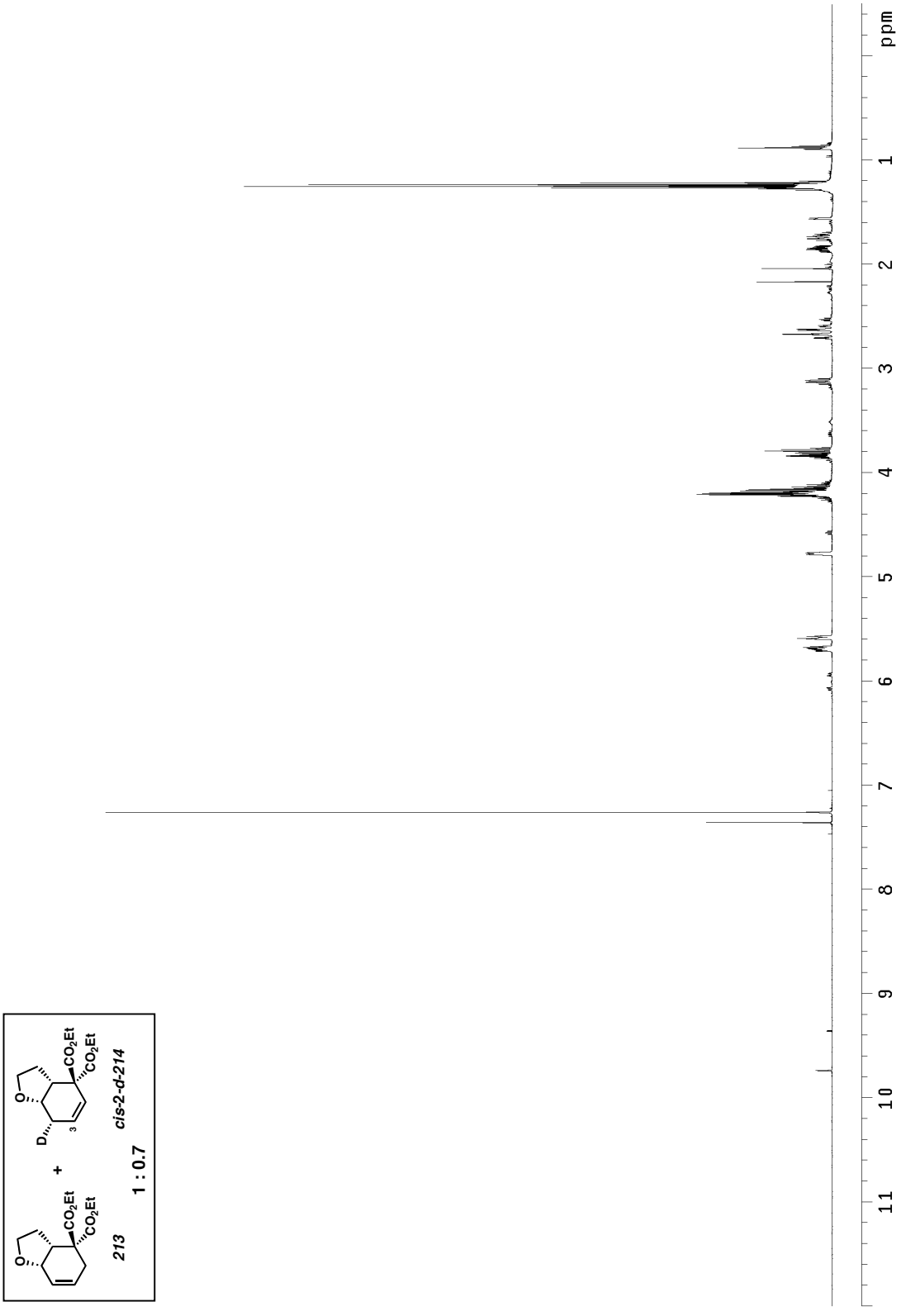

*Figure A3.1.24 ^{1}H NMR spectrum (500 MHz, $CDCl_3$) of **213** and **cis-2-d-214**.*

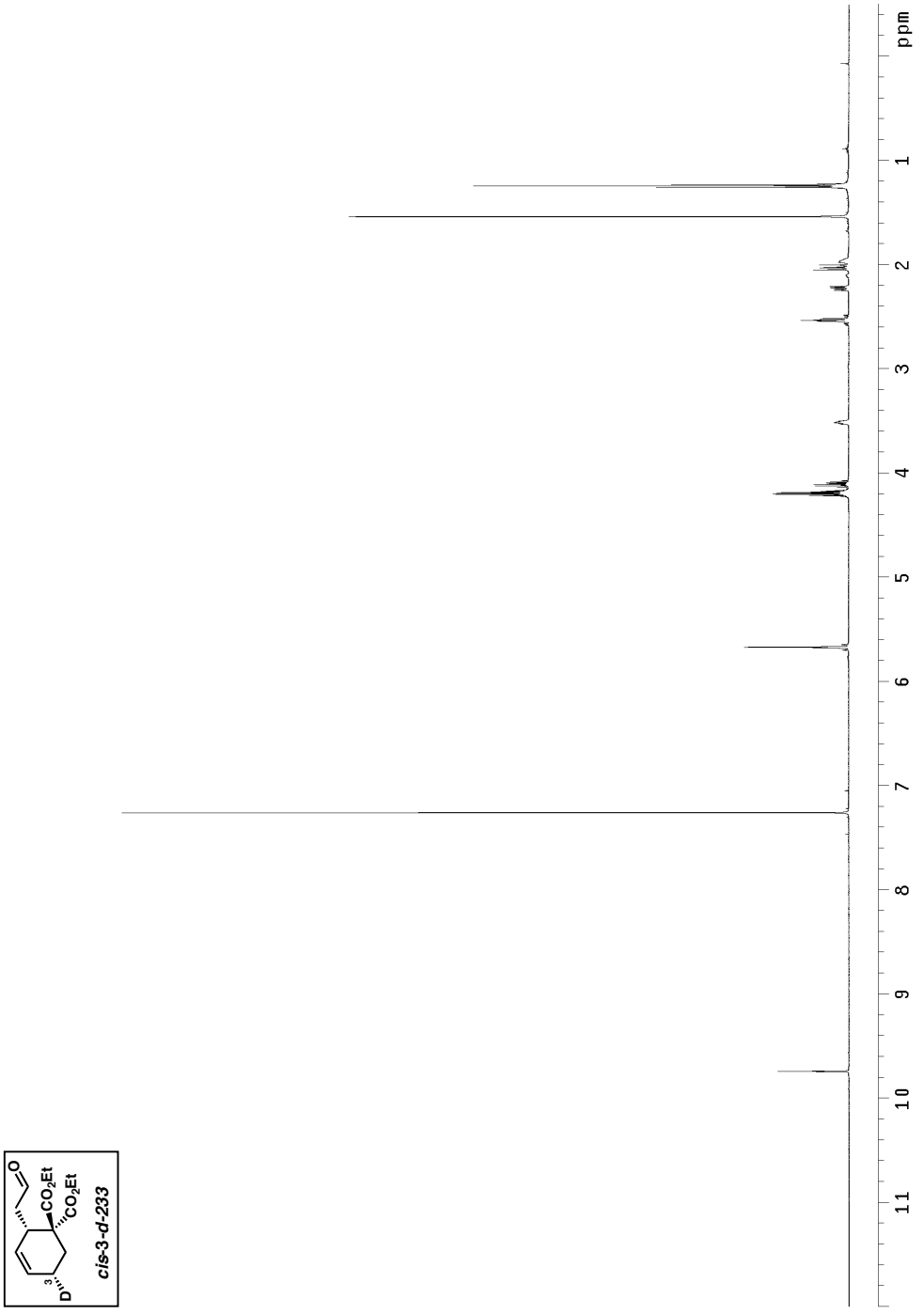

*Figure A3.1.25 ^{1}H NMR spectrum (500 MHz, $CDCl_3$) of **cis-3-d-233**.*

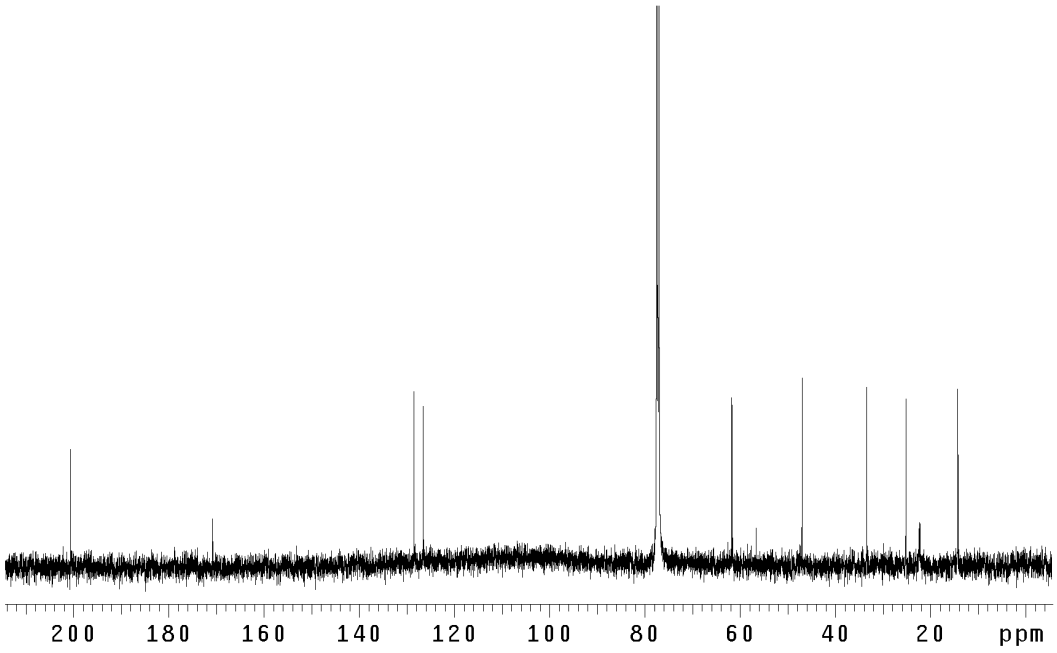

Figure A3.1.26 ^{13}C NMR spectrum (125 MHz, $CDCl_3$) of ***cis-3-d-233***.

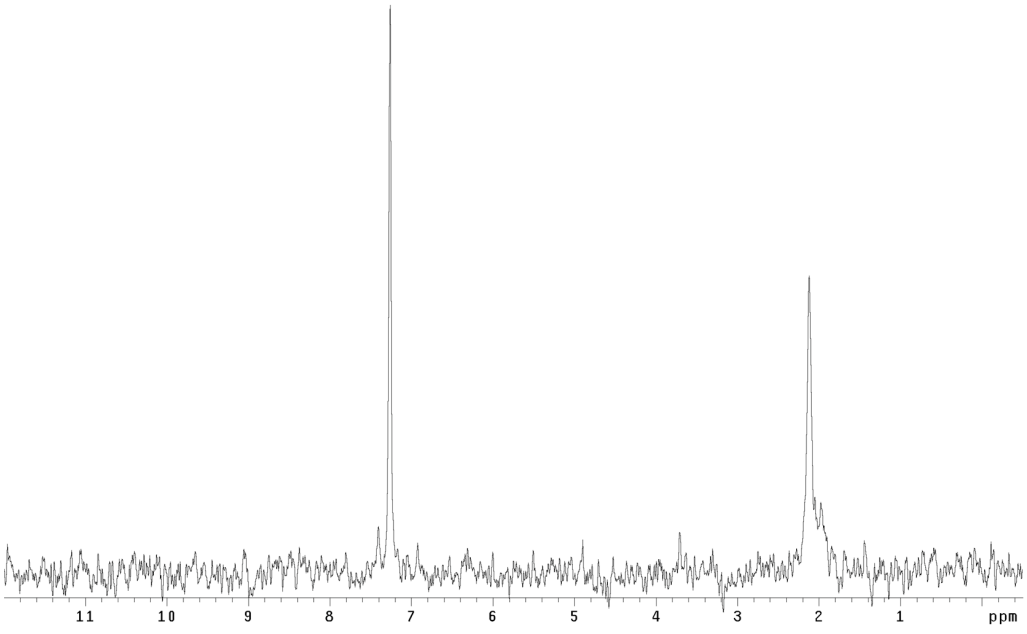

Figure A3.1.27 ^{2}H NMR spectrum (76 MHz, $CHCl_3$) of ***cis-3-d-233***.

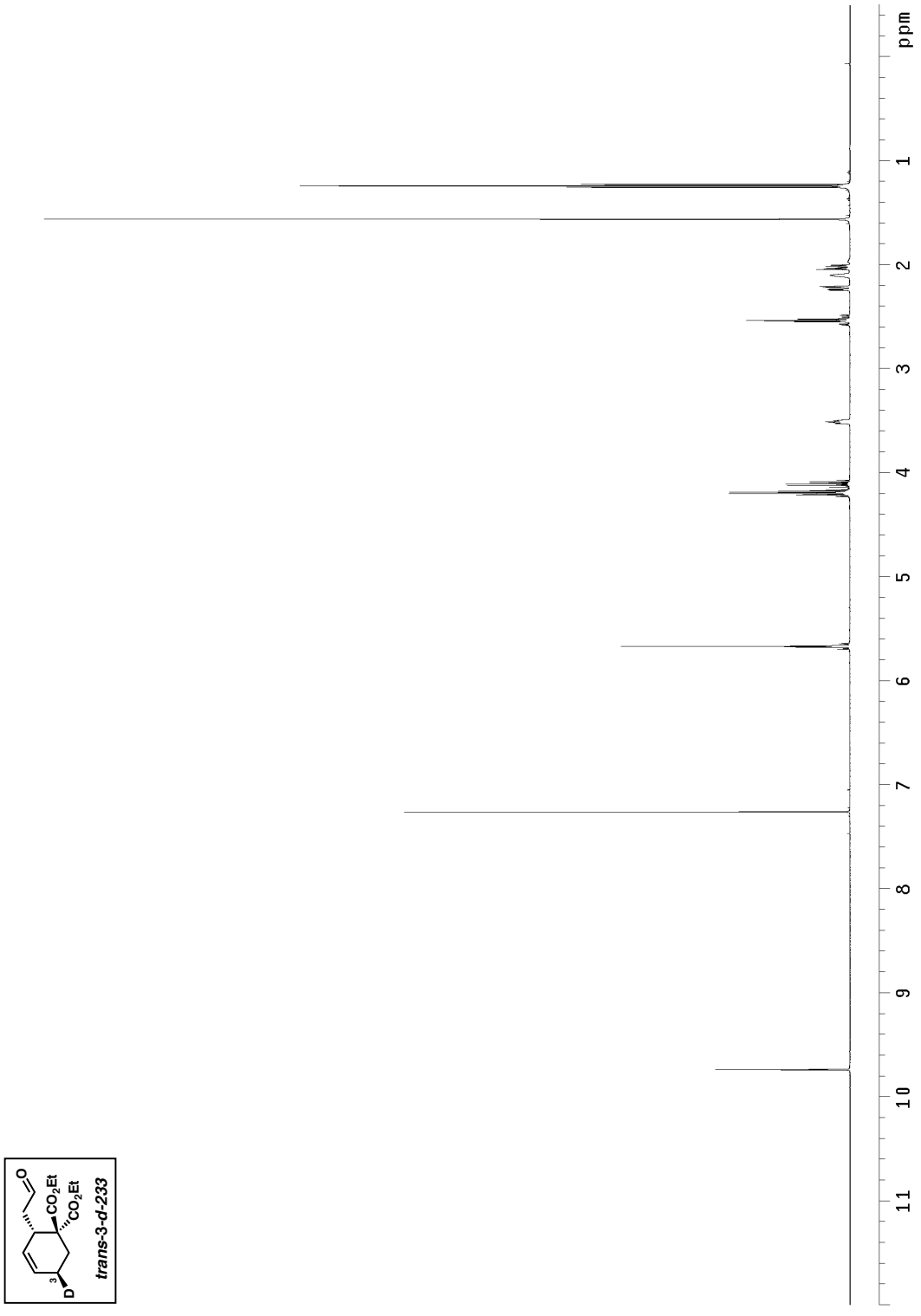

Figure A3.1.28 ^{1}H NMR spectrum (500 MHz, $CDCl_3$) of ***trans-3-d-233***.

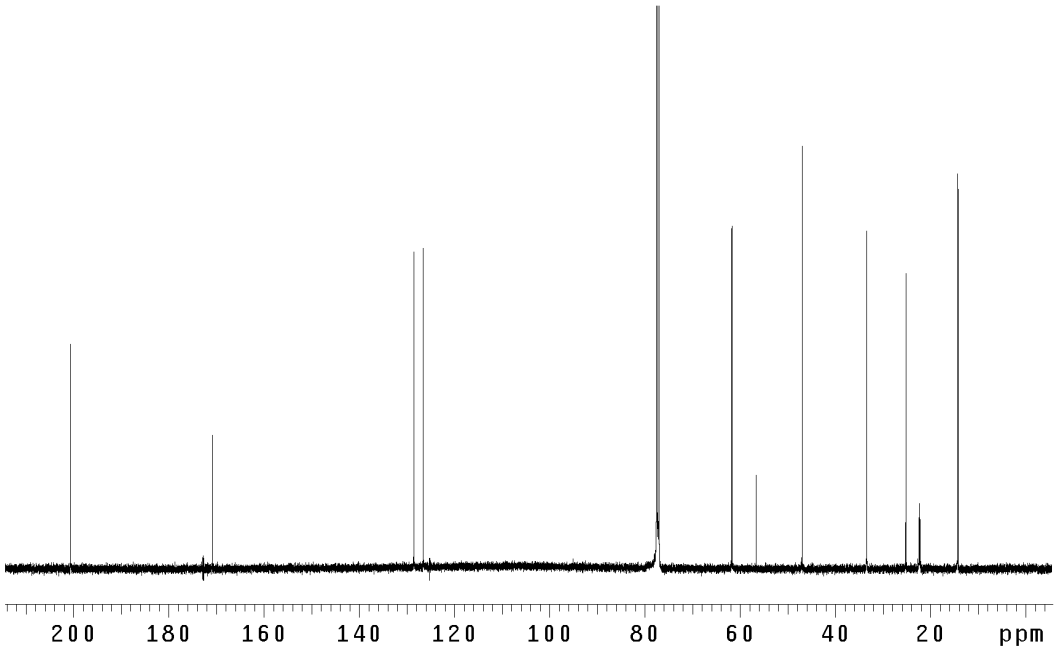

Figure A3.1.29 ^{13}C NMR spectrum (125 MHz, $CDCl_3$) of ***trans-3-d-233***.

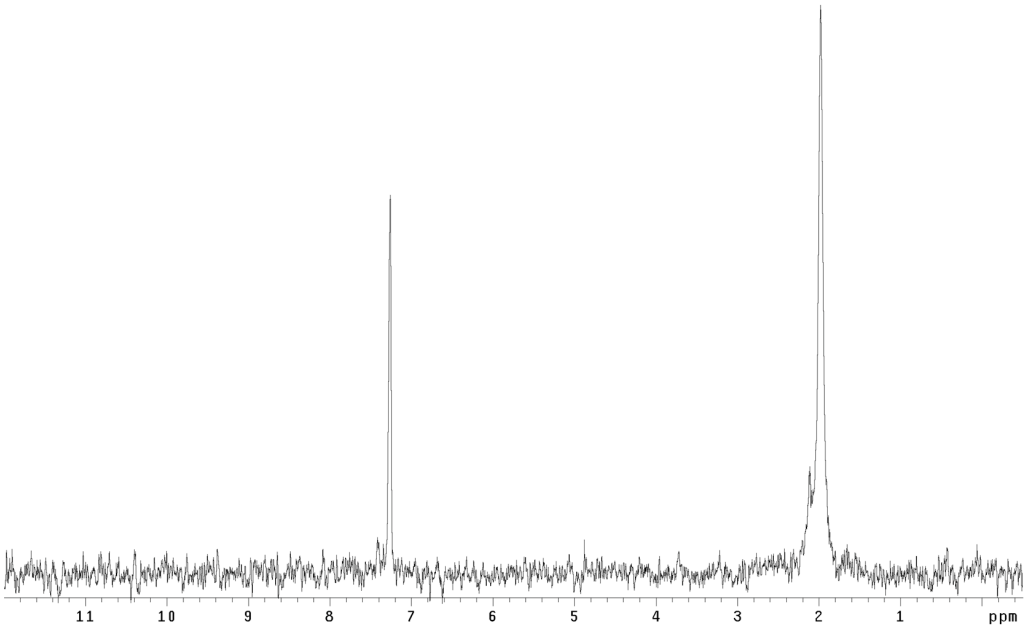

Figure A3.1.30 ^{2}H NMR spectrum (76 MHz, $CHCl_3$) of ***trans-3-d-233***.

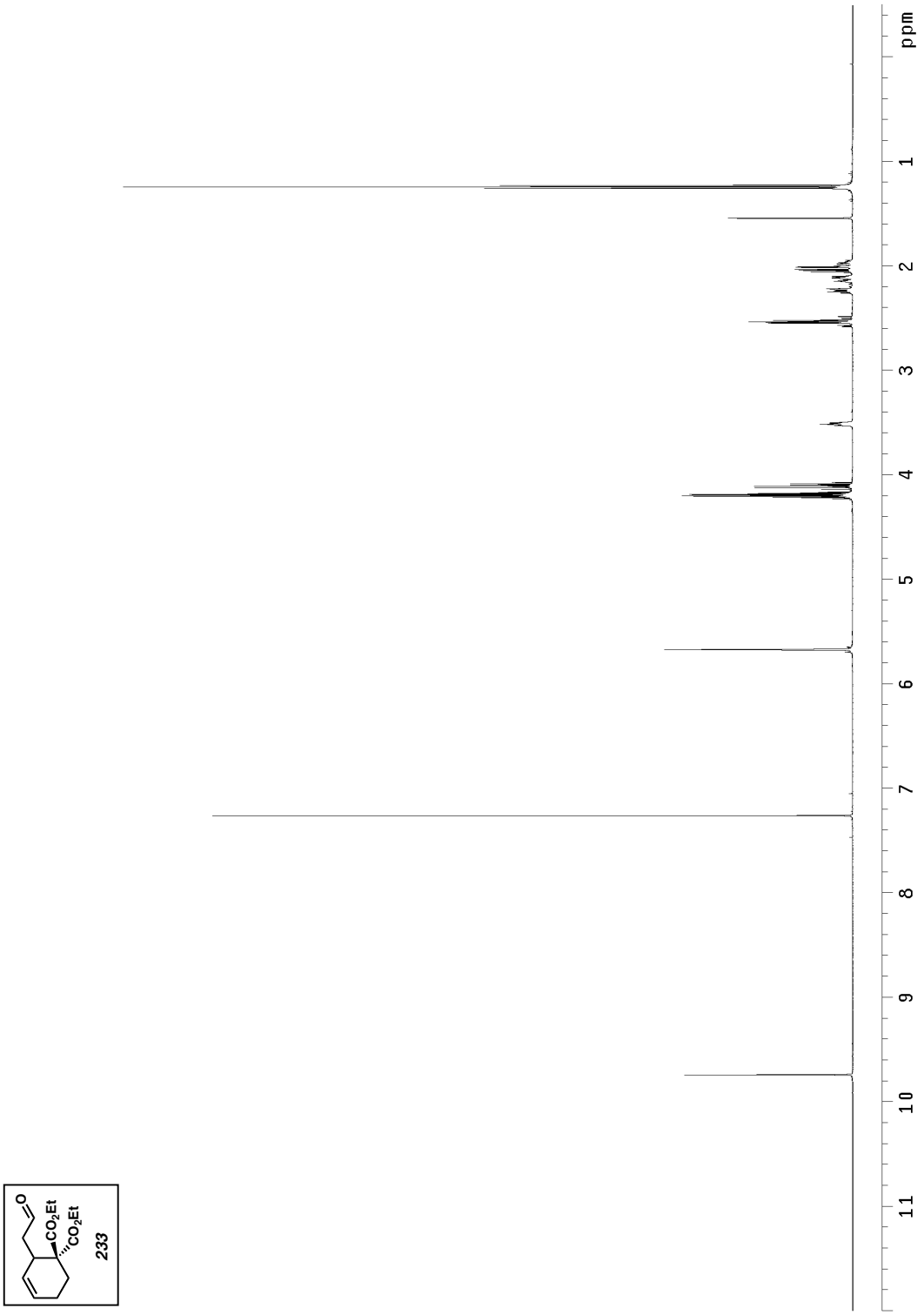

*Figure A3.1.31 ^{1}H NMR spectrum (500 MHz, $CDCl_3$) of **233**.*

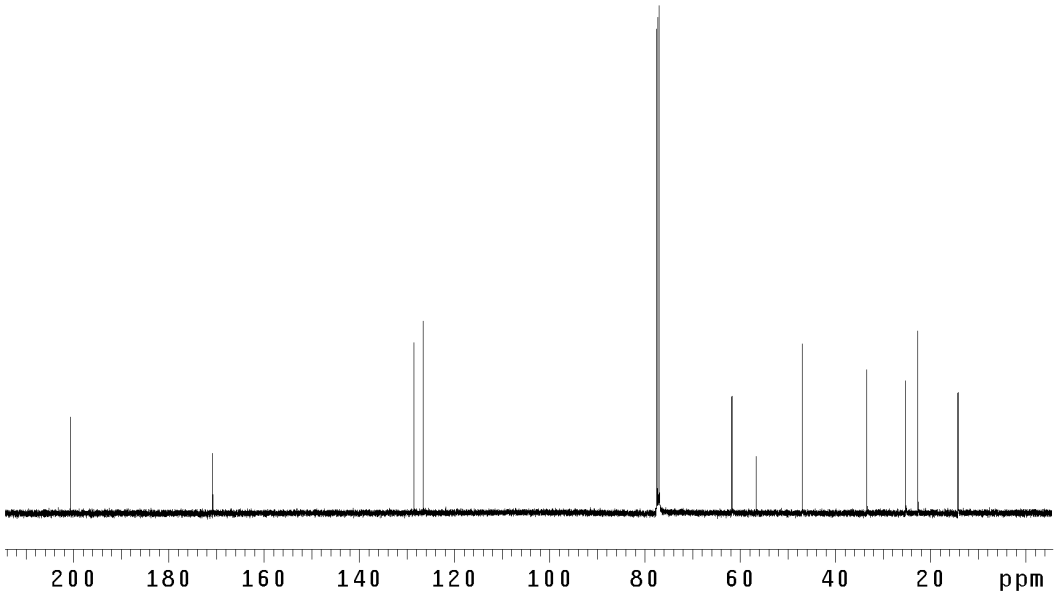

*Figure A3.1.32 ^{13}C NMR spectrum (125 MHz, $CDCl_3$) of **233**.*

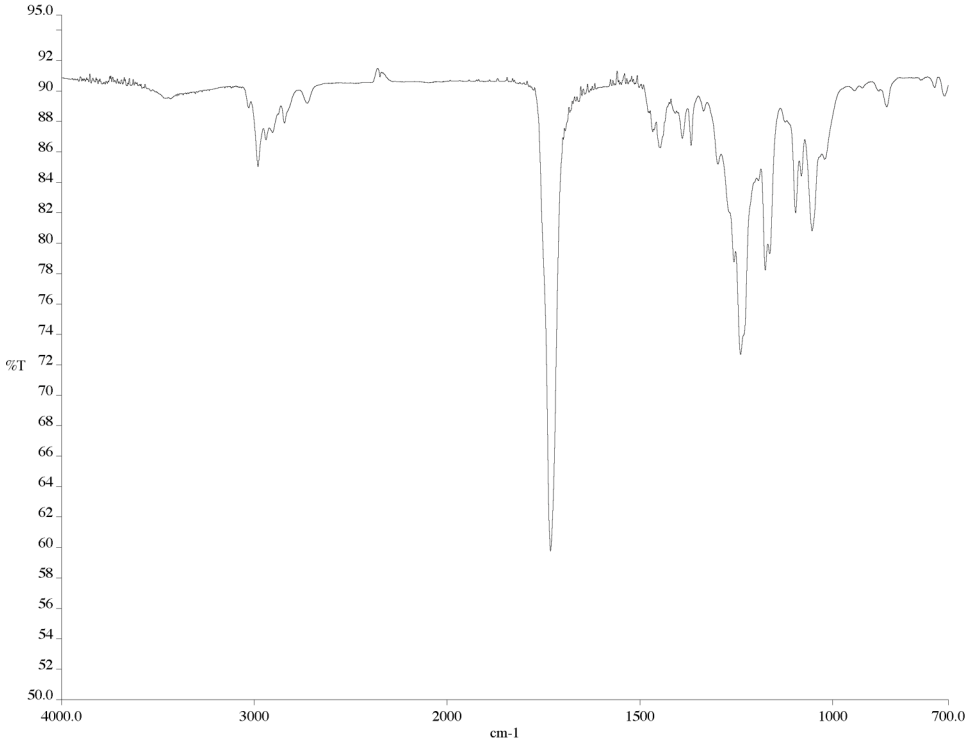

*Figure A3.1.33 IR spectrum (thin film/NaCl)) of **233**.*

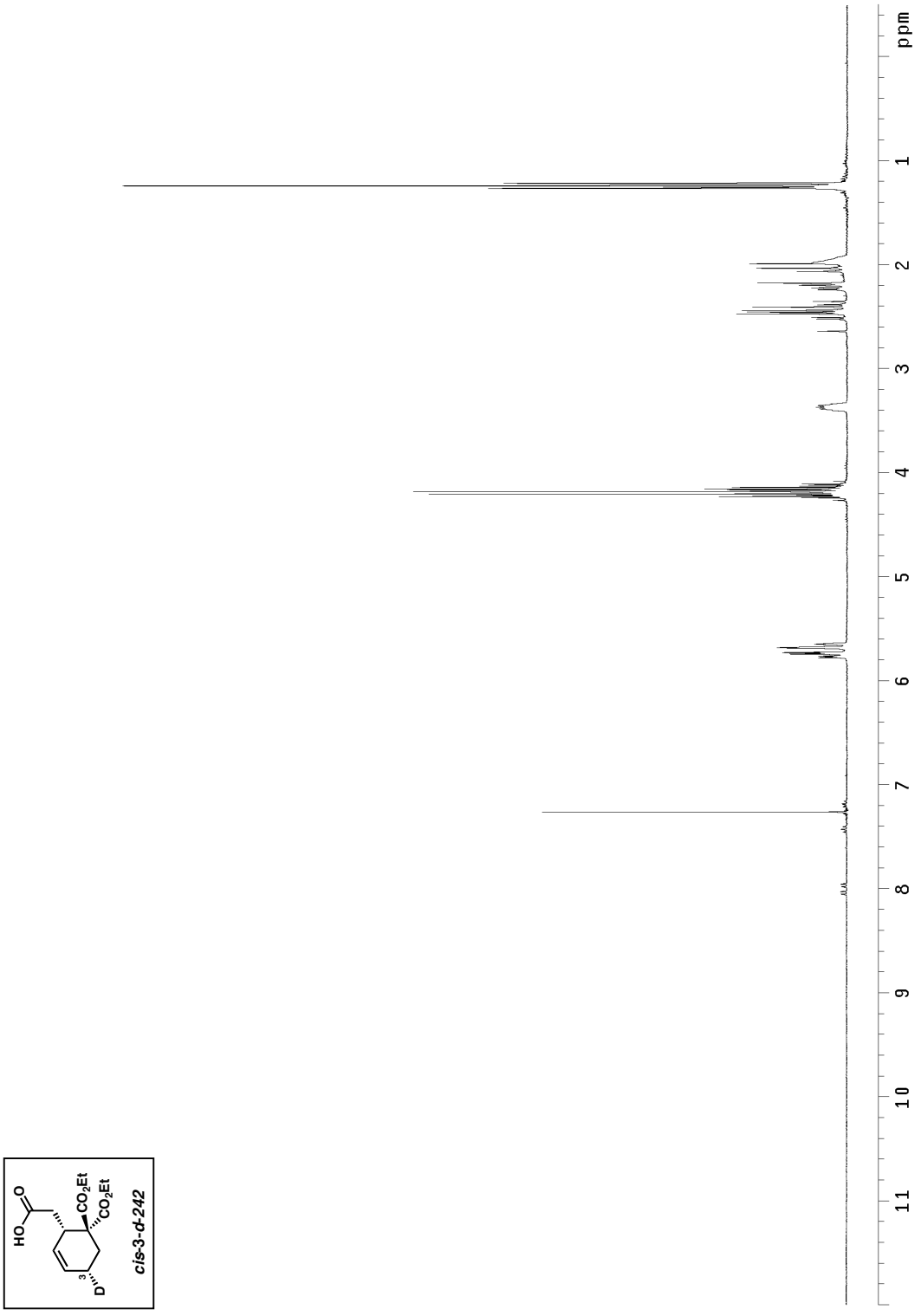

Figure A3.1.34 ^{1}H NMR spectrum (500 MHz, $CDCl_3$) of ***cis-3-d-242****.*

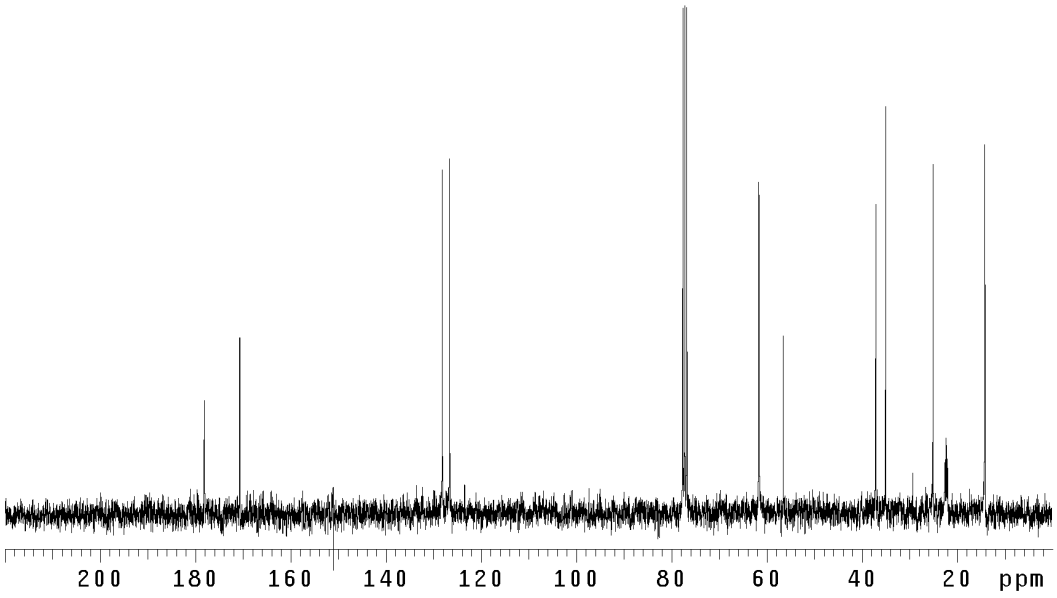

Figure A3.1.35 ^{13}C NMR spectrum (125 MHz, $CDCl_3$) of ***cis-3-d-242***.

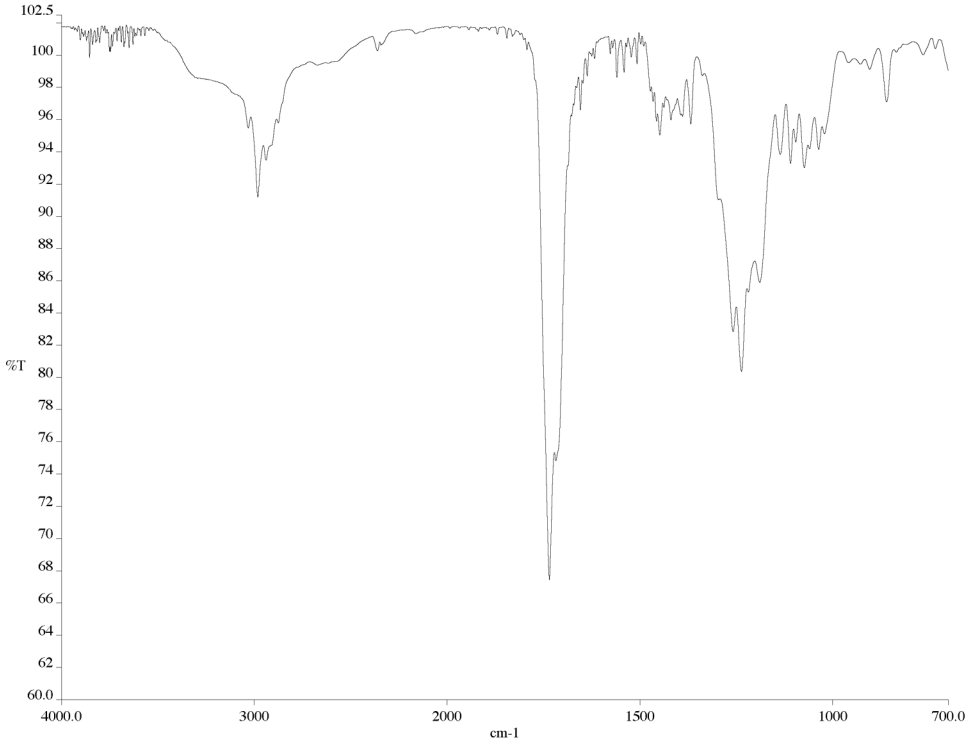

Figure A3.1.36 IR spectrum (thin film/NaCl)) of ***cis-3-d-242***.

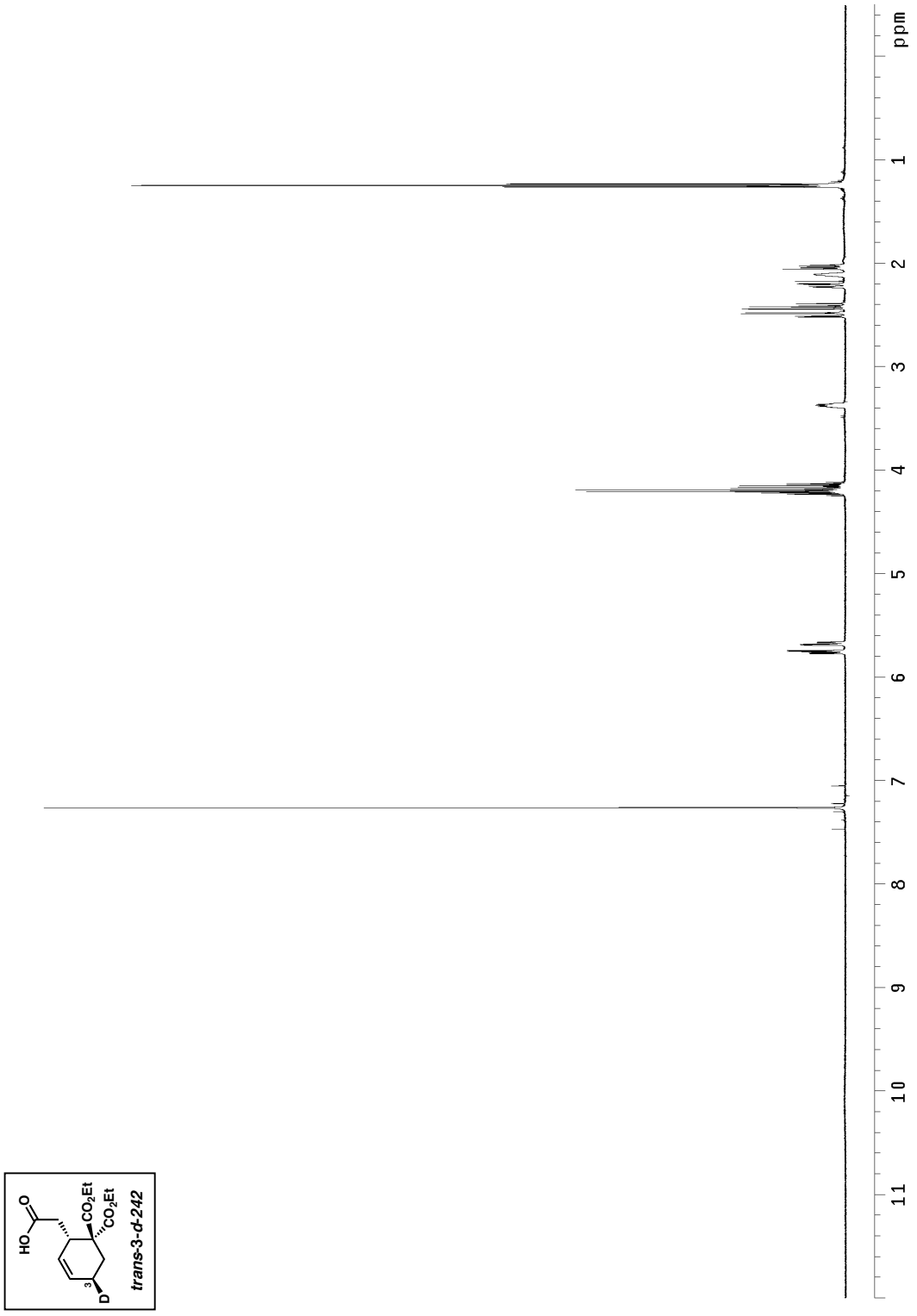

Figure A3.1.37 ^{1}H NMR spectrum (500 MHz, $CDCl_3$) of ***trans-3-d-242***.

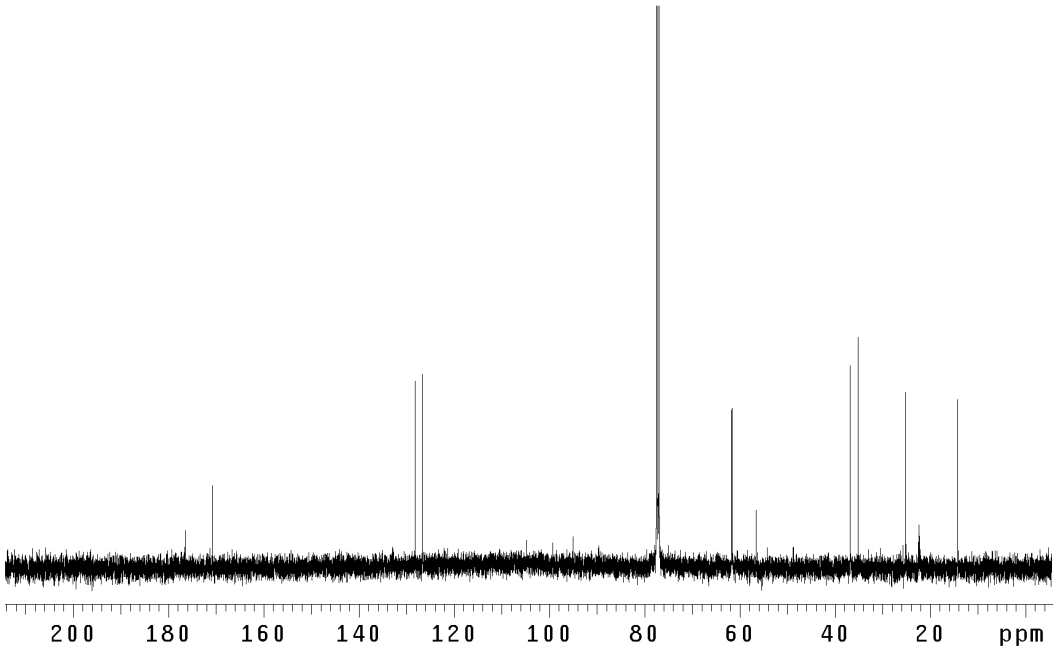

Figure A3.1.38 ^{13}C NMR spectrum (125 MHz, $CDCl_3$) of ***trans-3-d-242***.

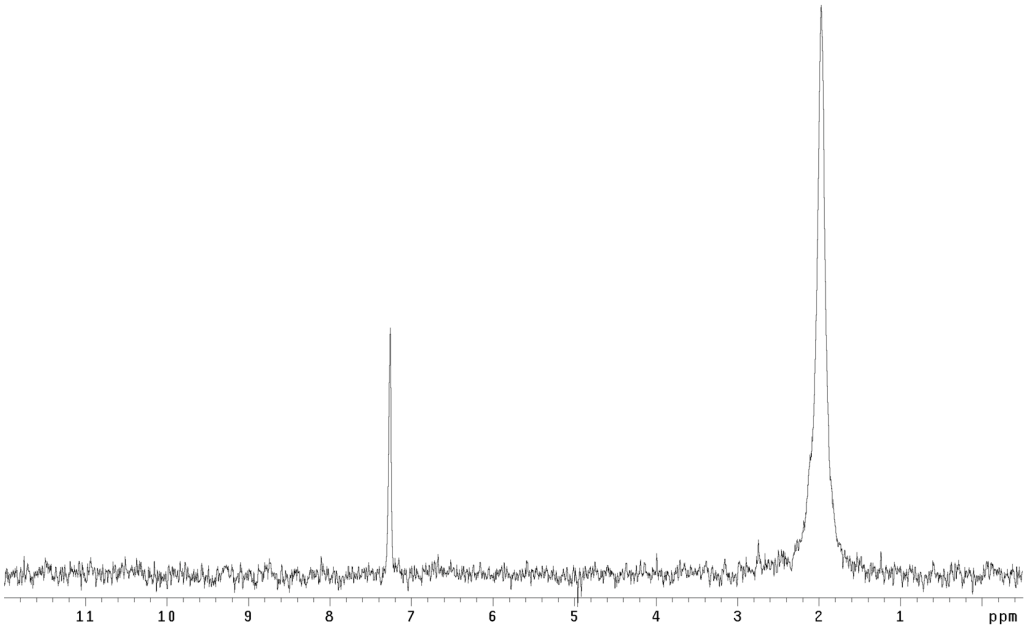

Figure A3.1.39 ^{2}H NMR spectrum (76 MHz, $CHCl_3$ of ***trans-3-d-242***.

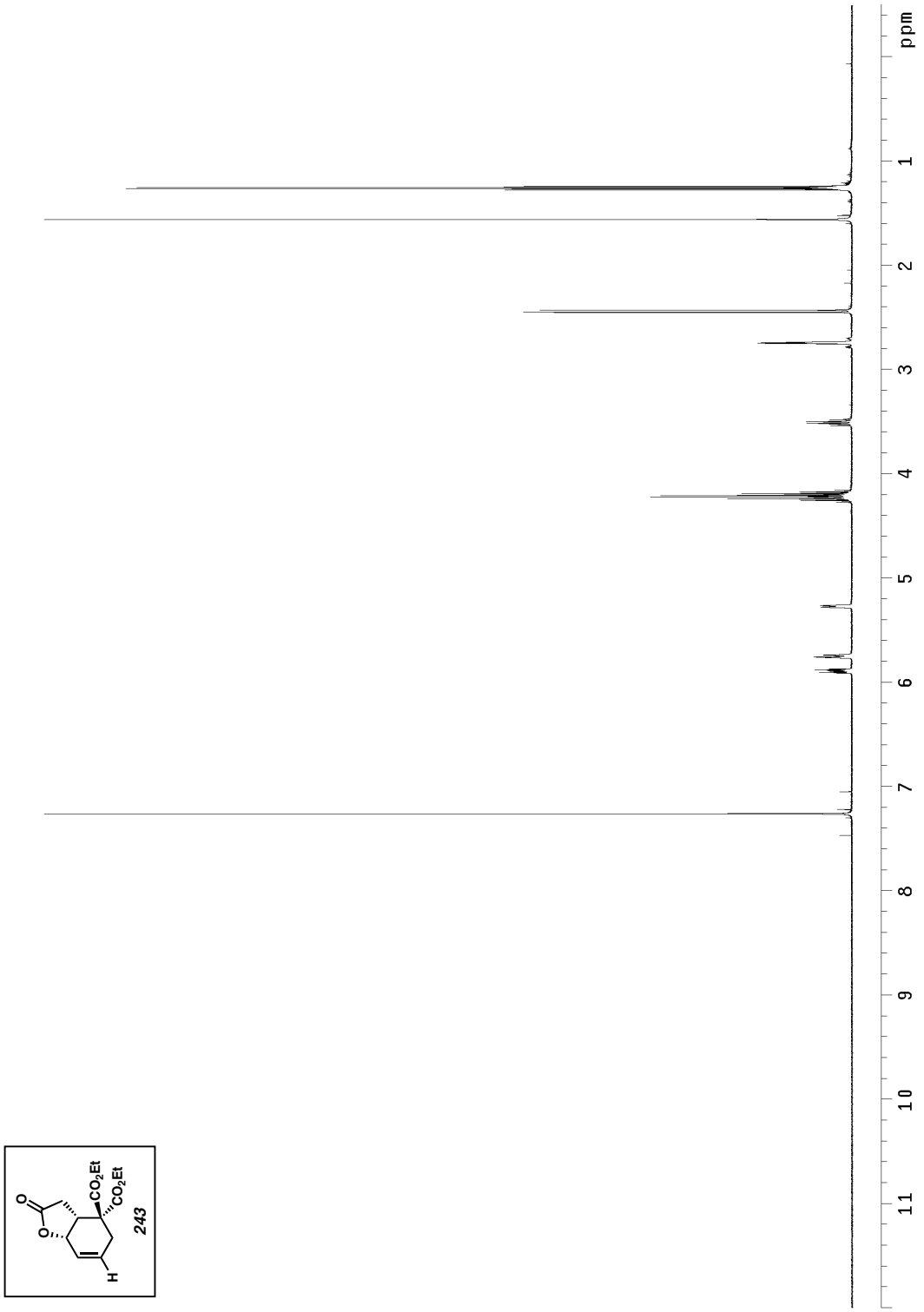

*Figure A3.1.40 ^{1}H NMR spectrum (500 MHz, $CDCl_3$) of **243**.*

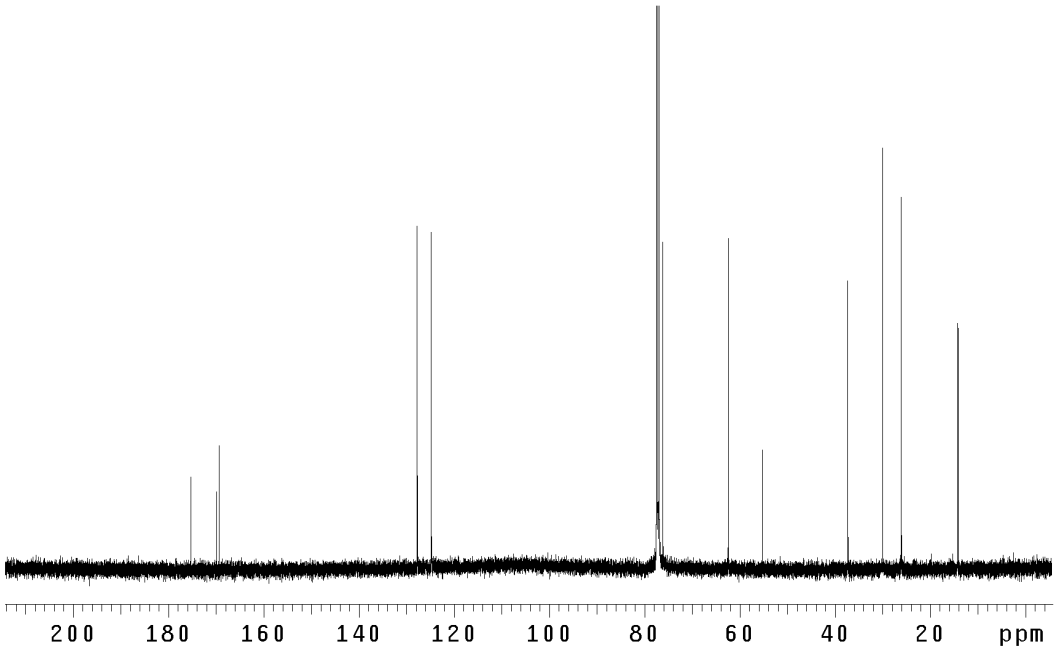

*Figure A3.1.41 ^{13}C NMR spectrum (125 MHz, $CDCl_3$) of **243**.*

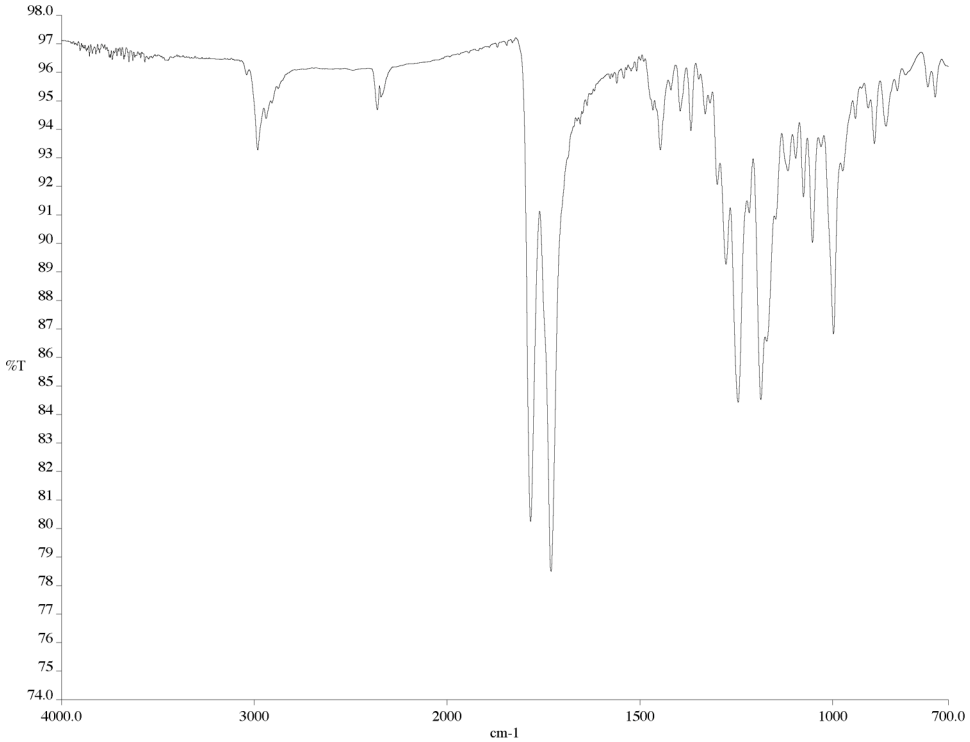

*Figure A3.1.42 IR spectrum (thin film/NaCl)) of **243**.*

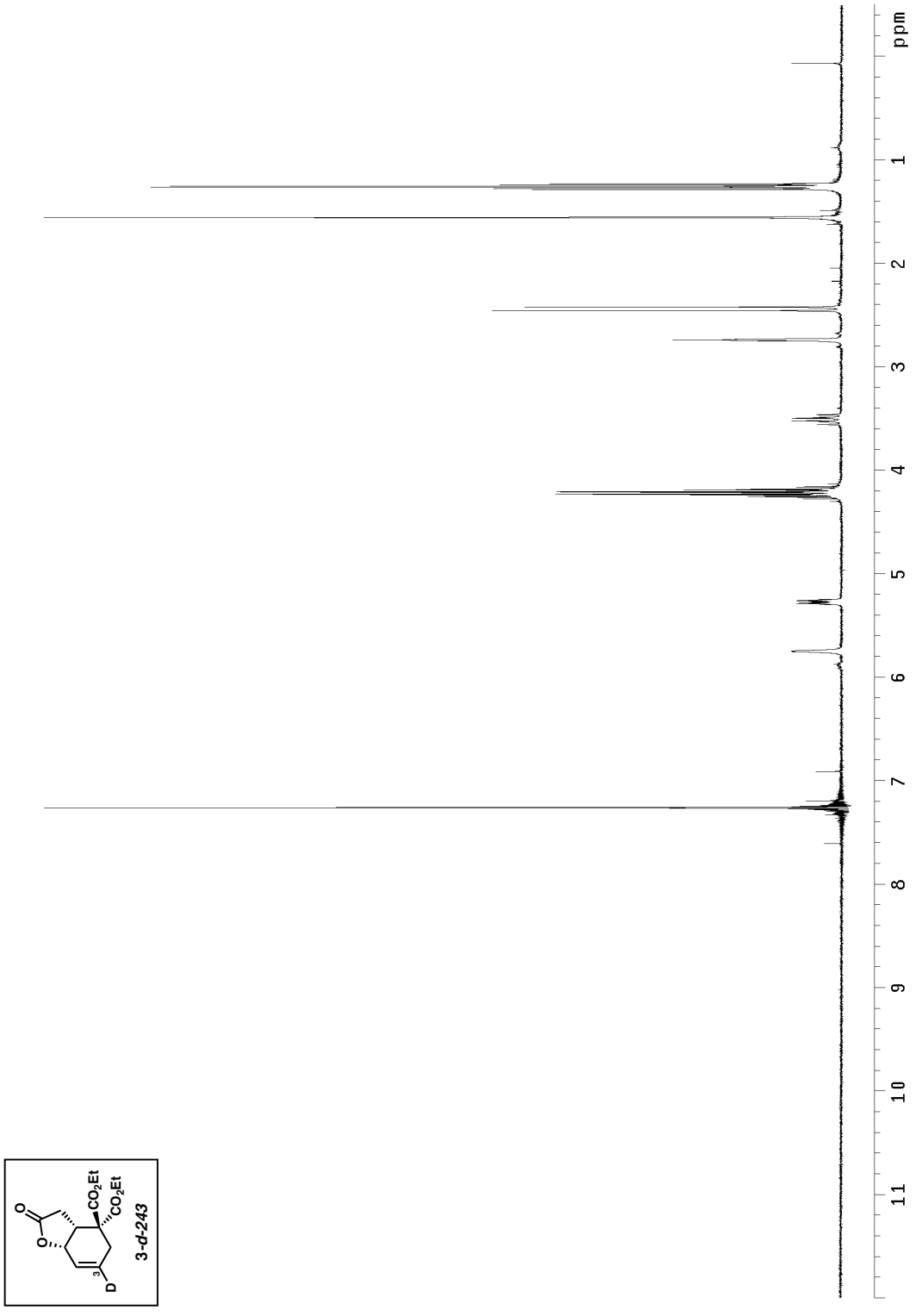

*Figure A3.1.43 ^{1}H NMR spectrum (300 MHz, $CDCl_3$) of **3-d-243**.*

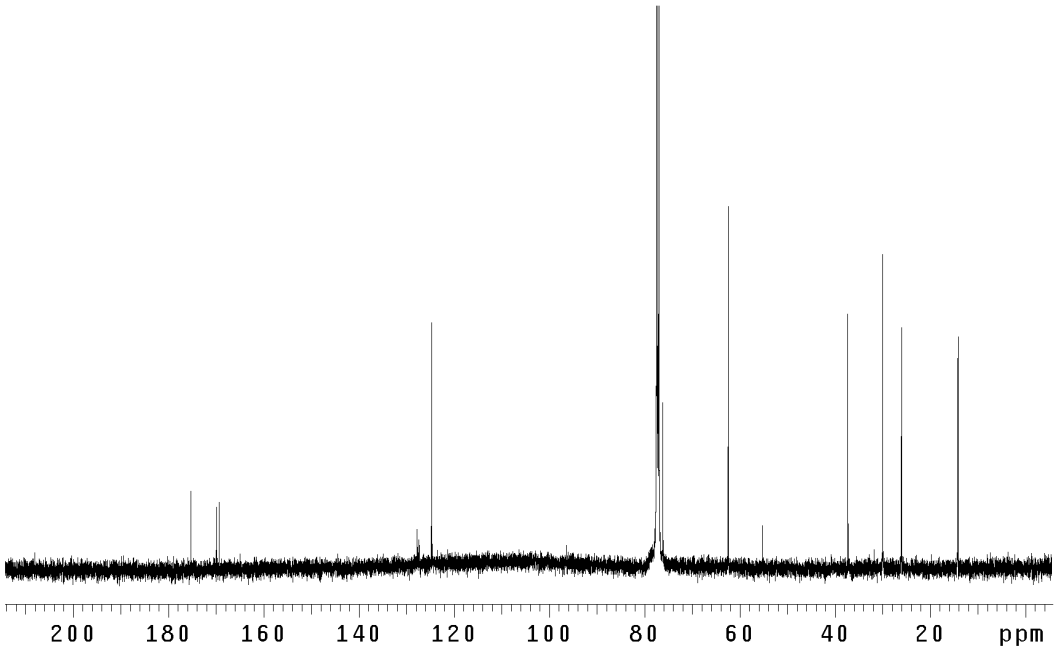

Figure A3.1.44 ^{13}C NMR spectrum (125 MHz, $CDCl_3$) of ***3-d-243***.

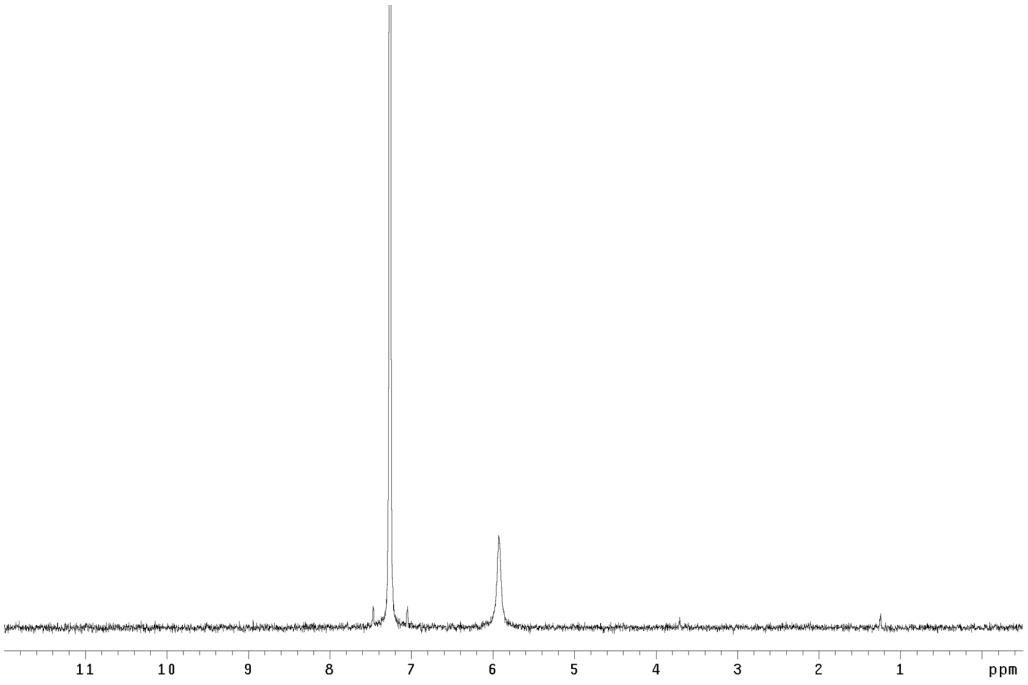

Figure A3.1.45 ^{2}H NMR spectrum (76 MHz, $CHCl_3$) of ***3-d-243***.